Aus der
Universitätsklinik für Anaesthesiologie und Intensivmedizin

Role of Sema4D on the primary immune function in Acute Respiratory Distress Syndrome

Thesis submitted as requirement to fulfill the degree ,,Doctor of Philosophy" in *Experimental Medicine* (PhD)

at the
Faculty of Medicine
Eberhard Karls Universität
Tübingen

by

Tang, Linyan

2023

Dean: Professor Dr. B. Pichler

Frist reviewer: Professor Dr. P. Rosenberger
Second reviewer: Professor Dr. R. Lukowski

Date of oral examination: 04.08.2023

Table of contents

List of Figures IV
List of abbreviations V
1 Introduction 1
1.1 Acute Respiratory Distress Syndrome (ARDS) 1
1.1.1 Definition 1
1.1.2 Epidemiology 2
1.1.3 Pathophysiology 3
1.2 Inflammation and leukocyte recruitment 7
1.2.1 Neutrophil polarization 7
1.2.2 Neutrophil rolling 11
1.2.3 Neutrophil firm adhesion 12
1.2.4 Neutrophil crawling 14
1.2.5 Neutrophil trans-endothelial migration (TEM) 15
1.2.6 Neutrophil effector functions 18
1.3 Sema4D and its receptors 20
1.4 Aims of the project 22
2. Materials and Methods 23
2.1 General materials 23
2.2 Methods and specific materials 25
2.2.1 Flow chamber 25
2.2.2 Isolation of neutrophils from human blood with Percoll-based density gradient 27
2.2.3 Isolation of neutrophils with Magnetic-activated cell sorting (MACS) system 28
2.2.4 Flow cytometry for fibrinogen binding assay 29
2.2.5 Expression of integrins on human neutrophils by flow cytometry 30
2.2.6 Chemotaxis assay 30
2.2.7 Immunofluorescence for PSGL-1 and CD11b on human neutrophils in chemotaxis 32
2.2.8 Length width ratio of human neutrophils 33
2.2.9 Immunofluorescence for RhoA and F-actin on human neutrophils in chemotaxis 33

2.2.10 Immunofluorescence for RhoA and F-actin on human neutrophils in the homogeneous concentration of fMLP 34
2.2.11 Proteomics analysis 35
2.2.12 Immunofluorescence for Sema4D and PlxnB2 on fMLP activated human neutrophils 35
2.2.13 Experimental mice 37
2.2.14 LPS-induced mouse lung injury model 38
2.2.15 Flow cytometry for mouse neutrophils in the blood 38
2.2.16 Flow cytometry for mouse bronchoalveolar lavage (BAL) 39
2.2.17 Flow cytometry for mouse lung 40
2.2.18 Immunofluorescence staining for Sema4d, and vWF or cytokeratin in mice lung sections 41
2.2.19 Protein analysis - Bicinchoninic acid assay (BCA) 44
2.2.20 MPO assay 44
2.2.21 Enzyme-linked immunosorbent assay (ELISA) 45
3. Results 47
3.1 Sema4D inhibits neutrophil rolling and adhesion in inflammation 47
3.2 Sema4D inhibits neutrophil polarization and PSGL-1 redistribution in inflammation 51
3.3 Sema4D inhibits neutrophil uropod formation and firm adhesion in inflammation 55
3.4 Sema4D regulates the Rho GTPase family proteins and consequently influences the intracellular cytoskeleton in neutrophils 59
3.5 Sema4D inhibits neutrophil polarization through binding to its receptors PlxnB1 and PlxnB2. 64
3.6 The expression of Sema4D and its receptors on neutrophils declines in inflammation 67
3.7 Inflammation induces increase in Sema4D expression on pulmonary endothelial and epithelial cells 71
3.8 Sema4D deficiency leads to a more aggressive inflammatory reaction in acute lung injury 74
4. Discussion 77
5. Summary 84
6. German summary 86
7. References 88
8. Declaration of Contributions to the Dissertation 96

9. Awards 97
10. Acknowledgments 98

List of Figures

Figure 1. Schematic representation of neutrophil polarization. 10

Figure 2. Schematic representation of neutrophil extravasation. 18

Figure 3. Schematic diagram of the flow chamber experiment. 26

Figure 4. Scheme of neutrophil isolation with Percoll-based density gradient. 27

Figure 5. LPS inhalation induced mice acute lung injury model. 38

Figure 6. Sema4D inhibits neutrophil adhesion in inflammation. 50

Figure 7. Sema4D inhibits neutrophil polarization and PSGL-1 redistribution in inflammation. 55

Figure 8. Sema4D inhibits neutrophil uropod formation and firm adhesion in inflammation. 58

Figure 9. Sema4D regulates Rho GTPase family proteins and consequently influences the intracellular cytoskeleton in neutrophils. 64

Figure 10. Sema4D inhibits neutrophil polarization through binding to its receptors PlxnB1 and PlxnB2. 66

Figure 11. Expression of Sema4D and its receptors on neutrophils declines in inflammation. 68

Figure 12. The expression of Sema4D on pulmonary epithelial and endothelial cells increases in inflammation. 73

Figure 13. Sema4D deficiency leads to a more aggressive inflammatory reaction in acute lung injury. 76

List of abbreviations

Abbreviations	Full name
AAV	antineutrophil cytoplasmic antibody (ANCA)-associated vasculitis
ADAM17	a disintegrin and metalloprotease
AECC	American-European consensus conference
AECI	type I alveolar epithelial cell
AECII	type II alveolar epithelial cell
AJs	adherens junctions
ALI	acute lung injury
ANCA	antineutrophil cytoplasmic antibody
ANOVA	analysis of variance
ARDS	acute respiratory distress syndrome
BAL	bronchoalveolar lavage
BCA	bicinchoninic acid assay
BSA	bovine serum albumin
BW	body weight
CD	cluster of differentiation
Cdc42	cell division control protein 42 homolog
CFTR	cystic fibrosis transmembrane conductance regulator
CR1	complement receptor type 1
CPAP	continuous positive airway pressure
Cx	connexin
CXCL1	chemokine (C-X-C motif) ligand 1
DAG	diacylglycerol
DAPI	4′,6-diamidino-2-phenylindole
DCs	dendritic cells
ECM	extracellular matrix
EDTA	ethylenediaminetetraacetic acid tetrasodium salt hydrate
ELAM-1	endothelial-leukocyte adhesion molecule 1
ELISA	enzyme-linked immunosorbent assay
ENaC	epithelial sodium channel
ER	endoplasmic reticulum
ERMs	ezrin, radixin and moesin
F-actin	actin filament
FACS	fluorescence-activated cell sorting
FFPE	formalin-fixed, paraffin-embedded
FiO2	fraction of inspired oxygen
fMLP	N-Formylmethionyl-leucyl-phenylalanine
FPR1	formyl peptide receptor 1
GAPs	GTPase-activating proteins
GDIs	guanine dissociation inhibitors
GEFs	guanine nucleotide exchange factors
GJs	gap junctions
GLYCAM1	glycosylation-dependent cell adhesion molecule 1
GMP-140	granule membrane protein 140
GPCR	G- protein-coupled receptor
GPI	glycosylphosphatidylinositol
GPIb	glycoprotein Ib
HBSS	Hanks´ balanced salt solution

HNSCC	head and neck squamous cell carcinoma
IFN-γ	interferon-gamma
IP3	inositol 1,4,5-trisphosphate
JAMs	junctional adhesion molecules
KC	keratinocytes-derived chemokine
LECAM2	leukocyte-endothelial cell adhesion molecule 2
LFA-1	lymphocyte function-associated antigen 1
ICAM-1	intercellular adhesion molecule 1
ICAM-2	intercellular adhesion molecule 2
IFN-γ	interferon gamma
IL-1	interleukin 1
IL-1β	interleukin 1 beta
IL-4	interleukin 4
IL-6	interleukin 6
IL-12	interleukin 12
IL-13	interleukin 13
IS	immune synapse
LBRC	lateral border recycling compartment
LPS	lipopolysaccharide
Mac-1	macrophage-1 antigen
MADCAM1	mucosal vascular addressin cell adhesion molecule 1
MFI	mean fluorescence intensity
MLCP	myosin light chain phosphatase
MMP9	metalloprotease 9
MMP25	metalloprotease 25
MPO	myeloperoxidase
MRLC	myosin regulatory light chain
MS	multiple sclerosis
NE	neutrophil elastase
NETs	neutrophils extracellular traps
NGPs	neuronal guidance proteins
PADGEM	platelet activation-dependent granule to external membrane protein
PaO2	partial pressure of arterial oxygen
PAWP	pulmonary artery wedge pressure
PBS	phosphate buffered saline
PECAM-1	platelet endothelial cell adhesion molecule 1
PEEP	positive end-expiratory pressure
PFA	paraformaldehyde
PI3Kγ	type 1B phosphoinositide 3-kinase
PIP2	phosphatidylinositol (4,5)-triphosphate, PtdIns(4,5) P2
PIP3	phosphatidylinositol (3,4,5)-triphosphate, PtdIns(3,4,5)P3
PLC	phospholipase C
PlxnB1	plexinB1
PlxnB2	plexinB2
PNCs	platelet-neutrophils complexes
PSGL1	P-selectin glycoprotein ligand 1
RA	rheumatoid arthritis
RhoA	ras homolog family member A
Rho GDI	Rho GDP-dissociation inhibitor
ROCK	Rho-associated protein kinase

ROI	reactive oxygen intermediates
ROS	reactive oxygen species
RT	room temperature
SCAMP	secretory carrier membrane protein
Sema4D	semaphorin4D
Sema4d$^{-/-}$	Sema4d-deficient
SELPLG	selectin P ligand
SPF	specific pathogen free
sSema4D	soluble fragment of Sema4D
TEM	trans-endothelial migration
TJs	tight junctions
TNFα	tumor necrosis factor α
VE-cadherin	vascular endothelial -cadherin
VLA-4	very late antigen-4
vWF	von Willebrand factor
WT	wild type
ZOs	zonula occludens

1 Introduction

1.1 Acute Respiratory Distress Syndrome (ARDS)

1.1.1 Definition

Acute respiratory distress syndrome (ARDS) is characterized by inflammation-induced rapidly progressed non-cardiogenic pulmonary edema and severe hypoxemia. It was initially described in 1967[1,2] by Ashbaugh et al. as 12 adult patients presented with acute tachypnea, hypoxemia and decreased lung compliance, whereby these symptoms could not be alleviated by standard common respiratory treatment at that time[2].

The specific definition and diagnostic criteria for ARDS were established in 1992 at the American-European Consensus Conference (AECC) on ARDS[3]. It defined ARDS as a severe inflammation syndrome with increased lung permeability which is represented as the acute onset of hypoxemia ($PaO_2/FiO_2 \leq 200$mmHg. FiO_2, the fraction of inspired oxygen; PaO_2, partial pressure of arterial oxygen) with bilateral infiltrates on frontal chest radiograph, without left atrial hypertension (Pulmonary Artery Wedge Pressure, PAWP ≤ 18mmHg). Besides the diagnostic criteria, this definition emphasized the crucial role of inflammation in ARDS development and indicated that the most frequent initial pathological conditions for ARDS are sepsis syndrome, aspiration, primary pneumonia or multiple traumas.

In 2012 the updated standard definition and classification for adult ARDS was proposed as the Berlin Definition[4] (table 1) by an international expert panel summoned by the European Society of Intensive Care Medicine, and supported by the American Thoracic Society and the Society of Critical Care Medicine. Compared to the AECC definition, the Berlin definition specified the ‘acute time frame’ to 1 week, clarified the chest radiograph criteria, removed the PAWP criteria, and added subgroups depending on oxygenation levels. Because the Berlin Definition is more explicit, sensitive and reliable, it has been broadly accepted by physicians and clinical researchers.

Acute lung injury (ALI)[3] was defined also first at AECC in 1992 as a wider definition for the continuous pathological process of ARDS. The clinical representation spectrum of ARDS, including arterial blood gas and chest radiographic abnormalities, is continuous. Before the patients develop severe ARDS ($PaO_2/FiO_2 \leq 200$mmHg), the pathological process has started, and earlier recognition and interference will benefit more patients.

Therefore, AECC defined the diagnosis criteria for ALI in oxygenation (PaO_2/FiO_2 ≤ 300mmHg) are wider than ARDS, but the same with ARDS in timing, chest radiograph, and pulmonary artery wedge pressure, and clarified ARDS as `the most severe end stage` of ALI. However, the term 'acute lung injury' was eliminated in the Berlin definition[4], because the expert panel believed that this term was 'misused' by clinicians to diagnose the patients only with better oxygenation (200mmHg ≤ PaO_2/FiO_2 ≤ 300mmHg), but not all the patients with this pathologic process. Instead, Berlin Definition categorized the patients with better oxygenation (200mmHg ≤ PaO_2/FiO_2 ≤ 300mmHg) as 'mild' ARDS, and the patients with 100mmHg ≤ PaO_2/FiO_2 ≤ 200mmHg and PaO_2/FiO_2 ≤ 100mmHg as 'moderate' and 'severe' ARDS respectively (table 1).

Table 1. The Berlin Definition of Acute Respiratory Distress Syndrome

	Acute Respiratory Distress Syndrome
Timing	Within 1 week of a known clinical insult or new or worsening respiratory symptoms
Chest imaging[a]	Bilateral opacities—not fully explained by effusions, lobar/lung collapse, or nodules
Origin of edema	Respiratory failure not fully explained by cardiac failure or fluid overload Need objective assessment (eg. echocardiography) to exclude hydrostatic edema if no risk factor presents
Oxygenation[b]	
Mild	200 mmHg < PaO_2/FiO_2 ≤ 300 mmHg with PEEP or CPAP < 5 cm H_2O[c]
Moderate	100 mmHg < PaO_2/FiO_2 ≤ 200 mmHg with PEEP > 5 cm H_2O
Severe	PaO_2/FiO_2 ≤ 100 mmHg with PEEP > 5 cm H_2O

Abbreviations: CPAP, continuous positive airway pressure; FiO_2, the fraction of inspired oxygen; PaO_2, partial pressure of arterial oxygen; PEEP, positive end-expiratory pressure.

[a] Chest radiograph or computed tomography scan.

[b] If altitude is higher than 1000 m, the correction factor should be calculated as follows: [PaO_2/FiO_2 × (barometric pressure/ 760)].

[c] This may be delivered noninvasively in the mild acute respiratory distress syndrome group

1.1.2 Epidemiology

ARDS is a syndrome with sobering mortality and public health impact. It is a frequent cause for acute respiratory failure and mechanical ventilation. In a prospective study for

the incidence of ALI in the United States from 1999 to 2000, it was estimated that the annual incidence of ALI in the United States is 190,600 cases which were attributed with 74,500 mortality cases and 3.6 million hospital days[5].

The Large observational study to Understand the Global impact of Severe Acute Respiratory Failure (LUNG SAFE) is the most famous epidemiologic study for ARDS. It observed patients from 459 ICUs in 50 countries in 2014 and revealed that 10.4% of all ICU patients fulfilled the diagnostic criteria of ARDS, of which 23.4% of them required invasive or noninvasive ventilation[6]. Among these patients hospital mortality rates for mild cases were 34.9%, moderate cases were 40.3%, and severe ARDS patients were 46.1%[6], which is accordant to the mortality in Berlin definition, which is 27%, 32%, and 45% in mild, moderate, and severe ARDS patients respectively[4].

1.1.3 Pathophysiology

1.1.3.1 Inflammation

Inflammation is the most critical pathologic process for ARDS, influencing the pathogenesis, progression and recovery of the disease. From the very beginning in 1967 when ARDS was first reported, Ashbaugh[1] et al indicated that all ARDS patients initially presented severe inflammation in lung or systemic inflammation, including 4 patients (33,3%) with viral pneumonia, 7 patients (58,3%) preceded from severe trauma, and 1 patient (8,33%) from acute pancreatitis. In the AECC in 1992 ARDS was defined as a 'syndrome of inflammation'[3]. A histopathological study with an autopsy of 712 patients who died in ICU over 2 decades showed that in all 356 patients who fulfilled the clinical criteria for ARDS in the Berlin definition, 290 (81,46%) patients presented intense neutrophil infiltration into the lung interstitium and alveolar space[7]. This study proved that the recruitment of inflammatory cells, particularly neutrophils, from the vasculature to the lung is the core pathophysiological process for ARDS. During the recruitment process, neutrophils undergo rolling, adhesion and transmigration, which are regulated by a large class of adhesion molecules, selectins, P-selectin glycoprotein ligand-1(PSGL-1) and integrins. Such molecules are found on cell surfaces of vascular endothelial cells and inflammatory cells[8].

1.1.3.2 Epithelial cell barrier function

Besides inflammation, lung epithelial and vascular endothelial injury also play critical roles in ARDS. The normal human lung is composed of the trachea (windpipe), bronchi,

bronchioles and alveoli. The surface of all these structures is covered with epithelial cells which function mainly as a barrier towards potential pathogens and tiny extraneous particles in the inspiratory air. The epithelial cells on the respiratory tract (trachea and bronchi) comprise of ciliated columnar epithelial cells, secretory goblet cells, club cells, and basal cells[9]. Goblet cells, together with the submucosal glands, secrete mucus glycoproteins to trap microorganisms and particles. These foreign particles are subsequently eliminated effectively from the respiratory tract by the coordinated beating of cilia across different ciliated epithelial cells to generate the propulsion of mucus. This function is called mucociliary clearance[10]. The alveolar epithelium, which covers 99% of the lung surface area, is composed of type I and type II alveolar epithelial cells (AECI and AECII). AECI and AECII occupy almost the same numbers but consist of 96% and 4% of the alveolar surface respectively[11]. The reason for this is because AECIs are membranous flat, and their main anatomic function is to form the extremely thin air-exchanging barrier. Differently, AECIIs are cuboidal and usually localize at the alveolar corners. AECIIs secrete protein components for the alveolar surfactant which lower the alveolar surface tension at the liquid-air interface to prevent alveolar collapse during breathing.

Not only the surface of the alveolar, but also the surface of the bronchi and bronchioles are covered with lining liquid, which is regulated by different kinds of ions and water channels on epithelial cells, including the functional epithelial sodium channel (ENaC)[12], cystic fibrosis transmembrane conductance regulator (CFTR)[13], and tight junction proteins[14], including claudins, occludin, and their scaffold proteins zonula occludens (ZOs). All of these molecules cooperate to secrete or clear ions and water molecules to maintain the proper depth of liquid on the surface of the respiratory tract and alveolar space, which is essential for the efficient directional beat of cilia and subsequently, mucociliary clearance function[10].

ARDS is characterized by an abundant liquid accumulation in the lung interstitium and the alveolar space. In this pathological process lung epithelial cells play an important role. In ARDS lung epithelium could be injured directly by viruses, bacterial toxins, physical injury from aspiration, and mechanical forces, or indirectly by cytokines from inflammatory cells.

Without question epithelial cell necroptosis or apoptosis will lead to the dysfunction of all the ion and water channels we mentioned above and influence the regulation of liquid on

the surface of respiratory ducts and alveoli. However, researchers illustrated that inflammation could regulate epithelial permeability, by influencing the epithelium barrier function actively. For instance, the expression of ZO-1, Claudin-2, and Claudin-4 was altered in acute lung inflammation[15]. Cytokines, including tumor necrosis factor-α (TNF-α), decrease the expression of ENaC on epithelial cell[16]. All these changes induce liquid accumulation in the lung interstitium, bronchioles, and alveolar spaces which increase the oxygen diffusion distance, block the respiratory tract, induce arteriovenous shunt, and eventually lead to severe hypoxemia.

1.1.3.3 Endothelial barrier function

The endothelium in lung vessels constructs a semipermeable barrier that restricts its permeability towards molecules in a size-selective manner[17]. Molecules smaller than 3nm in radius, such as H_2O, O_2, and CO_2, permeate through endothelium following concentration gradients, while larger molecules such as albumin and blood cells are restricted in the vessels[18]. Lung endothelial cells are connected by three protein complexes, the inter-endothelial junctions, including tight junctions (TJs), adherens junctions (AJs), and gap junctions (GJs). All of them are crucial for the endothelial selective permeability towards certain molecules and cells, and consequently influence tissue liquid homeostasis and inflammatory cell accumulation in the lung interstitium and alveolar space.

The most important AJs between adjacent endothelial cells are the vascular endothelial-cadherin (VE-cadherin) and associated α-, β- and p120-catenin adhesion complexes[17] which anchor the cadherin to the cytoskeleton. Cadherins are calcium-dependent adhesion molecules that mediate intercellular connection formation. VE-cadherin is crucial for the assembly and remodeling of the vasculature in embryo development[19]. Knock-out VE-cadherin gene leads to endothelial cell apoptosis[20], and blocking VE-cadherin in vitro inhibits angiogenesis[21]. VE-cadherin is the core player for the integrity of endothelium and is pathologically responsible for increasing endothelial permeability. For instance, phosphorylation of Tyr-658 and Tyr-731 leads to the loss of endothelial barrier function[22]. During inflammation, intercellular adhesion molecule 1 (ICAM-1) activation or inflammatory mediators exposure influence RhoA-dependent stress fibre formation and cell contraction, which dissemble cadherin and enhance endothelial permeability. Xiong et al. demonstrated that lipopolysaccharides (LPS) or interleukin 1 beta (IL-1β) stimulation

decreases the transcription of VE-cadherin and the formation of endothelial adherens junctions in the lung[23]. Broermann et al. showed that during LPS-induced pulmonary inflammation, alterations to VE-cadherin function resulted in the inhibition of protein leakage due to loss in the regulation of endothelial cell contacts[24]. All these studies prove the importance of VE-cadherin in regulating endothelial permeability in inflammatory lung injury.

The TJs on endothelium in the lung are mainly junctional adhesion molecules (JAMs), including JAM-1, JAM-2, and JAM-3 (also named as JAM-A, -B, and -C). They are demonstrated to be concentrated at the apical intercellular junction and are mainly involved in leukocyte paracellular transmigration[24-27]. Inflammatory cytokines, such as TNF-α and interferon-gamma (IFN-γ), induce JAM-1 redistribution from the intercellular junction to the luminal surface of endothelial cell[25], and on the luminal surface, it cooperates with leukocyte integrin αLβ2 (also named lymphocyte function-associated antigen 1, LFA-1) to control leukocyte transendothelial migration (TEM)[26]. JAM-2 performs its role in regulation leukocyte rolling and firm adhesion by cooperating with integrin α4β1 (also named very late antigen-4, VLA-4) [27]. Endothelial JAM-3 plays an important role in leukocyte TEM. It cooperates with the integrin αMβ2 (also named macrophage-1 antigen, Mac-1) expressed on leukocytes to regulate their transmigration direction. Increasing JAM-3 expression promotes neutrophil TEM in an abluminal to luminal direction by preventing reverse transmigration[28]. While blocking JAM-3 reduces the number of monocytes in the inflammatory position and increases reverse-transmigration back to circulated blood simultaneously[29].

GJs were originally described as low-resistance ion channels joining neurons and myocytes to propagate excitation[30]. Studies demonstrated that GJs connect all types of cells in solid tissues. Human GJs channels are constructed of six connexin molecules, including connexin37 (Cx37), connexin40 (Cx40), and connexin43 (Cx43), Cx43, which are the three major isoforms in endothelial cells[17]. They connect the endothelial-endothelial junction and endothelial-smooth muscle cells and regulate blood pressure[31,32]. Cx43 is also shown to induce lung capillaries endothelial cells to express P-selectin[33], which is critical for the adhesion of leukocytes and platelets to the inflammatory area.

1.2 Inflammation and leukocyte recruitment

ARDS is characterized by serious inflammation in the lung, with or without systemic inflammation involved in other organs. The inflammatory reaction is initialized through neutrophil adhesion and transmigration into the lung interstitial or alveolar space. Neutrophil granulocyte (short for neutrophil) recruitment plays a central role in the pathogenesis and progression of ARDS. Several independent investigations showed that in ARDS patients the number of neutrophils in bronchoalveolar lavage (BAL) was always elevated and the higher concentration of neutrophils was associated with increased protein concentration in BAL, worse oxygenation and higher mortality, especially in ARDS patients with sepsis[34,35,36]. Neutrophil infiltration into inflammatory sites, also named adhesion cascade or extravasation, is a pathological process composed of neutrophil rolling, adhesion, and transmigration. A more specific description of this process has been raised in recent decades, including slow rolling, adhesion strengthening, crawling on endothelium, paracellular or transcellular transmigration, and basement membrane transmigration[8]. Different sorts of molecules expressed on the membrane of neutrophils and endothelial cells cooperate effectively to regulate this orchestrated cascade. Simultaneously the cytoskeleton inside both types of cells reorganizes responsively to provide mechanical support for cell movement and transformation. This reorganization leads to neutrophil polarization which is a characterized feature of inflammation-activated neutrophils.

1.2.1 Neutrophil polarization

The polarization of neutrophils is seen as the hallmark of inflammatory states[37,38] and is the physical foundation for efficient migration of neutrophils following the chemoattractant gradient. In the recent two decades this process has been focused on and intensively investigated[39-45]. Chemoattractants bind to the G- protein-coupled receptor (GPCR), such as formyl peptide receptor 1 (FPR1), on cell surfaces of neutrophils to initiate signal transduction cascades by inducing the α subunit of G protein to dissociate from the β and γ subunits. Both α and βγ subunits recruit phospholipase C (PLC) that hydrolyses phosphatidylinositol 4,5-bisphosphate (PtdIns(4,5) P2, PIP2) on the plasma membrane into inositol 1,4,5-trisphosphate (IP3) and diacylglycerol (DAG)[40]. IP3 triggers Ca^{2+} releasing from the smooth endoplasmic reticulum (ER) by binding to IP3 receptor. βγ subunits of G protein activate type 1B phosphoinositide 3-kinase (PI3Kγ) which

phosphorylates PIP2 into phosphatidylinositol (3,4,5)-triphosphate (PtdIns(3,4,5)P3, PIP3)[41]. PIP3 activates guanine nucleotide exchange factors (GEFs), such as P-Rex1[42], which activates the small Rho GTPases Rac[42] and cell division control protein 42 homolog (Cdc42)[43] by exchanging the binding GDP to GTP. Subsequently, Rac and Cdc42 promote actin filament (F-actin) polymerization to push the membrane to form protrusion at the cell front[43,44]. At the same time, another small Rho GTPases Ras homolog family member A (RhoA) is activated in the cell rear by blocking its inhibitor Rho GDP-dissociation inhibitor (Rho GDI). Activated RhoA stimulates Rho-associated protein kinase (ROCK), which subsequently phosphorylates the myosin regulatory light chain (MRLC) to stimulate actomyosin contraction and form the uropod[43,45]. Additionally, the F-actin polymerization-induced front protrusion is instantaneously coupled with the myosin contraction in the uropod and positively reinforces each other to achieve efficient migration and turning around of neutrophils towards the pathogen[43].

The traditional view believes that the traction forces for cells transmigration were originally produced by the adhesion of cells leading edge to the substratum and towing forward. In this theory hypothesis, the function of transmigrating cells uropod is to contract and efficiently release the rear from the substratum passively. That means, in cells uropod, myosin contractility accompanies by low adhesive membrane protein distribution, and this combination enables cells to move towards the chemoattractant by pulling forward the leading edge, compressing the rear and releasing the uropod adhesion from the surrounding environment[46]. However, there is growing substantial evidence that this type of traction force generation may only promote the transmigration of mesenchymal cells and even macrophages, but not neutrophils[43,44].

In neutrophils, uropod formation is substantial and plays a more critical role than just passive contraction and posterior release. Smith L.A. et al.[47] performed traction force microscopy and proved in vitro that the traction force in transmigrating neutrophils is continuously generated at the rear, but rare or never in the leading edge. The traction stresses generating area (uropod) could change orientation and location immediately after the chemotaxis direction is altered and this change generates a new transmigration force toward the chemotaxis gradient. This traction force from backward continuously pushes

neutrophils to move forward and this traction stress, but not the pulling stress from the lamellipodia, is the main or only mobility mechanism for neutrophil transmigration.

Several studies[46,47] demonstrated the intensive correlation between myosin-induced uropod formation and firm adhesion and extravasation in leukocytes. Vadillo E. et al.[48] employed Myosin 1e deficient mice to illustrate that myosin deficiency significantly damaged the process of neutrophils extravasation, this dysfunction was mainly due to the diminished uropod formation and firm adhesion of neutrophils to the vascular endothelium. Guinoa J. et al.[49] proved that actomyosin induces vinculin, a protein linking the actin cytoskeleton with integrins, to recruit to the B lymphocytes uropod and at the same time, LFA-1 enriches to this ring-shaped immune synapse, actively regulate epithelial permeability, in another word, the epithelium barrier function.

Hyun Y.M. et al.[50] proved that uropod elongation is a universal final process in neutrophil extravasation. Uropod contract and detachment from endothelial cells happens much later than neutrophil protrusion extravasation. Even when the leading edge of neutrophils is penetrating through the vessel basement membrane and migrating into the inflammatory location, the uropod could still be firm adhering and stationary on the luminal surface of endothelial cells, which produces a long-stretched rear of the neutrophil.

Neutrophil polarization does not only mean the rearrangement of the cytoskeleton to achieve cell transformation and motility, but also presents the redistribution of membrane proteins[44] which is critical for cooperating with other cell types, such as endothelial cells and platelets. The asymmetrical redistribution of membrane proteins seems to follow special patterns: highly glycosylated receptors involved in adhesion concentrate to the uropod, including P-Selectin Glycoprotein Ligand 1 (PSGL-1), LFA-1 (integrin αLβ2), ICAMs, L-selectin, and others[46,50,51], while other receptors, such as chemokine receptor CXCR2[51] and fMLP receptors[44], accumulate to the leading edge of neutrophils. These polarized proteins redistribution is essential for neutrophil interaction with chemokine-stimulus, platelets, endothelial cells and consequently plays a central role in neutrophil recruitment to the inflammatory sites.

In the process of neutrophil polarization, the redistribution of membranal proteins and the activation of the cytoskeleton are not two independent procedures, but intensively correlated and interacted[52-54]. Lorant D. E. et al.[54] indicated that activated neutrophils

polarized to form a PSGL-1 enriched uropod and the redistribution of PSGL-1 to the uropod could be inhibited by cytochalasin D, which proved that this process depended on cytoskeleton activation. When Cdc42 was deleted, the neutrophil polarization, especially the uropod formation was significantly diminished, and synchronously PSGL-1 could not concentrate to form the cluster, which subsequently impaired the interaction between platelet and neutrophils and compromised neutrophils crawling[53].

Above all, neutrophil polarization is a critical and fundamental process in neutrophil extravasation. During polarization, the intracellular cytoskeleton system is organized to produce the mechanical force for cell transformation, protrusion, adhesion, and detachment. At the same time, the membranal proteins are activated or redistributed coordinating neutrophil motility and to cooperate with other types of cells, such as endothelial cells or platelets.

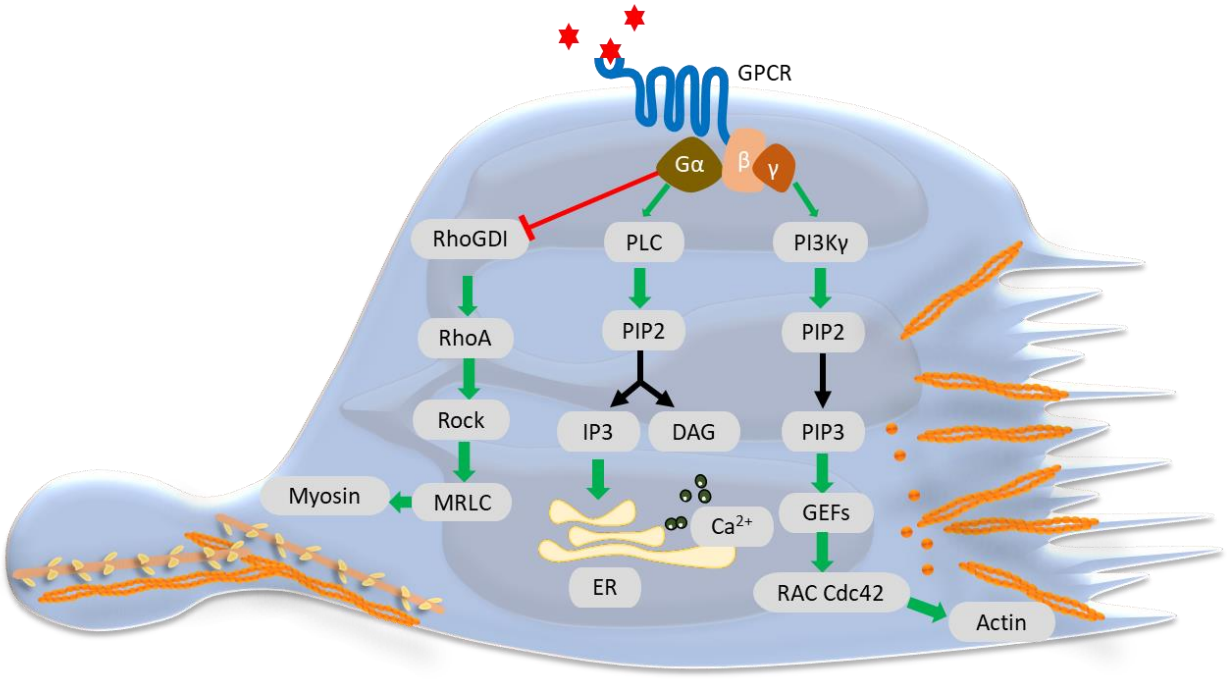

Figure 1. Schematic representation of neutrophil polarization.
Stimulus binds to GPCR to dissociate α subunit of G protein from the βγ subunits. PLC is recruited by subunits of G protein and hydrolyses PIP2 into DAG and IP3 which triggers Ca2+ releasing from ER. βγ subunits of G protein activate PI3Kγ which phosphorylates PIP2 into PIP3. PIP3 activates GEFs, such as P-Rex1, which activates Rac and Cdc42 to promote actin polymerization in the leading edge of neutrophils. In the cell rear Rho GDI is blocked and this activates RhoA. Activated RhoA stimulates ROCK which subsequently phosphorylates MRLC to stimulate myosin contraction and form the uropod.

1.2.2 Neutrophil rolling

The rolling of neutrophils on the surface of endothelium is triggered by the selectins on the endothelium or platelets and PSGL-1 on neutrophils. The selectin family is composed of P-selectin, E-selectin and L-selectin. P-selectin, also known as cluster of differentiation 62P (CD62P), previously named as granule membrane protein 140 (GMP-140)[55] and platelet activation-dependent granule to external membrane protein (PADGEM)[56], is synthesized and stored in Weibel-Palade bodies of endothelial cells, megakaryocytes and α-granules of platelets. Agonists such as histamine, thrombin, and inflammatory cytokines Interleukin-4 (IL-4) and Interleukin-13 (IL-13) could induce rapid translocation of P-selectin from intracellular granules to the cell surface, accompanied by von Willebrand Factor (vWF) releasing from the same components.

E-selectin is also named endothelial-leukocyte adhesion molecule 1 (ELAM-1), leukocyte-endothelial cell adhesion molecule 2 (LECAM2) or CD62E. Different from P-selectin, E-selectin expresses only in stimulated or activated endothelial cells[57]. It is undetectable in unstimulated endothelial cells, but is synthesized and expressed on the surface after two hours of stimulation with TNFα, LPS, Interleukin 1 (IL-1), or Interleukin 1β (IL-1β)[58]. Its expression peaks after three to six hours of stimulation and subsequently declines to basal levels within 24 to 48 hours on account of shedding off and internalization[59]. It is believed that this temporary upregulation is coordinated with the function of promoting neutrophil rolling and adhesion[60] and the rapidly declined expression will limit neutrophil accumulation and negatively regulate local inflammation.

L-selectin, also named CD62L, is expressed in almost all leukocytes. But the function of L-selectin is only well-invested in lymphocytes. Binding to its ligands, including glycosylation-dependent cell adhesion molecule 1 (GLYCAM1) on high endothelial venules of lymph nodes, or mucosal vascular addressin cell adhesion molecule 1 (MADCAM1) on mucosal endothelial cells, L-selectin assists lymphocytes to ‘homing’ secondary lymphoid tissues[61,62]. It is thought that L-selectin also contributes to neutrophil transmigration, since neutrophil recruitment is significantly decreased in L-selectin-null mice in a thioglycollate-induced peritonitis model. However, the molecular mechanism is not yet completely understood.

P-selectin and E-selectin are crucial for initializing neutrophil rolling on endothelial cells and their function mainly depends on binding to their ligand PSGL-1. PSGL-1, also named selectin P ligand (SELPLG), or CD162, is expressed by most of the leukocytes. It binds to P-selectin, E-selectin, and L-selectin, but the affinity towards P-selectin and E-selectin is high, while is low with L-selectin. As described previously, PSGL-1 is redistributed and concentrated to the uropod of the activated neutrophils and regulates the binding of neutrophils to endothelial cells (via E-selectin or P-selectin) or platelets (P-selectin). The distribution of PSGL-1 from the whole cell body to the uropod reduces the adhesion of the leading edge of neutrophils, but enhances the adhesion of the uropod to other cells[46]. This process may happen after rolling, synchronously with neutrophil firm adhesion and transmigration.

PSGL-1 functions also as a receptor to transfer the extracellular signal into cells[53,54]. The binding of P-selectin on platelets or endothelial cells to PSGL-1 enhances the binding of neutrophils to immobilized fibrinogen and ICAM-1, probably because it activates integrins and changes the affinity towards their ligand , because the total expression of integrin $\alpha M\beta_2$ (Mac-1) or integrin $\alpha L\beta_2$ (LFA-1) are not altered[63]. Deletion of the cytoplasmic domain of PSGL-1 only, without influencing the membranal part, also diminished the LFA-1 activation and binding to ICAM-1[64]. The binding of neutrophils integrins to ICAM-1 or to fibrinogen will induce the next step in neutrophil extravasation, which is firm adhesion.

1.2.3 Neutrophil firm adhesion

It is well established that firm adhesion of neutrophils is induced by the binding of integrins to their ligands on endothelial cells[8,65]. Integrins are a big family of cell adhesion molecules which are composed of heterodimeric α and β subunits. In vertebrates, 18 α subunits and 8 β subunits assemble 24 integrins[66]. The different structures of α subunits mainly determine the specificity of their ligands[67]. The β subunit contains a homology cytoplasmic tail that can bind to several cytoskeleton proteins. Integrins play important roles in mediating cell attachment to the extracellular matrix (ECM) or other cell types and in supporting cell transmigration through ECM and cell layers. To fulfill their challenging tasks, integrins are not only adjusted for their concentrated expression on the cell membrane, so-called ‘clustering’, but also are modulated conformationally to change their affinity toward specific ligands[66,68].

Integrins expressed by neutrophils include integrin αL/β2 (CD11a/CD18; LFA-1) and αM/β2 (CD11b/CD18; CR3; Mac-1)[69]. The binding of LFA-1 to endothelial ICAM-1 provides the main bond strength for neutrophil firm adhesion[70,71]. The expression of ICAM-1 on endothelial cells is significantly upregulated in inflammation. Blocking LFA-1 or ICAM-1 significantly inhibits neutrophil adhesion and transmigration through endothelial layers[72]. The binding of LFA-1 to intercellular adhesion molecule 2 (ICAM-2) also enhances neutrophil adhesion, but the bond force is weaker compared to ICAM-1. LFA-1 also binds to JAM-1 on endothelial cells to promote neutrophil trans-endothelial migration. This will be introduced in the following chapter.

Mac-1[69] binds to ICAM-1, ICAM-2 and JAM-3 on the endothelial cells, glycoprotein Ib (GPIb) on the platelets[73], and fibrinogen, factor X and heparin. Mac-1 promotes neutrophil adhesion to endothelial cells directly by binding ICAM-1 and ICAM-2, but the bond strength is not as strong as LFA-1 - ICAM-1 binding. However, it binds also to adhered platelets[73] or fibrinogen[74], which deposit on the inflammatory or injured endothelial cells, and bridges the neutrophils efficiently to endothelial cells. That is the reason why Mac-1 influences leukocyte trans-endothelial migration and recruitment in inflammation significantly[73,74].

Integrin clustering on the cell membrane is dramatically induced by proinflammatory agonists[69]. As an example, LFA-1 and Mac-1 are trafficked and redistributed from intracellular vesicles or membrane to specific areas of the membrane and enhance local adhesion of neutrophils. The integrin endocytosis, trafficking and clustering on membrane employ Rho GTPase signaling and cytoskeleton system[75].

During the rolling phase, neutrophils interact with endothelial cells and platelets through the binding of PSGL-1 to P-selectin or E-selectin. As described previously[58,59] this binding modulates integrin conformation and subsequently upregulates the affinity of neutrophil integrins, including LFA-1 and Mac-1, to their ligands. In recent years many researchers demonstrated that the conformation modulation of integrins is regulated by the binding of cytoskeleton proteins to the β subunit cytoplasmic tail. For instance, the binding of talin1[76], talin2[77], vinculin[49], and kindlin 1-3[78] to β subunit cytoplasmic tail transforms the extracellular ‘head’ of integrins from bent to extension, which regulate the affinity of

integrins to their ligands from low to high. While filamin A interacts with integrin β subunit and competitively down-regulate talin-dependent integrin activation[79].

Besides the 'inside-out' signaling, integrins also function as receptors for the 'outside-in' signal[69,69-75]. The binding of integrins subsequently influences the small GTPase pathway, including the Ras-dependent MAP kinase pathway[80,81]and the Rho GTPase pathway[82] which regulate the intracellular cytoskeleton rearrangement[83,84], reactive oxygen intermediates (ROI) generation and release[84,85], and apoptosis[86]. Following cytoskeleton re-organization, the binding of integrins to specific ligands induces neutrophil polarization, spreading, and intraluminal crawling, which is the next step in the transmigration cascade. This 'outside-in' signaling is mainly induced by Mac-1, but not LFA-1[70].

1.2.4 Neutrophil crawling

After neutrophils adhere to the surface of activated endothelial cells, they start crawling continuously until they find the proper transmigration location[87]. The average leukocyte crawling distance is usually approximately 20μm-30μm from the adhesion point[87]. The intraluminal velocity of neutrophils is around 7.6 ± 0.4 μm/min[88] and the speed is even slower than neutrophils' motility speed in tissue after trans-endothelial migration, which is 15-20μm/min[89]. This suggests separate adhesion mechanisms play characteristic roles in different transmigration phase[90].

The crawling of neutrophils mainly depends on neutrophil integrin Mac-1, but not LFA-1[91,92]. Blocking Mac-1, but not LFA-1, reduces the neutrophils crawling significantly, and subsequently inhibits TNFα-induced neutrophils extravasation. During crawling neutrophil integrins attach to and detach from their ligands on endothelial cells to maintain the coordinated adhesion force[93].

Neutrophil crawling ends at the transmigration location. It is believed that endothelial ICAM-1 and ICAM-2 are important for ending neutrophils crawling and prompting transmigration. The slower crawling and trans-endothelial migration usually occur on special 'portals' where ICAM-1, but not P-selectin, is redistributed and enriched in a tricellular endothelial junctional area in inflammatory endothelial cells[87]. Blocking the extracellular domain of ICAM-1 strongly inhibits the sensing capacity of neutrophils to this portal. At the same time, ICAM-1 also works as a receptor to transduce signals

intracellularly to rearrange VE-Cadherin, which is critical for controlling leukocyte transmigration[87].

Halai K. et al.[94] demonstrated that ICAM-2 on the endothelial cells is also critical for neutrophil crawling whereby ICAM-2 blockade decreases crawling velocity, and prolongs crawling process prior to trans-endothelial migration. This suggests that ICAM-2 plays a similar role as ICAM-1, to lead neutrophils to the proper portal.

During neutrophil crawling, the characteristic locomotion is that neutrophils polarize to extend numerous tiny protrusions in the forward direction which is called the leading edge or the lamellipodia and to form the uropod in the back, as we described in 1.2.1. F-actin in the lamellipodia ae very dynamic structures undergoing rapid filament polymerization and depolymerization. Polymerized F-actin extends the cell body which push the local membrane forward to form the protrusion. It is the continuous F-actin polymerization and depolymerization that allow the cell to propel in the forward direction. Myosin is another key component involved in composing this dynamic network. Myosin contraction generates essential force to form the uropod and to push the cell forward during crawling[47]. As previously described the small GTPase family, including Cdc42, Rac, and RhoA play a fundamental role in this process.

1.2.5 Neutrophil trans-endothelial migration (TEM)

After neutrophils crawl to the suitable location, they transmigrate through the endothelium, a process termed ‘diapedesis’, in the paracellular pathway or transcellular pathway. Emigrating neutrophils cooperate with endothelial cells to compose a harmonized system to facilitate neutrophil transmigration as well as to control the leakage of other substances in the bloodstream simultaneously.

A particular structure named ‘the transmigration cup’ forms on endothelial cells during both paracellular and transcellular TEM[95,96]. ICAM-1 re-localizes intensively on the endothelial membrane, which protrudes by actin-rich filipodia and surrounds the neutrophils. Integrin LFA-1 on neutrophils coordinately clusters on the membrane where neutrophils contact with endothelial cells and robustly colocalizes with endothelial ICAM-1 cup-like protrusion. The interaction of LFA-1 and ICAM-1 subsequently phosphorylates VE-cadherin and loosens the endothelial junctions[22,23]. Most likely ICAM-2 plays a similar role and promotes neutrophil transmigration in this early step, since in ICAM-2$^{-/-}$ mice

neutrophils were trapped in the condition where they just started to penetrate the endothelial junction[97].

In the following step, neutrophil LFA-1 cooperates with JAM-1 which is redistributed efficiently to the necessary membrane contact and facilitates leukocytes transmigration through endothelial cells[24,25,98]. Blocking JAM-1 interferes with this process and leads to trapped neutrophils within the endothelial paracellular junction[97]. JAM-3 is critical for controlling the neutrophils reverse transmigration by binding to integrin Mac-1[27].

After neutrophils transmigrate through the endothelial cells, the basement membrane is the next anatomical layer to overstep. In this phase, platelet endothelial cell adhesion molecule-1 (PECAM-1)[97], CD99[99,100], and CD99L2[100,101] are critical molecules to support neutrophil migration. For instance, in PECAM-1 knockout mice this process is impaired and the neutrophils are stopped between endothelial cells and base membrane[97]. Similarly blocking CD99L2 in mice trapped neutrophils in the space between endothelial cells and basement membrane and the function of CD99L2 is independent of PECAM-1[100].

During neutrophil TEM, PECAM-1, JAMs, and CD99 in the endothelial cells are transported and redistributed into the target location in form of the lateral border recycling compartment (LBRC)[102,103]. LBRC is essentially invaginated junctional membrane and is transported by microtubules to efficiently traffick molecules to the neutrophils interacted membrane in endothelial cells[102]. Interfering microtubules function impaired the enrichment of PECAM-1 to the leukocyte interface in endothelial cells.

After neutrophils transmigrate through the endothelium, adjacent endothelial cells must be sewn together quickly and efficiently to prevent plasma leakage. VE-cadherin[103] is essential for this response and controls vascular permeability in inflammation.

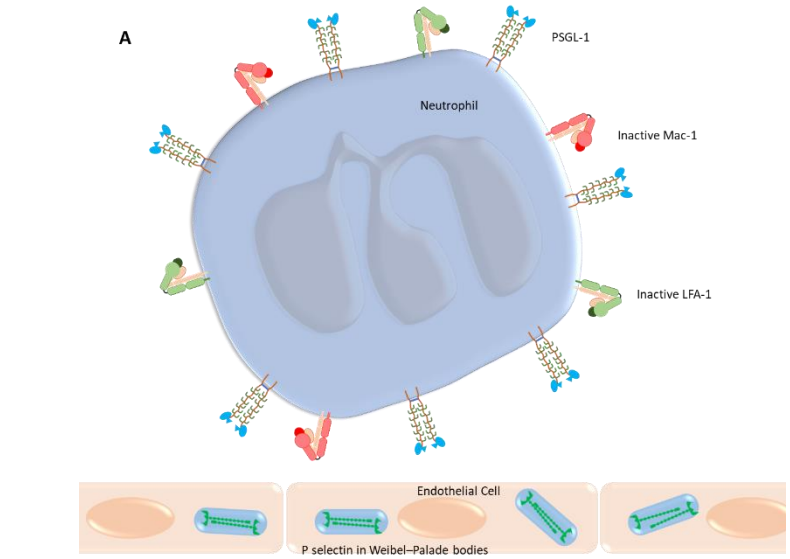
A
PSGL-1
Neutrophil
Inactive Mac-1
Inactive LFA-1
Endothelial Cell
P selectin in Weibel–Palade bodies

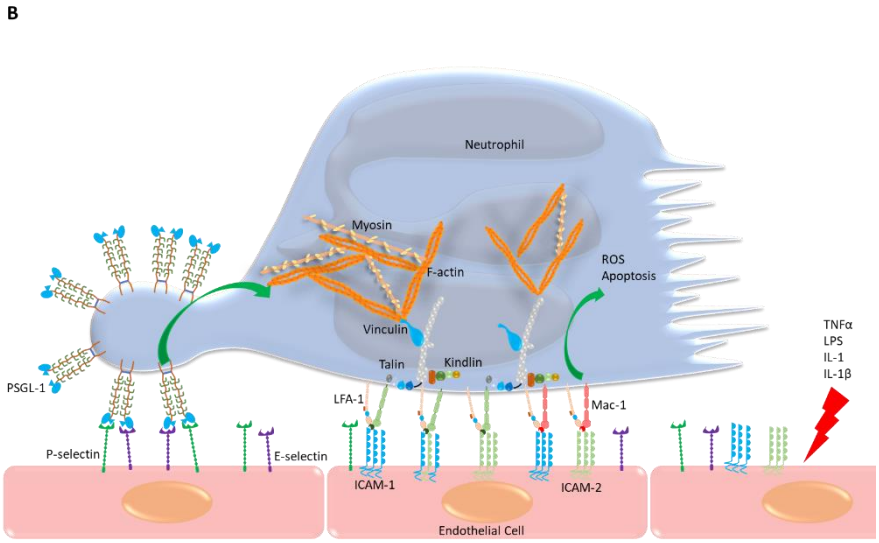
B
Neutrophil
Myosin
F-actin
ROS
Apoptosis
Vinculin
Talin
Kindlin
TNFα
LPS
IL-1
IL-1β
PSGL-1
LFA-1
Mac-1
P-selectin
E-selectin
ICAM-1
ICAM-2
Endothelial Cell

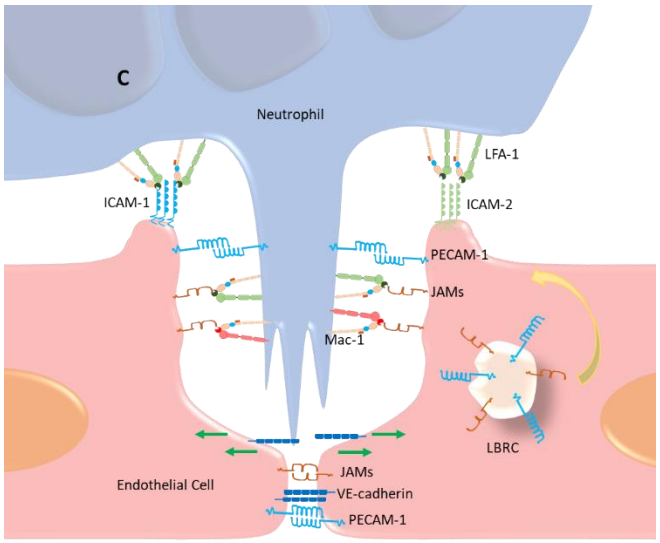
C
Neutrophil
LFA-1
ICAM-1
ICAM-2
PECAM-1
JAMs
Mac-1
LBRC
JAMs
VE-cadherin
PECAM-1
Endothelial Cell

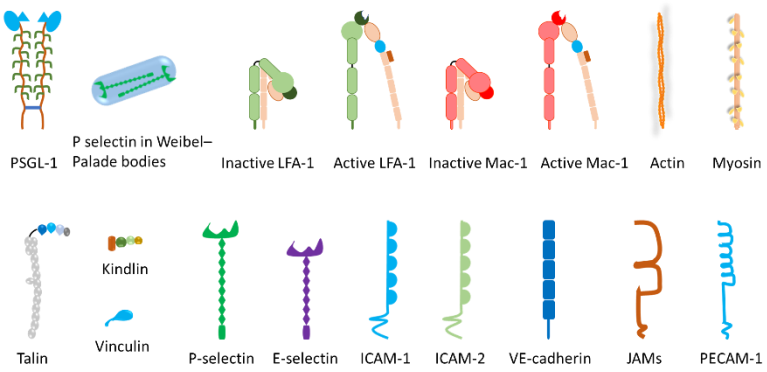

Figure 2. Schematic representation of neutrophil extravasation.

(A) In stationary condition PSGL-1 distributes evenly on neutrophil surface, and neutrophil integrins LFA-1 and Mac-1 are inactive. In endothelial cells P-selectin is storied in Weibel–Palade bodies and E-selectin is not expressed on cell surface. **(B)** In inflammatory condition, PSGL-1 redistributes and concentrates on the uropod membrane and binds to P-selectin on the endothelial cells. This binding activates intracellular cytoskeleton and vinculin, talins and kindlins which subsequently activate integrins LFA-1 and Mac-1 to upregulate the affinity of them towards ICAM-1 and ICAM-2 (Inside-out signal). Clustered ICAM-1 and ICAM-2 bind to Mac-1 and this process promotes neutrophils to apoptosis and produce ROS (Outside-in signal). The binding of LFA-1 and Mac-1 to ICAM-1 and ICAM-2 support neutrophils crawling on the endothelial cells to search for the proper transmigration location. **(C)** Endothelial cells form 'the transmigration cup' which intensively expressed ICAM-1 and ICAM-2 to promote neutrophil TEM. Integrin LFA-1 binds to ICAM-1, ICAM-2 and JAMs to loosen VE-cadherin binding between adjacent endothelial cells and assist neutrophils transmigration. Mac-1 cooperates with JAM-3 to inhibit neutrophil reverse transmigration. LBRC transports and redistributes PECAM-1 and JAMs into the target location to support neutrophil TEM.

1.2.6 Neutrophil effector functions

Once neutrophils extravasate and migrate to the target inflammatory site, they perform their principal duties which is efficiently killing invaded pathogenic microorganisms. To accomplish this challenging task, neutrophils are equipped with three effector functions: degranulation, phagocytosis, and formation of neutrophils extracellular traps (NETs)[104].

Mature differentiated human neutrophils contain four types of releasable membrane-bound vesicles, azurophil granules, specific granules, gelatinase granules and secretory vesicles[105]. Primary or azurophilic granules store myeloperoxidase (MPO), elastase, and other proteolytic and bactericidal proteins[106]. These enzymes and bactericidal proteins

can be released to the extracellular space for killing or digesting pathogens, but can also combine and decorate decondensed DNA to form the NET fibers and will be released to microbicidal vesicles during phagocytosis[107]. Contrarily, secondary or specific granules and third or gelatinase granules are both peroxidase-negative and contain mainly integrins like Mac-1, gelatinase (metalloprotease 9, MMP9), and leukolysin (metalloprotease 25, MMP25) which are critical for neutrophil adhesion and transmigration through endothelial layer and basement membrane. All of these proteins are synthesized when neutrophils are developed in bone marrow and can be released very fast without translational or transcriptional reaction[104]. Secretory vesicles are different from the three types of granules since they are much smaller and do not contain compact intensive proteins [105]. They are membranes combined with proteins such as Mac-1, complement receptor type 1 (CR1), CD16 and secretory carrier membrane protein (SCAMP)[105,108]. They integrate fast with the plasma membrane under stimulation and promote proteins to distribute and recruit to membrane efficiently[105].

After neutrophils sense pathogens and other inflammatory activators, the local membrane protrudes and forms ruffles[109]. Ruffles stretch out to contact pathogens and bind targets with receptors to trap them. Then the membrane protrusion collapses and coalesces to form membrane-bound intracellular vesicles named phagosomes. Primary granules merge with phagosomes to produce an enclosed microbicidal compartment containing reactive oxygen species (ROS), elastase, and other proteolytic and bactericidal proteins[107]. In this process, the intracellular cytoskeleton system, which is regulated by the Rho GTPase family, provides motility and transformation force[109].

The formation and release of NETs is another antimicrobial strategy of neutrophils[110]. Exposure to agonists such as LPS or PMA promotes the NOX enzyme to assemble and produce ROS in neutrophils. Subsequently, the granules membrane and nucleus membrane are broken down, followed by the release of MPO and neutrophil elastase (NE) from primary granules. MPO and NE then facilitate the citrullination of histones and chromatin de-condensation. Finally, the cytoplasmic membrane is disintegrated and enzyme-decorated DNA strains are released to extracellular space which can stick, trap and degrade pathogens efficiently[110]. In this NETosis process, the neutrophils will not survive, so it is called the suicide NETosis[111]. On the contrary, neutrophils can produce

NETs with part of their molecules and release them to extracellular space, named vital NETosis, and still are able to perform chemotaxis and phagocytosis after this process[112].

1.3 Sema4D and its receptors

Neuronal guidance proteins (NGPs), composed of netrins, Slit-2, neogenin, semaphorins, and plexins, were originally identified for their guidance function in growing axons[113]. They sense chemoattractive or chemorepulsive signals to induce the assembly or collapse of growth cones[114], suppress or promote the growth of axons and dendrites[115], modulate the synaptic contacts[116] and prune axons[117] to refine the neuronal circuits.

Semaphorins are evolutionarily conserved proteins, more than 30 members in 8 subclasses share one versatile extracellular sema domain which employs a 7-blade β-propeller structure[118,119]. Semaphorins in vertebrates include 20 proteins that belong to subclasses III to VII. Subclass III semaphorins (Sema3A-G) are secreted proteins, subclass IV, V, and VI are transmembrane molecules, and Semaphorin VII is connected to the membrane through a glycosylphosphatidylinositol (GPI) anchor[120]. Membrane binding semaphorins including subclass IV, V, VI, and VII, directly bind to plexin receptors through the extracellular sema domain to transduce signals. Plexins are structurally conserved receptors that comprise nine members in mammals which could be divided into four classes: class A (A1-A4), class B (B1-B3), PlexinC1, and PlexinD1[121]. They contain a Rho and Ras-family-specific GTPase-activating protein (GAP) domain in the cytoplasmic region which regulates the cytoskeleton arrangement[122] as downstream signals.

The actin cytoskeleton rearrangement fundamentally generates force for cell motility and is apparently crucial for cell shape change, migration, and contact with the extracellular matrix and other cells[123]. During the effective immune reaction, immune cells adopt all types of motility, including polarization, adhesion, and transmigration to eliminate invasive pathogens. Therefore, it is not astonishing that in recent years the function of neuronal guidance protein in regulating immune reaction is highlighted by tremendous research[113,120]. For instance, Sema3A is found to inhibit the proliferation and cytokines secretion of primary T-cells by upregulating the activation of the Ras family small GTPase Rap1[124]. Sema4A is also proven to promote T cell proliferation and increase cytokine production[125]. Our research group has shown that Sema7A is induced to express on

endothelial and epithelial cells during lung inflammation and facilitates neutrophil trans-endothelial migration (TEM)[126]. In myocardial ischemia-reperfusion injury, Sema7A enhances platelet-neutrophils complexes (PNCs) formation and facilitates the inflammation reaction[127].

My research project focuses on the function of Semaphorin 4D (Sema4D) in inflammation. Sema4D, a member of subclass IV of semaphorins, is a transmembrane protein expressed on various cell types, including neutrophils, T cells, B cells, platelets, monocytes and dendritic cells (DCs) in the immune system and can be found in the organs of brain, kidney, heart, and spleen[120,128-130]. It was initially recognized on human T lymphocytes as CD100[131] in 1992 and categorized as a member of the semaphorin family in 1996[132], and was the primary evidence for semaphorin expression in the immune system[128].

Sema4D[128,129] is composed of 862 amino acids and the molecular weight is 150 kDa. Structural analysis reveals that the extracellular region of Sema4D consists of a plexin-semaphorin-integrin domain, a sema domain, an Ig-like domain and a lysine-rich stretch, followed by the hydrophobic transmembrane region and a cytoplasmic tail which contains numerous tyrosine and serine phosphorylation sites. On the cell membrane, Sema4D exists as homodimers which are linked by disulfide bridging[133]. The extracellular region of Sema4D can be cleaved off to release a soluble form with a molecular weight of 120 kDa[134] and this exodomain cleavage is proceeded by metalloprotease ADAM17[135].

Sema4D links to its receptors PlexinB1 (PlxnB1), PlexinB2 (Plxnb2) and CD72[130,136]. The binding affinity of Sema4D to its different receptors seems various depending on the receptors-expressed cell types and cell condition[136]. For instance, B cells highly express CD72 as the receptor towards Sema4D[137], but not myeloid lineage cells. While PlxnB1 and PlxnB2 are highly expressed on T cells and myeloid lineage cells, including dendritic cells (DCs) and monocytes.

Tremendous research has demonstrated that Sema4D and its receptors play a critical function in the immune system. For example, Ponnat I. et al. proved that Sema4D binds to PlxnB1 on monocytes and DCs to impair the migration process[138]. Sema4D knockout mice recruit fewer macrophages to glomeruli in a foreign antigen-induced crescentic glomerulonephritis model and exhibit less activated T and B cells in lymph nodes[139].

Nishide M. et. al [130] illustrated that soluble Sema4D concentration rises in patients with antineutrophil cytoplasmic antibody (ANCA)-associated vasculitis (AAV), companied with a declined expression of Sema4D on neutrophils surface. Soluble Sema4D facilitates the inflammation of endothelial cells, while PlxnB2 on the endothelial cells binds to membranal Sema4D on the neutrophils and inhibits NET formation.

1.4 Aims of the project

As we described above, ARDS is a syndrome with extreme mortality and excessive public health impact. The research to identify effective prevention and treatment solutions for ARDS is of significant importance and meaning. Neutrophil recruitment plays a central role in the pathogenesis and progression of ARDS. Sema4D is a very promising candidate for its significant influences towards immune reactions in other diseases/models. However so far, only a few studies have illustrated the function of Sema4D in lung and inflammation. For this reason, in this project we will investigate whether Sema4D influences ARDS and the mechanism of its functions. In detail, we will figure out

2. Materials and Methods

2.1 General materials

Product name	Product No.	Company	Headquarter
Dulbecco's Phosphate Buffered Saline, -$CaCl_2$, -$MgCl_2$, $PBS^{-/-}$, 500ml	D8537-500ML	Sigma Aldrich	3050 Spruce Street, Saint Louis, MO 63103, U.S.A.
Dulbecco's Phosphate Buffered Saline, +$CaCl_2$, +$MgCl_2$, $PBS^{+/+}$, 500ml	D8662-500ML	Sigma Aldrich	3050 Spruce Street, Saint Louis, MO 63103, U.S.A.
Gibco™ RPMI Medium 1640, no Phenol red, 500ml	11835-063	Thermo Fisher Scientific Inc.	Neuhofstrasse 11, CH 4153 Reinach, Switzerland
Gibco™ Hanks´Balanced Salt Solution, -$CaCl_2$, -$MgCl_2$, $HBSS^{-/-}$, 500ml	14175-053	Thermo Fisher Scientific Inc.	Neuhofstrasse 11, CH 4153 Reinach, Switzerland
Gibco™ Hanks´Balanced Salt Solution, +$CaCl_2$, +$MgCl_2$, $HBSS^{+/+}$, 500ml	14025-050	Thermo Fisher Scientific Inc.	Neuhofstrasse 11, CH 4153 Reinach, Switzerland
Gibco™ PBS Tablets, Phosphate-buffered saline, -$CaCl_2$, -$MgCl_2$, 1×	18912-014	Thermo Fisher Scientific Inc.	Neuhofstrasse 11, CH 4153 Reinach, Switzerland
Sodium chloride physiological solution, tablet	231-598-3	Sigma Aldrich	3050 Spruce Street, Saint Louis, MO 63103, U.S.A.
Trizma™ base, Tris base	T1503-500G	Sigma Aldrich	3050 Spruce Street, Saint Louis, MO 63103, U.S.A.
Isotonic sodium chloride solution, NaCl, 0.9%, 20×10ml	2350748	B. Braun Melsungen AG	Carl-Braun-Str. 1, 34212, Melsungen, Germany
AQUA AD injectabilia, Mini-plasco connect	2351744	B. Braun Melsungen AG	Carl-Braun-Str. 1, 34212, Melsungen, Germany
Eppendorf® Safe-Lock Tubes, 0.5 ml, 1.5 ml, 2.0ml	30121023, 30120086, 30120094	Eppendorf	Barkhausenweg 1, 22339 Hamburg, Germany
Eppendorf® Tubes 5.0ml with snap cap	30119401	Eppendorf	Barkhausenweg 1, 22339 Hamburg, Germany
Corning Falcon 50 mL Conical Centrifuge Tubes	10788561, Corning 352070	Corning, Thermo Fisher Scientific Inc.	Neuhofstrasse 11, CH 4153 Reinach, Switzerland
Corning Falcon 15 mL Conical Centrifuge Tubes	11507411, Corning 352196	Corning, Thermo Fisher Scientific Inc.	Neuhofstrasse 11, CH 4153 Reinach, Switzerland
Eppendorf Combitips® advanced - positive displacement pipette tips, 1.0ml, 2.5ml, 5.0ml	0030089430 0030089650 0030089456	Eppendorf	Barkhausenweg 1, 22339 Hamburg, Germany
Eppendorf Multipette M4	4982000012	Eppendorf	Barkhausenweg 1, 22339 Hamburg, Germany
ROTH Reaction vials Mμlti® SafeSeal, colorless, 0.5 ml, 1.5ml, 2ml	7060.1 7080.1 7083.1	Carl Roth GmbH	Schoemperlenstr. 3-5, 76185 Karlsruhe, Germany

Product name	Product No.	Company	Headquarter
Pipette tip, transparent, PCR Performance Tested, 1000µl, 200µl	70.3060 70.3030	SARSTEDT AG & Co. KG	Sarstedtstraße 1, 51588 Nümbrecht , Germany
Pipette tip 10µl transparent	720011	Biozym Scientific GmbH	Steinbrinksweg 27, 31840 Hessisch, Oldendorf, Germany
Falcon® 5 mL Round Bottom Polystyrene Test Tube	352052	Corning, Thermo Fisher Scientific Inc.	Neuhofstrasse 11, CH 4153 Reinach, Switzerland
Corning™ Falcon™ Polystyrene Serological Pipets, Sterile 5ml, 10ml, 25ml	356543 356551 356525	Corning, Thermo Fisher Scientific Inc.	Neuhofstrasse 11, CH 4153 Reinach, Switzerland
Injekt, two-part disposable fine dosing single syringe, 1ml, 2ml, 5ml, 10ml, 20ml	9166017V 4606027V 4606051V 4606108V 4606205V	B. Braun Melsungen AG	Carl-Braun-Str. 1, 34212, Melsungen, Germany
Easystrainer for 50ml tubes, 70µm, 40µm	542070 542040	Greiner Bio-One International GmbH	Maybachstraße 2, 72636 Frickenhausen, Germany
SuperFrost Plus Adhesion slides	03-0060	Novoglas Labortechnik Langenbrinck	Stöckackerstr. 103 CH - 3018 Bern, Switzerland
Microscopical Cover Glasses, 24 x 32 mm, 24 x 50 mm, 24 x 60 mm,	01-2432/x 01-2450/x 01-2460/x	Novoglas Labortechnik Langenbrinck	Stöckackerstr. 103 CH - 3018 Bern, Switzerland
S-Monovette 10ml Citrat 3,2% syringe	02.1067.001	Sarstedt AG & Co. KG	Sarstedtstraße 1, 51588 Nümbrecht , Germany
S-Monovette® neutral 9 ml syringe	02.1726.021	Sarstedt AG & Co. KG	Sarstedtstraße 1, 51588 Nümbrecht , Germany
S-Monovette® Kalium-EDTA 2,7 ml	04.1915.100	Sarstedt AG & Co. KG	Sarstedtstraße 1, 51588 Nümbrecht , Germany
Safety-Multifly® needle, 21G x 3/4"	85.1638.235	Sarstedt AG & Co. KG	Sarstedtstraße 1, 51588 Nümbrecht , Germany
Ethylenediaminetetraacetic acid tetrasodium salt hydrate, EDTA	ED4S	Sigma Aldrich	3050 Spruce Street, Saint Louis, MO 63103, U.S.A.
Sodium azide, NaN_3	S8032	Sigma Aldrich	3050 Spruce Street, Saint Louis, MO 63103, U.S.A.
Trypan Blue solution	T8154	Sigma Aldrich	3050 Spruce Street, Saint Louis, MO 63103, U.S.A.
Natriumhydrogencarbonat, NaHCO3	1.06329.0500	Sigma Aldrich	3050 Spruce Street, Saint Louis, MO 63103, U.S.A.
Ammonium chloride, NH_4Cl	A9434	Sigma Aldrich	3050 Spruce Street, Saint Louis, MO 63103, U.S.A.

Product name	Product No.	Company	Headquarter
Heparin-Natrium-25000-Ratiopharm	N68542.03	Ratiopharm GmbH	Graf-Arco-Straße 3, D-89079 Ulm, Germany
Bovine Serum Albumin, BSA	A3294-100G	Sigma Aldrich	3050 Spruce Street, Saint Louis, MO 63103, U.S.A.
FBS superior	S0615	Sigma Aldrich	3050 Spruce Street, Saint Louis, MO 63103, U.S.A.
Heraeus Megafuge 1.0R Centrifuge	05718	Thermo Fisher Scientific Inc.	Neuhofstrasse 11, CH 4153 Reinach, Switzerland
Eppendorf Centrifuge 5417 R	5417 R	Eppendorf	Barkhausenweg 1, 22339 Hamburg, Germany
Incubator with shaker	Infors AG CH-4103	Infors AG	Rittergasse 27 CH-4103 Bottmingen, Switzerland
BD FACS CantoTM II Flow Cytometry System	BD FACS Canto™ II	BD biosciences	2350 QUME DR, San Jose, California, U.S.A.
Confocal microscope Stellaris 8	SP8	Leica Mikrosysteme Vertrieb GmbH	Ernst-Leitz-Strasse 17-37 Wetzlar, 35578, Germany

2.2 Methods and specific materials

2.2.1 Flow chamber

Product name	Product No.	Company	Headquarter
SuperFrost Plus Adhesion slides	03-0060	Novoglas Labortechnik Langenbrinck	Stöckackerstr. 103 CH - 3018 Bern, Switzerland
Microscopical Cover Glasses, 24 x 32 mm,	01-2432/x	Novoglas Labortechnik Langenbrinck	Stöckackerstr. 103 CH - 3018 Bern, Switzerland
Rectangle Boro Tubing, 0.02×0.20mm	5002-600	CM Scientific Ryefield (EU) Ltd, VitroCom	GD House, Whitestown Drive, Tallaght Business Park Dublin, D24 FR60, Republic of Ireland
Recombinant Human E-selecin/CD62E, rh E-selectin	724-ES	R&D Systems, Inc. Bio-Techne.	614 McKinley Place NE Minneapolis, MN 55413, U.S.A.
fibrinogen from human plasma	F4883	Sigma Aldrich	3050 Spruce Street, Saint Louis, MO 63103, U.S.A.
Recombinant Human Semaphorin 4D Fc Chimera Protein, rhSEMA4D FC.	7470-S4	R&D Systems, Inc. Bio-Techne.	614 McKinley Place NE Minneapolis, MN 55413, U.S.A.
Leitz wetzlar microscope	D64600	Leica Mikrosysteme Vertrieb GmbH	Ernst-Leitz-Strasse 17-37 Wetzlar, 35578, Germany
Hamamatsu Orca R2 Digital camera	C10600, Orca R2	Hamamatsu Photonics K. K	325-6, Sunayama-cho, Naka-ku, Hamamatsu City, Shizuoka Pref., 430-8587, Japan

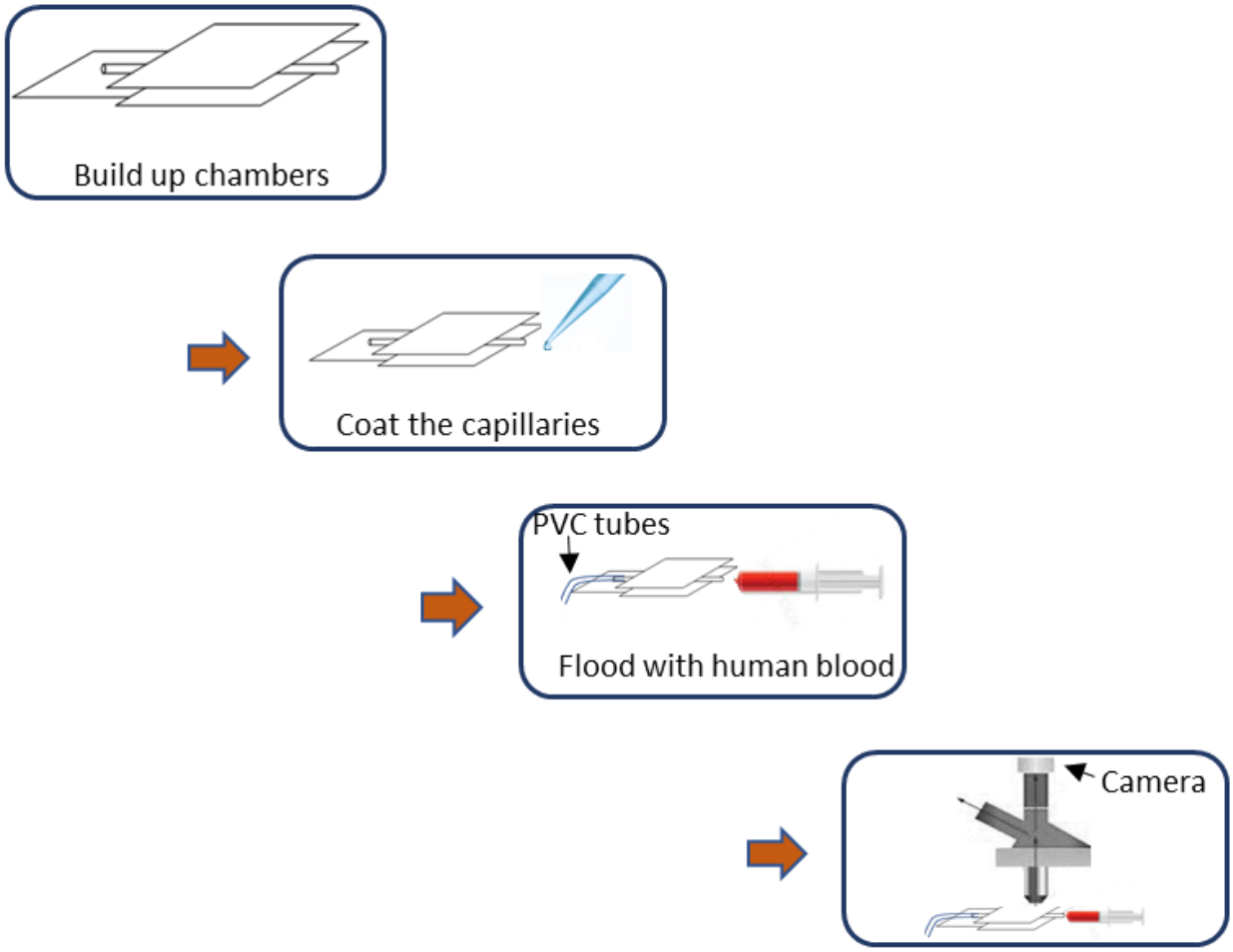

Figure 3. Schematic diagram of the flow chamber experiment.

Flow chamber experiments were performed as shown in Figure 1. The chambers were built on object slides fastening the capillary, a glass tubing (0.02×0.20 mm, VitroCom, 5002-600) which was cut to pieces in the length of 35mm. After the chambers were fixed, the capillary was coated for 2 hours at Room Temperature (RT) with 3.0 µg/ml E-selectin (Recombinant Human E-selectin/CD62E, R&D, 724-ES), with or without 100 µg/ml fibrinogen (from human plasma, SIGMA, F4883), with or without 2 µg/ml SEMA4D (rhSEMA4D FC, R&D, 7470-S4). The PVC tubes were fractionally filled with NaCl and connected to the glass capillaries to avoid capillary dryness and to produce the force for the flowing later. Consequently, the capillary was coated again with 10% casein in NaCl for blocking and incubated for an hour at RT. Human blood was drawn from healthy donors with S-Monovette syringe containing heparin for anti-coagulation (1 ml blood with 10 units heparin). Whole blood was stimulated with 10 ng/ml fMLP (N-FORMYL-MET-LEU-PHE, SIGMA, F3506) at 37^{o}C if necessary. Then, the flow chamber was mounted onto a Leitz Wetzlar microscope with a 20× lens (NA=0.32). The blood was flowed through the

capillary, observed under the microscope, and the videos were recorded with a black-and-white Hamamatsu Orca R2 digital camera (C10600, Hamamatsu). Each video was recorded for 10 seconds and later analyzed manually using Nikon 'NIS-Elements AR420:02 64bit' software.

2.2.2 Isolation of neutrophils from human blood with Percoll-based density gradient

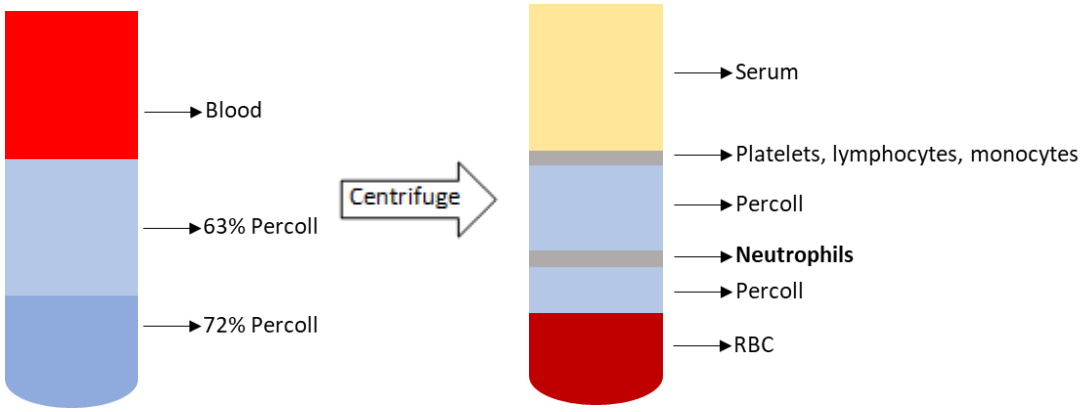

Figure 4. Scheme of neutrophil isolation with Percoll-based density gradient.

Product name	Product No.	Company	Headquarter
Percoll cytiva	17089101	Scientific Laboratory Supplies Ltd	Orchard House, The Square, East Yorkshire Hessle, HU13 0AE United Kingdom
Ammonium chloride, NH_4Cl	A9434	Sigma Aldrich	3050 Spruce Street, Saint Louis, MO 63103, U.S.A.
Ethylenediaminetetraacetic acid tetrasodium salt hydrate, EDTA	ED4S	Sigma Aldrich	3050 Spruce Street, Saint Louis, MO 63103, U.S.A.
Natriumhydrogencarbonat, NaHCO3	1.06329.0500	Sigma Aldrich	3050 Spruce Street, Saint Louis, MO 63103, U.S.A.

Human blood was drawn with S-Monovette blood collection system with trisodium citrate solution (10 % of nominal volume) for anti-coagulation and was cooled down to RT. 4 ml of the 72% Percoll (Cytiva, Scientific Laboratory Supplies Ltd, 17089101, 1.130 g/ml. Percoll 36 ml + $PBS^{-/-}$ 10x 4 ml + $PBS^{-/-}$ 1x 10 ml) was pipetted into 10 ml plastic tubes, then 4 ml 63% Percoll solution (Percoll 31.5 ml + $PBS^{-/-}$ 10x 3.5 ml + $PBS^{-/-}$ 1x 15 ml) was overlaid without mixing the interface. 4 ml of human whole blood was pipetted on top of Percoll as shown in Figure 2. The percoll-blood tubes were centrifuged at 1700 rpm, 25°C for 29 minutes without brake. After centrifugation the blood components were separated and distributed as shown in Figure 2. The upper waste (serum + platelets) was taken out carefully and discarded. The neutrophils under the Percoll layer was collected into a 50

mL falcon tube (on ice). The RBCs in the neutrophil fraction were lysed with ice-cold 'Erythrocyte Lyse Buffer' (8 g NH_4Cl + 840 mg $NaHCO_3$ + 37 mg EDTA in 1 Liter deionized water (dH_2O)) for 10 minutes on ice. Then the sample was centrifuged with 1300 rpm for 10 minutes at 4°C (with brake). The lysis buffer was poured out and the neutrophil pellet was resuspended with 10ml $HBSS^-$. 10µl of cells were diluted with Trypan Blue (SIGMA, T8154) for cell counting. The remaining cells were washed in final volume of 50 ml $HBSS^{-/-}$.The neutrophils were spun down again and adjusted to the proper concentration according to the following experiments.

2.2.3 Isolation of neutrophils with Magnetic-activated cell sorting (MACS) system

Product name	Product No.	Company	Headquarter
BD Lysing buffer 10X	555899	BD Biosciences	Tullastrasse 8-12, 69126 Heidelberg, Germany
Trypan blue solution	T8154	Sigma Aldrich	3050 Spruce Street, Saint Louis, MO 63103, U.S.A.
CD15 MACSiBeads Kit, human	130-093-580	Miltenyi Biotec B.V. & Co. KG	Friedrich-Ebert-Straße 68, 51429 Bergisch, Gladbach, Germany
MACS LS Columns	130-042-401	Miltenyi Biotec B.V. & Co. KG	Friedrich-Ebert-Straße 68, 51429 Bergisch, Gladbach, Germany
MidiMACS separators	130-042-302	Miltenyi Biotec B.V. & Co. KG	Friedrich-Ebert-Straße 68, 51429 Bergisch, Gladbach, Germany

MACS-wash-buffer ($PBS^{-/-}$ 500 ml + 2.5 g BSA + 380 mg EDTA) was prepared 2 hours before experiment and pre-warmed to 37 °C. Human whole blood was collected in a heparin-coated syringes (1ml blood with 10 Unit heparin) and mixed gently. Then 5 ml blood was added to 45ml pre-warmed erythrocyte lysing buffer (BD Pharm Lyse, 10*, diluted 1:10 with dH_2O) and incubated for 2 minutes at RT, followed by centrifugation at 4 °C, 500 g for 10 minutes. The supernatant was poured out and the pellet was resuspended in 3 ml MACS-wash buffer and mixed gently, followed by another centrifugation. The pellet was re-suspended with 1 ml MACS-wash-buffer and the number of cells was acquired under the microscope using Trypan blue (Sigma Aldrich, T8154) staining. Anti-CD15 MicroBeads (Miltenyi Biotec, 130-046-601) were added to the leukocyte suspension (20 µl per 10^7 cells), followed by a gentle mix, and incubation for 15 minutes at 4 °C. During the incubation time, the LS column (Miltenyi Biotec, 130-042-401) was fixed to MidiMACS separators (Miltenyi Biotec, 130-042-302) and rinsed 3 times with 3 ml MACS-wash-buffer. After incubation, 3 ml MACS-wash-buffer was added to anti-CD15 - MicroBeads

leukocytes mixture for washing, followed by centrifuging and resuspending with another 3 ml MACS-wash-buffer. The leukocyte - anti-CD15 MicroBeads mix was loaded on prepared LS column and flown through, followed by 3-5 times rinsing with 3 ml warm MACS-wash buffer. Then the LS column was disconnected from the MidiMACS separator and flushed immediately with 3 ml MACS-wash-buffer to flush neutrophils out of the column and collect them. The neutrophil suspension obtained was centrifuged again and adjusted to the correct concentration according to the following experiments.

2.2.4 Flow cytometry for fibrinogen binding assay

Product name	Product No.	Company	Headquarter
N-Formyl-Met-Leu-Phe, fMLP	F3506	Sigma Aldrich	3050 Spruce Street, Saint Louis, MO 63103, U.S.A.
Recombinant Human Semaphorin 4D Fc Chimera Protein, rhSEMA4D FC.	7470-S4	R&D Systems, Inc. Bio-Techne.	614 McKinley Place NE Minneapolis, MN 55413, U.S.A.
Fibrinogen from Human Plasma, Alexa Fluor™ 647 Conjugate	F35200	Thermo Fisher Scientific Inc.	Neuhofstrasse 11, CH 4153 Reinach, Switzerland
CellFix™ Tissue Processing Reagent, BD	340181	Thermo Fisher Scientific	Neuhofstrasse 11, CH 4153 Reinach, Switzerland
Mouse-anti-Human CD18 (Activation Epitope) FITC	MCA2086F	Bio-Rad Laboratories GmbH	1000 Alfred Nobel Drive Hercules, California 94547, U.S.A.
Brilliant Violet 421™ anti-human CD11b Antibody	301324	Biolegend	8999 BioLegend Way, San Diego, CA 92121, U.S.A.

Human neutrophils were isolated with the MACS system as mentioned in 2.2.3. In 100 µl RPMI medium $2x10^5$ neutrophils were incubated with 10 ng/ml fMLP (N-Formyl-Met-Leu-Phe, Sigma, F3506) or PBS as control, with or without 2.5 µg/ml rhSEMA4D (rhSEMA4D FC, R&D, 7470-S4), together with human Fibrinogen-Alexa Fluor 647 (Thermo Fisher, F35200) 10 µl for 5 minutes at 37 °C. After incubation, neutrophils were immediately put on ice, and fixed with 100 µl CellFix (Tissue Processing Reagent, BD, 340181) for 10 minutes. Then neutrophils were washed with 2 ml FACS buffer ($PBS^{-/-}$ + 1% BSA + 2 mM/L EDTA + 2 mM/L NaN_3) on ice and centrifuged with 500 g for 10 minutes at 4 °C. For the next step, the antibody cocktail (if necessary, FITC - CD18a antibody, MCA 2086F, BioRad; Brilliant Violet 421 - CD11b antibody, 301324, BioLegend) was added to neutrophils and incubated for 30 minutes on ice. After washing with 2 ml FACS buffer, the neutrophils were resuspended into 300 µl FACS buffer, and measured by Flow cytometry.

The experiment used a BD FACS Canto™ II running the BD FACS Diva™ software. The data were analyzed with the software FlowJo V10.0.8.

2.2.5 Expression of integrins on human neutrophils by flow cytometry

Product name	Product No.	Company	Headquarter
Alexa Fluor® 488 anti-human CD11a/CD18 (LFA-1) antibody	363404	BioLegend	8999 BioLegend Way, San Diego, CA 92121, U.S.A.
Brilliant Violet 421™ anti-human CD11b antibody	301324	Biolegend	8999 BioLegend Way, San Diego, CA 92121, U.S.A.
PerCP/Cyanine5.5 anti-human CD49d antibody	304312	Biolegend	8999 BioLegend Way, San Diego, CA 92121, U.S.A.
Recombinant Human Semaphorin 4D Fc, rhSEMA4D FC	7470-S4	R&D Systems, Inc. Bio-Techne	614 McKinley Place NE Minneapolis, MN 55413, U.S.A.
N-Formyl-Met-Leu-Phe, fMLP	F3506	Sigma Aldrich	3050 Spruce Street, Saint Louis, MO 63103, U.S.A.
BD Lysing buffer 10X	555899	BD Biosciences	Tullastrasse 8-12, 69126 Heidelberg, Germany
CellFix™ Tissue Processing Reagent, BD	340181	Thermo Fisher Scientific	Neuhofstrasse 11, CH 4153 Reinach, Switzerland

Human blood was drawn with S-Monovette blood collection system with trisodium citrate solution for anticoagulation. Antibodies (Alexa Fluor 488 – LFA-1 antibody, 363404, BioLegend; Brilliant Violet 421 - CD11b antibody, 301324, BioLegend; PerCp - Cy5.5 - CD49d antibody, 304312, BioLegend) were added to tubes first, then 100 µl whole blood was added, followed by adding rhSEMA4D 2.5 µg/ml (rhSEMA4D FC, R&D, 7470-S4) and / or 10 ng/ml fMLP (N-Formyl-Met-Leu-Phe, Sigma, F3506). The tubes were briefly vortexed for mixing and then incubated at 37 ºC for 30 minutes. After incubation, the erythrocytes in the blood sample were lysed for 2 minutes with 2 ml pre-warmed BD lysis buffer (BD Lysing buffer 10x, BD, 555899, pre-diluted 1:10 with dH_2O), followed by centrifugation with 400 g for 5 minutes at 4 ºC. The supernatant was discarded and 100 µl warm fix buffer (Tissue Processing Reagent, BD, Thermo Fisher Scientific, 340181) was added to fix the neutrophils for 10 minutes at RT. After washing with 2 ml FACS buffer, the neutrophils were resuspended in 1 ml FACS buffer and measured by flow cytometry. For the experiment we used a BD FACS Canto™ II running with BD FACS Diva™ software. The data were analyzed with software FlowJo V10.0.8.

2.2.6 Chemotaxis assay

Product name	Product No.	Company	Headquarter
Chemotaxis chamber	80326	Ibidi GmbH	Am Klopferspitz 19, 82152 Martinsried, Germany.
Type I Bovine Collagen solution	5005-100ml	Advanced BioMatrix, Inc.	5930 Sea Lion Place, Carlsbad, CA 92010, U.S.A.

Product name	Product No.	Company	Headquarter
Human PlexinB1 antibody	MAB3749	R&D Systems, Inc. Bio-Techne	614 McKinley Place NE Minneapolis, MN 55413, U.S.A.
Human PlexinB2 antibody	MAB5329	R&D Systems, Inc. Bio-Techne.	614 McKinley Place NE Minneapolis, MN 55413, U.S.A.
Recombinant Human Semaphorin 4D Fc, rhSEMA4D FC.	7470-S4	R&D Systems, Inc. Bio-Techne.	614 McKinley Place NE Minneapolis, MN 55413, U.S.A.
FBS superior	S0615	Sigma Aldrich	3050 Spruce Street, Saint Louis, MO 63103, U.S.A.
N-Formyl-Met-Leu-Phe, fMLP	F3506	Sigma Aldrich	3050 Spruce Street, Saint Louis, MO 63103, U.S.A.
CellFix™ Tissue Processing Reagent, BD	340181	Thermo Fisher Scientific	Neuhofstrasse 11, CH 4153 Reinach, Switzerland

Chemotaxis chambers (ibidi, µ-Slide, Chemotaxis, 80326) were coated with 100 µg/ml Collagen I (PureCol, 5005) at RT overnight and washed with $HBSS^-$ once before use. Neutrophils were isolated from human whole blood with the Percoll-based density gradient method as mentioned in 2.2.2 and were resuspended in $HBSS^+$ to $1x10^7$ /ml, then pre-incubated with or without anti-PlxnB1 (Human PlexinB1 antibody, 10 µg/ml, R&D, MAB3749) or anti-PlxnB2 (Human PlexinB2 antibody, 10 µg/ml, R&D, MAB5329) antibody for 30 minutes at 37 °C. In the following step the mixture was incubated with or without rhSEMA4D 1 µg/ml (rhSEMA4D FC, R&D, 7470-S4) for 30 minutes at 37 °C. Both side chambers were filled with 70µl RPMI + 10 % FBS and the middle chambers were filled with 10 µl RPMI + 10 % FBS. The pre-incubated neutrophils were diluted to 3×10^6 /L in RPMI + 10 % FBS and 10 µl was added to the middle chamber again. The chambers were incubated at 37 °C for 30 minutes to settle down neutrophils and then the buffer in the left side chambers was replaced with 70 µl RPMI + 10 % FBS with 10 ng/ml fMLP (N-Formyl-Met-Leu-Phe, Sigma, F3506) for chemotaxis. In the next step, neutrophils were observed with a Zeiss confocal microscopy and recorded with a Orca R^2 digital camera. The videos were analyzed manually with 'NIS-Elements AR Analysis 4.20.00 64-bit' software. For immunofluorescence staining, neutrophils were incubated for 15 minutes at 37 °C, followed by fixation with BD CellFix (Tissue Processing Reagent, BD, 340181) for 10 minutes on ice. After washing once with $HBSS^-$, the chambers were dried at 60 °C for 30 minutes.

2.2.7 Immunofluorescence for PSGL-1 and CD11b on human neutrophils in chemotaxis

Product name	Product No.	Company	Headquarter
Tween® 20 for molecular biology	A4974	AppliChem GmbH	Ottoweg 4, D-64291, Darmstadt, Germany
normal goat serum	S-1000	Vector Laboratories	6737 Mowry Ave Newark, CA 94560 United States
Bovine Serum Albumin	A3294-100G	Sigma Aldrich	3050 Spruce Street, Saint Louis, MO 63103, U.S.A.
Purified anti-mouse / human CD11b Antibody	101202	Biolegend	8999 BioLegend Way, San Diego, CA 92121, U.S.A.
normal rat IgG	sc-2026	Santa Cruz Biotechnology, Inc.	10410 Finnell Street Dallas, Texas, 75220 U.S.A.
Goat anti-Rat antibody Alexa Fluor™ 546	A11081	Invitrogen, Thermo Fisher Scientific	Neuhofstrasse 11, CH 4153 Reinach, Switzerland
normal donkey serum	ab7475	abcam	Bertha-Benz-Straße 5, 10557 Berlin, Germany
Purified anti-human CD162 Antibody	328802	Biolegend	8999 BioLegend Way, San Diego, CA 92121, U.S.A.
normal mouse IgG	sc-2025	Santa Cruz Biotechnology, Inc.	10410 Finnell Street Dallas, Texas, 75220 U.S.A.
Donkey anti-Mouse Antibody, Alexa Fluor™ 488	A21202	Invitrogen, Thermo Fisher Scientific	Neuhofstrasse 11, CH 4153 Reinach, Switzerland
ROTI® Mount FluorCare DAPI	HP20.1	Carl Roth GmbH	Schoemperlenstr. 3-5, 76185 Karlsruhe, Germany
Confocal microscope Stellaris 8	SP8	Leica Mikrosysteme Vertrieb GmbH	Ernst-Leitz-Strasse 17-37 Wetzlar, 35578, Germany

Human neutrophils were isolated, stimulated and fixed in the chemotaxis chamber as described before in 2.2.6. Neutrophils were washed with 0.1% Tween (Tween® 20 for molecular biology, AppliChem, A4974) in PBS for 5 minutes 3 times and then directly blocked with 5 % normal goat serum in 5 % BSA + 0.1 % Tween in PBS at RT for an hour to reduce unspecific staining. Anti-human CD11b antibody (purified anti-mouse / human CD11b antibody, BioLegend, 101202) or rat IgG (Santa Cruz, sc-2026) as control or blank for second antibody control, was diluted to 10 µg/ml with 1 % BSA + 0.1 % Tween in PBS and was added to neutrophils for incubation at 4 ^{o}C in humid chamber overnight. On the second day, neutrophils were washed with 0.1 % Tween in PBS for 5 minutes 3 times first, followed by incubation with anti-rat second antibody Alexa Flour 546 (Goat anti-Rat antibody Alexa Fluor™ 546, Invitrogen, A11081) which was diluted with 1 % BSA + 0.1 % Tween in PBS for 60 minutes at RT in a dark humid chamber. After incubation neutrophils were washed with 0.1 % Tween in PBS for 5 minutes 3 times and then incubated with 5 % normal serum donkey + 5 % BSA + 0.1 % Tween in PBS for an hour at RT for blocking. Subsequently, anti-human PSGL-1/CD162 antibody (purified mouse-anti-human CD162

antibody, Biolegend, 328802) or mouse IgG (Santa Cruz, sc-2025) as control or blank as 2nd antibody control was diluted with 1 % BSA + 0.1 % Tween in PBS and added to neutrophils to incubate at RT for an hour in a dark humid chamber. After washing with 0.1 % Tween in PBS for 5 minutes 3 times, anti-mouse Alexa 488 antibody (Donkey anti-Mouse antibody, Alexa Fluor™ 488, Invitrogen, A21202) was diluted with 1 % BSA + 0.1% Tween in PBS and incubated together with neutrophils for 60 minutes at RT in a dark humid chamber. Then neutrophils were washed with 0.1 % Tween in PBS for 5 minutes 3 times and ROTI® Mount FluorCare DAPI (4′,6-diamidino-2-phenylindole (DAPI), Carl Roth, HP20.1) was added to the chambers. The filling cups were then sealed using nail polish and dried in dark at RT for 2 hours and stored at 4 °C in the dark. The micrographs were acquired on a Leica SP8 Stellaris confocal microscope and analyzed and processed with the software Leica Application Suite X.

2.2.8 Length width ratio of human neutrophils

The human neutrophils were isolated and stained in the chemotaxis chamber as described in 2.2.6 and 2.2.7. The length of the neutrophil was determined as the length of the major axis which connected the two furthest poles of the neutrophil. The width of the neutrophil was determined as the length of the shortest minor axis which must pass the middle point of the major axis. The length-width ratio was defined by the length of neutrophils divided by the width of neutrophils.

2.2.9 Immunofluorescence for RhoA and F-actin on human neutrophils in chemotaxis

Product name	Product No.	Company	Headquarter
Tween® 20 for molecular biology	A4974	AppliChem GmbH	Ottoweg 4, D-64291, Darmstadt, Germany
Triton® X-100	X 100 – 100ML	Sigma Aldrich	3050 Spruce Street, Saint Louis, MO 63103, U.S.A.
normal donkey serum	ab7475	abcam	Bertha-Benz-Straße 5, 10557 Berlin, Germany
Recombinant Anti-RhoA antibody [EPR18134]	ab187027	abcam	Bertha-Benz-Straße 5, 10557 Berlin, Germany
Rabbit IgG Isotype Control	31235	Thermo Fisher Scientific	Neuhofstrasse 11, CH 4153 Reinach, Switzerland
Donkey anti-Rabbit Second Antibody Alexa Fluor™ Plus 488	A32790	Invitrogen, Thermo Fisher Scientific	Neuhofstrasse 11, CH 4153 Reinach, Switzerland

Product name	Product No.	Company	Headquarter
rhodamine Phalloidin	R415	Thermo Fisher Scientific	Neuhofstrasse 11, CH 4153 Reinach, Switzerland
ROTI® Mount FluorCare DAPI	HP20.1	Carl Roth GmbH	Schoemperlenstr. 3-5, 76185 Karlsruhe, Germany
Confocal microscope Stellaris 8	SP8	Leica Mikrosysteme Vertrieb GmbH	Ernst-Leitz-Strasse 17-37, Wetzlar, 35578, Germany

Human neutrophils were isolated, stimulated and fixed in the chemotaxis chamber as described in 2.2.6. Neutrophils were washed with 0.1 % Tween (Tween® 20 for molecular biology, AppliChem, A4974) in PBS for 5 minutes twice and then permeabilized with 0.5 % Triton® X-100 (Sigma, X 100 - 100ml) in PBS for 5 minutes on ice, following 3 times washing with 0.1 % Tween in PBS. Then the slides were blocked with 5 % normal donkey serum in 5 % BSA + 0.1 % Tween in PBS at RT for an hour to block unspecific staining. Anti - human, RhoA antibody (rabbit anti-human RhoA antibody, abcam, ab187027) or IgG (rabbit IgG isotype control, Thermo Fisher, 31235) as control or blank for second antibody control, was diluted to 8.3 µg/ml with 1 % BSA + 0.1 % Tween in PBS and added to neutrophils for incubation at 4 ^{o}C in humid chambers overnight. On the second day, neutrophils were washed with 0.1 % Tween in PBS for 5 minutes 3 times, followed by incubation with anti - rabbit second antibody Alexa488 (Alexa Fluor™ Plus 488 donkey anti-rabbit second antibody, A32790, Invitrogen) in 1 % BSA + 0.1 % Tween in PBS for 40 minutes at RT in a dark humid chamber. After incubation neutrophils were washed with 0.1 % Tween in PBS for 5 minutes 3 times and then incubated with 5 % BSA + 0.1 % Tween in PBS for an hour at RT for blocking. Subsequently neutrophils were incubated with 5 µg/ml rhodamine Phalloidin (Thermo Fisher, R415) for 20 minutes at RT in a dark humid chamber. Then neutrophils were washed with 0.1 % Tween in PBS for 5 minutes 3 times and ROTI® Mount FluorCare DAPI (Carl Roth, HP20.1) was added. Following the chambers were sealed with nail polish and dried in dark at RT for 2 hours and stored at 4 ^{o}C in the darkness. The micrographs were acquired on a Leica SP8 Stellaris confocal microscope and analyzed the Leica software Application Suite X.

2.2.10 Immunofluorescence for RhoA and F-actin on human neutrophils in the homogeneous concentration of fMLP

Product name	Product No.	Company	Headquarter
Recombinant Human Semaphorin 4D Fc, rhSEMA4D FC	7470-S4	R&D Systems, Inc. Bio-Techne	614 McKinley Place NE Minneapolis, MN 55413, U.S.A.
N-Formyl-Met-Leu-Phe, fMLP	F3506	Sigma Aldrich	3050 Spruce Street, Saint Louis, MO 63103, U.S.A.
ROTI® Mount FluorCare DAPI	HP20.1	Carl Roth GmbH	Schoemperlenstr. 3-5, 76185 Karlsruhe, Germany
Confocal microscope Stellaris 8	SP8	Leica Mikrosysteme Vertrieb GmbH	Ernst-Leitz-Strasse 17-37 Wetzlar, 35578, Germany

Human neutrophils were isolated with the MACS system as mentioned in 2.2.3 and resuspended to 4 x 10^7 /ml. 1 x 10^6 neutrophils (50 µl) were stimulated in 100 µl $HBSS^+$ with or without 1 µg/ml Sema4D (rhSEMA4D FC, R&D, 7470-S4) for 30 minutes and with or without 10 ng/ml fMLP (N-Formyl-Met-Leu-Phe, Sigma, F3506) for 15 minutes at 37 °C. After incubation neutrophils were washed with 1 ml NaCl and then centrifuged down at 1300 rpm for 10 minutes at RT. Then neutrophil pellets were resuspended and fixed with 4 % PFA 1.5 ml for 5 minutes. After centrifuging with 1300 rpm for 10 minutes RT, neutrophils pellets were then resuspended with 500 µl NaCl and each 50 µl were dropped onto triethoxysilan pretreated slides and dried on a hot plate at 60 °C for 10 minutes. The immunofluorescence staining protocol described in 2.2.9 was used. After the neutrophils were washed with 0.1 % Tween in PBS for 5 minutes 3 times, in the last step ROTI Mount FluorCare DAPI (Carl Roth, HP20.1) was added to the slides and the coverslips were mounted. The slides were dried in dark at RT for 2 hours and stored at 4 °C. The micrographs were acquired on a Leica SP8 Stellaris confocal microscope and analyzed with Leica software Application Suite X.

2.2.11 Proteomics analysis

Neutrophils were isolated from human whole blood with the Percoll-based density gradient method as mentioned in 2.2.2 and were resuspended in $HBSS^+$ to 1 x 10^7 /ml. Subsequently neutrophils were preincubated in 1 µg/ml SEMA4D (rhSEMA4D Fc, R&D, 7470-S4) for 30 minutes at 37 °C. The preincubated neutrophils were then processed and analyzed in the core facility for Medical Bioanalytics in Institute for Ophthalmic Research in University Hospital Tübingen. The enrichment ratio for pathways was calculated with https://metascape.org. The enrichment plot and heatmap were plotted by embedded software on http://www.bioinformatics.com.cn.

2.2.12 Immunofluorescence for Sema4D and PlxnB2 on fMLP activated human neutrophils

Product name	Product No.	Company	Headquarter
Recombinant Human Semaphorin 4D Fc, rhSEMA4D FC.	7470-S4	R&D Systems, Inc. Bio-Techne.	614 McKinley Place NE Minneapolis, MN 55413, U.S.A.
N-Formyl-Met-Leu-Phe, fMLP	F3506	Sigma Aldrich	3050 Spruce Street, Saint Louis, MO 63103, U.S.A.
Tween® 20 for molecular biology	A4974	AppliChem GmbH	Ottoweg 4, D-64291, Darmstadt, Germany
Triton® X-100	X 100 – 100ML	Sigma Aldrich	3050 Spruce Street, Saint Louis, MO 63103, U.S.A.
normal donkey serum	ab7475	abcam	Bertha-Benz-Straße 5, 10557 Berlin, Germany
Human Semaphorin 4D/CD100 Antibody	Ab134128	abcam	Bertha-Benz-Straße 5, 10557 Berlin, Germany
Rabbit IgG Isotype Control	31235	Thermo Fisher Scientific	Neuhofstrasse 11, CH 4153 Reinach, Switzerland
Donkey anti-Rabbit Antibody, Alexa Fluor™ 488	A32790	Invitrogen, Thermo Fisher Scientific	Neuhofstrasse 11, CH 4153 Reinach, Switzerland
normal goat serum	S-1000	Vector Laboratories	6737 Mowry Ave Newark, CA 94560 U.S.A.
Anti-PlexinB2 antibody	MAB5329	R&D Systems, Inc. Bio-Techne.	614 McKinley Place NE Minneapolis, MN 55413, U.S.A.
normal mouse IgG	sc-2025	Santa Cruz Biotechnology, Inc.	10410 Finnell Street Dallas, Texas, 75220 U.S.A.
Goat anti-Mouse Antibody, Alexa™ 594	A11005	Invitrogen, Thermo Fisher Scientific	Neuhofstrasse 11, CH 4153 Reinach, Switzerland
ROTI® Mount FluorCare DAPI	HP20.1	Carl Roth GmbH	Schoemperlenstr. 3-5, 76185 Karlsruhe, Germany
Confocal microscope Stellaris 8	SP8	Leica Mikrosysteme Vertrieb GmbH	Ernst-Leitz-Strasse 17-37 Wetzlar, 35578, Germany

Human neutrophils were isolated with the MACS system as mentioned in 2.2.3 and resuspended to 4 x10^7/ml. 1 x 10^6 neutrophils were stimulated in 100 µl $HBSS^+$ with 10 ng/ml fMLP (N-Formyl-Met-Leu-Phe, Sigma, F3506) or NaCl was used as control with 15 minutes incubation time at 37^{o}C. After incubation neutrophils were washed with 1 ml NaCl and centrifuged at 1300 rpm for 10 minutes at RT. Then neutrophil pellets were resuspended and fixed with 4% PFA for 5 minutes. After centrifugation at 1300 rpm for 10 RT, neutrophil pellets were resuspended in 500 µl NaCl and each 50 µl was dropped on triethoxysilan pretreated slides. Then probes were fixed on a hot plate at 60 ^{o}C for 10 minutes. The staining for Sema4D and PlxnB2 started with a washing using 0.1 % Tween (Tween® 20 for molecular biology, AppliChem, A4974) in PBS for 5 minutes 3 times. Then the slides were blocked with 5% normal donkey serum in 5% BSA + 0.1% Tween in PBS at RT for an hour to block unspecific staining. Anti - human Sema4D antibody (rabbit-anti-human Semaphorin 4D/CD100 Antibody, abcam, ab134128) or rabbit IgG (Invitrogen,

ThermoFisher, #31235) as control or blank for second antibody control, was diluted to 12.07 µg/ml with 1 % BSA + 0.1 % Tween in PBS and added to neutrophils for incubation at 4 °C in humid chamber overnight. On the second day, neutrophils were washed with 0.1 % Tween in PBS for 5 minutes 3 times, followed by incubation with secondary antibody Alexa488 (Donkey anti-rabbit second antibody Alexa Fluor™ 488, Invitrogen, A21202) diluted 1:500 in 1 % BSA + 0.1 % Tween in PBS for 60 minutes at RT in a dark humid chamber. After incubation neutrophils were washed with 0.1 % Tween in PBS for 5 minutes 3 times and then incubated with 5 % normal goat serum in 5 % BSA + 0.1 % Tween in PBS for an hour at RT for blocking. Subsequently, neutrophils were incubated with 10 µg/ml mouse anti-human PlxnB2 antibody (anti-PlxnB2 antibody, R&D, MAB5329) or norm mouse IgG (Santa Cruz, sc-2025) as control, or blank as second antibody control, in 1 % BSA + 0.1 % Tween in PBS, and incubated at RT for 60 minutes. After incubation neutrophils were washed with 0.1 % Tween in PBS for 5 minutes 3 times, followed by incubation with second antibody Alexa594 (goat anti-mouse second antibody Alexa Fluor™ 594, Invitrogen, A11005) in 1 % BSA + 0.1 % Tween in PBS for 60 minutes at RT in a dark humid chamber. Then neutrophils were washed with 0.1 % Tween in PBS for 5 minutes 3 times. Then ROTI Mount FluorCare DAPI (Carl Roth, HP20.1) was added to the slides and the coverslips were mounted. The slides were dried in the dark at RT for 2 hours and stored at 4 °C in the dark. The micrographs were acquired on a Leica SP8 Stellaris confocal microscope and analyzed and processed with ImageJ software.

2.2.13 Experimental mice

All animal experiments in this project have been approved by the regional council of Tübingen and were performed in accordance with the German Animal Welfare Act. All animals used in this project, including *Sema4d*$^{-/-}$ mice (C.129P2-Sema4d<tm1Kik>) and littermate controls wild type BALB/c mice were bred in animal faculty from 2012 onwards in the institute of Pharmacology, Department of Anesthesiology and Intensive Care Medicine, AG Rosenberger in Wilhelmstr. 56 (Lothar Meyer Bau), 72074, Tübingen. In *Sema4d*$^{-/-}$ mice the expression of Sema4d was disrupted by replacing a 1.6kb genomic region with a neomycin (neo) resistance gene cassette. This region covers the first exon and the initiation codon for sema4d[134]. The mice were kept in cages under specific pathogen-free (SPF) condition. At the time of experimentation, the age of the mice was 12 - 16 weeks with an average body weight of 25 g.

2.2.14 LPS-induced mouse lung injury model

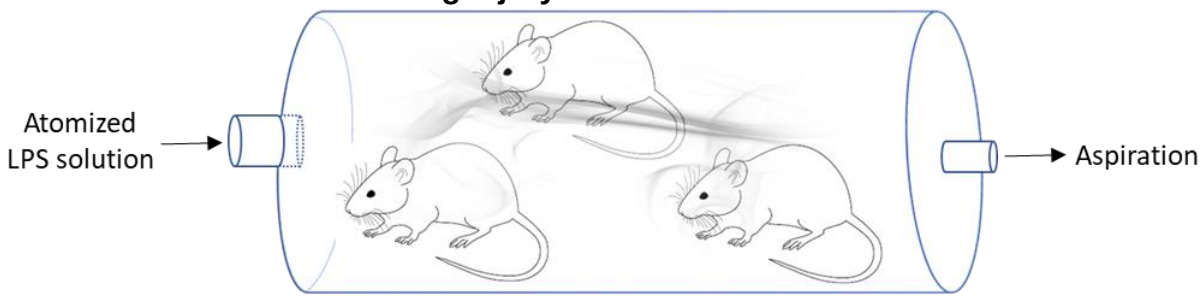

Figure 5. LPS inhalation induced mice acute lung injury model.

Product name	Product No.	Company	Headquarter
Lipopolysaccharides from Escherichia coli O26:B6	L8274-10MG	Sigma Aldrich	3050 Spruce Street, Saint Louis, MO 63103, U.S.A.
Omron micro A-I-R atomizer	U22	Omron Healthcare Co., Ltd	53 Kunotsubo Terado-cho Muko, 617-0002 Japan

As shown in Figure 3, the chamber was connected with an atomizer on one side, and negative pressure aspiration on the other side. Lipopolysaccharides (LPS, L8274-10MG, Sigma) were diluted to 0.5 mg/ml in NaCl and nebulized with a vaporizer (Omicron, U22). When the chamber was filled with atomized LPS, mice were put into the chamber and underwent LPS inhalation for 45 minutes. After inhalation, mice were put back into residential cages and incubated for 4 hours or 24 hours to induce acute lung injury. For saving experimental animals, the experiments for harvesting blood in 2.2.15, BAL in 2.2.16 and lungs in 2.2.17 were performed in the same mice, and the experiments for BAL in 2.2.19, 2.2.20 and 2.2.21 were carried out in the same animals.

2.2.15 Flow cytometry for mouse neutrophils in the blood

Product name	Product No.	Company	Headquarter
BD Lysing buffer 10X	555899	BD Biosciences	Tullastrasse 8-12, 69126 Heidelberg, Germany
CellFix™ Tissue Processing Reagent, BD	340181	Thermo Fisher Scientific	Neuhofstrasse 11, CH 4153 Reinach, Switzerland
APC anti-mouse CD100 (SEMA4D)	147606	BioLegend, Thermo Fisher Scientific	Neuhofstrasse 11, CH 4153 Reinach, Switzerland
PE/Cyanine7 anti-mouse Ly-6G/Ly-6C (Gr-1) Antibody	108416	BioLegend, Thermo Fisher Scientific	Neuhofstrasse 11, CH 4153 Reinach, Switzerland
Plexin-B1 Antibody, (A-8), Alexa Fluor® 647	Sc-28372 AF647	Santa Cruz Biotechnology, Inc.	10410 Finnell Street Dallas, Texas, 75220 U.S.A.
PE anti-mouse PlexinB2 Antibody	145903	BioLegend, Thermo Fisher Scientific	Neuhofstrasse 11, CH 4153 Reinach, Switzerland

Wild-type BALB/c mice underwent NaCl or LPS inhalation for 45 minutes followed by 4 hours incubation time as described in 2.2.14. Then the mouse was finally anesthetized with Pentobarbital (240 mg/kg body weight (BW)) and 500 µl blood of each mouse was harvested through right ventricle puncture with a syringe containing 100 µl trisodium citrate solution for anti-coagulation. The erythrocytes in the blood were then lysed with warm BD lysis buffer (BD Lysing buffer 10x, BD, 555899, pre-diluted 1:10 with dH_2O) 8 ml for 3 minutes. Then the blood sample was centrifuged with 500 g for 10 minutes at 4 ^oC, and the supernatant was discarded. The pellet was resuspended and fixed with 400 µl CellFix buffer (Tissue Processing Reagent, BD, Thermo Fisher Scientific, 340181) on ice for 10 minutes, and then washed with 8 ml FACS buffer ($PBS^{-/-}$ + 1 % BSA + 2 mM/L EDTA + 2 mM/L NaN_3). After centrifugation, the pellet was resuspended in 200 µl FACS buffer, and each 100 µl was transferred to a FACS glass tube and added antibody cocktail (APC anti-mouse Sema4d, and PE/Cyanine7 anti-mouse Ly-6G/Ly-6C; or Alexa Fluor® 647 anti-mouse PlxnB1, and PE anti-mouse PlxnB2) for staining 30 minutes at RT. After washing with 2 ml FACS buffer, the cells were resuspended into 300 µl FACS buffer, flow cytometry was performed immediately. The experiment used a BD FACS Canto™ II running the BD FACS Diva™ software. The data were analyzed with the software FlowJo V10.0.8.

2.2.16 Flow cytometry for mouse bronchoalveolar lavage (BAL)

Product name	Product No.	Company	Headquarter
CellFix™ Tissue Processing Reagent, BD	340181	Thermo Fisher Scientific	Neuhofstrasse 11, CH 4153 Reinach, Switzerland
APC anti-mouse CD100 (SEMA4D)	147606	BioLegend, Thermo Fisher Scientific	Neuhofstrasse 11, CH 4153 Reinach, Switzerland
PE/Cyanine7 anti-mouse Ly-6G/Ly-6C (Gr-1) Antibody	108416	BioLegend, Thermo Fisher Scientific	Neuhofstrasse 11, CH 4153 Reinach, Switzerland
Plexin-B1 Antibody, (A-8), Alexa Fluor® 647	Sc-28372 AF647	Santa Cruz Biotechnology, Inc.	10410 Finnell Street Dallas, Texas, 75220 U.S.A.
PE anti-mouse PlexinB2 Antibody	145903	BioLegend, Thermo Fisher Scientific	Neuhofstrasse 11, CH 4153 Reinach, Switzerland

Wild-type BALB/c mice underwent NaCl or LPS inhalation for 45 minutes following 4 hours incubation time as described in 2.2.14. Then the mouse was finally anesthetized with Pentobarbital (240 mg/kg BW) and tracheotomized and intubated. The tracheal tube was fixed with a ligature. The blood was acquired as described in 2.2.15. Then), the thorax and abdomen were incised, the abdominal aorta was cut, and the blood in lung circulation

was flushed with 10 ml $PBS^{-/-}$ through right ventricle puncture. Following the lung was lavaged 3 times with 0.6 ml PBS and the lavage was kept on ice. Then the BAL was centrifuged with 500 g for 10 minutes at 4 °C, and the supernatant was discarded. The pellet was resuspended and fixed with 400 µl fix buffer (Tissue Processing Reagent, BD, Thermo Fisher Scientific, 340181) on ice for 10 minutes, and then washed with 8 ml FACS buffer. After centrifugation, the pellet was resuspended with 200 µl FACS buffer, and 100 µl was moved to the FACS tube and antibody cocktail (APC anti-mouse Sema4d and PE/Cyanine7 anti-mouse Ly-6G/Ly-6C; or Alexa Fluor® 647 anti-mouse PlxnB1 and PE anti-mouse PlxnB2) was added for staining 30 minutes at RT. After washing with 2 ml FACS buffer, the cells were resuspended in 300 µl FACS buffer, and measured by flow cytometry. For cell counts in the BAL, 1:100 diluted SPHERO beads (Spherotech, 4µm, PP-40-10) 10 µl were added to the final FACS buffer before measurement. During flow cytometry, the beads were specifically gated and counted to 10000 events as the stopping criterion. For the experiment a BD FACS Canto™ II running the BD FACS Diva™ software was used. The data were analyzed with FlowJo V10.0.8 software.

2.2.17 Flow cytometry for mouse lung

Product name	Product No.	Company	Headquarter
collagenase/dispase, Collagenase from *Vibrio alginolyticus*, Dispase from *Bacillus polymyxa*	11097113001	Roche, Sigma-Aldrich Chemie GmbH	Eschenstr. 5, 82024, Taufkirchen, Germany
Deoxyribonuclease I from bovine pancreas	D4527	Sigma Aldrich	3050 Spruce Street, Saint Louis, MO 63103, U.S.A.
APC anti-mouse CD100 (SEMA4D)	147606	BioLegend, Thermo Fisher Scientific	Neuhofstrasse 11, CH 4153 Reinach, Switzerland
PE/Cyanine7 anti-mouse Ly-6G/Ly-6C (Gr-1) Antibody	108416	BioLegend, Thermo Fisher Scientific	Neuhofstrasse 11, CH 4153 Reinach, Switzerland
Plexin-B1 Antibody, (A-8), Alexa Fluor® 647	Sc-28372 AF647	Santa Cruz Biotechnology, Inc.	10410 Finnell Street Dallas, Texas, 75220 U.S.A.
PE anti-mouse PlexinB2 Antibody	145903	BioLegend, Thermo Fisher Scientific	Neuhofstrasse 11, CH 4153 Reinach, Switzerland
Brilliant Violet 421™ anti-mouse CD144 (VE-cadherin) Antibody	138013	BioLegend, Thermo Fisher Scientific	Neuhofstrasse 11, CH 4153 Reinach, Switzerland
Brilliant Violet 510™ anti-mouse CD326 (Ep-CAM) Antibody	118231	BioLegend, Thermo Fisher Scientific	Neuhofstrasse 11, CH 4153 Reinach, Switzerland

Wild type BALB/c mice underwent NaCl or LPS inhalation for 45 minutes and incubated for 4 hours as described in 2.2.14. After the mouse was finally anesthetized with

Pentobarbital (240 mg/kg BW), blood and BAL were acquired as described 2.2.15 and 2.2.16. After the blood in lung circulation was flushed and the lung was lavaged with 600 µl $PBS^{-/-}$ 3 times as described in 2.2.16, the left lung was cut off and washed once in $PBS^{-/-}$. The left lung was minced thoroughly in 2.5 ml digesting solution ($PBS^{-/-}$ + 0.5 % BSA + 1 mg/ml collagenase / dispase (Roche, Sigma, 11097113001) + 100 µg/ml Deoxyribonuclease I (Sigma, D4527)) and then incubated on a shaker for 60 minutes at 37 ºC. The lung tissue was disrupted every 5 minutes during digesting. After digestion, the lung tissue was filtered through a 70 µm filter which was pre-washed once with 2 ml $PBS^{-/-}$ + 0.5 % BSA. The lung tissue in buffer was centrifuged at 500 g for 10 minutes at 4 ºC and the cell pellet was resuspended and fixed with 1 ml fix buffer (Tissue Processing Reagent, BD, Thermo Fisher Scientific, 340181) for 10 minutes RT. After washing with 20 ml FACS buffer, the lung tissue buffer was filtered with a pre-washed 40 µm filter again, centrifuged at 500 g for 10 minutes at 4º C and resuspended with 1 ml FACS buffer. Each 100 µl lung cell suspension was stained 30 minutes at RT with antibody cocktail (APC anti-mouse Sema4d; PE/Cyanine7 anti-mouse Ly-6G/Ly-6C; or Alexa Fluor 647 anti-mouse PlxnB1 and PE anti-mouse PlxnB2; Brilliant Violet 421 anti-mouse CD144 (VE-cadherin) or Brilliant Violet 510 anti-mouse CD326 (Ep-CAM) antibody). After washing with 2 ml FACS buffer, the cells were resuspended into 300 µl FACS buffer and measured by flow cytometry. The experiment was performed with a BD FACS Canto™ II running the BD FACS Diva™ software. The data was analyzed using FlowJo V10.0.8 software.

2.2.18 Immunofluorescence staining for Sema4d, and vWF or cytokeratin in mice lung sections

Product name	Product No.	Company	Headquarter
Automatic benchtop tissue processor	TP1020	Leica Mikrosysteme Vertrieb GmbH Mikroskopie und Histologie	Ernst-Leitz-Strasse 17-37 35578 Wetzlar, Germany
Leica modular tissue embedding center	EG1150	Leica Mikrosysteme Vertrieb GmbH Mikroskopie und Histologie	Ernst-Leitz-Strasse 17-37 35578 Wetzlar, Germany
Manual rotary microtome for Routine Sectioning	RM2235	Leica Mikrosysteme Vertrieb GmbH Mikroskopie und Histologie	Ernst-Leitz-Strasse 17-37 35578 Wetzlar, Germany
Antigen Unmasking Solution, Citrate-Based	H-3300-250	Vector Laboratories	6737 Mowry Ave Newark, CA 94560, U.S.A.
normal goat serum	S-1000	Vector Laboratories	6737 Mowry Ave Newark, CA 94560, U.S.A.

Product name	Product No.	Company	Headquarter
Tween® 20 for molecular biology	A4974	AppliChem GmbH	Ottoweg 4, D-64291, Darmstadt, Germany
SEMA4D Polyclonal Antibody	bs-6965R	Bioss, Thermo Fisher Scientific	Neuhofstrasse 11, CH 4153 Reinach, Switzerland
Rabbit IgG Isotype Control	31235	Thermo Fisher Scientific	Neuhofstrasse 11, CH 4153 Reinach, Switzerland
Goat anti-Rabbit IgG Secondary Antibody, Alexa Fluor™ 488	A-11008	Invitrogen, Thermo Fisher Scientific	Neuhofstrasse 11, CH 4153 Reinach, Switzerland
normal donkey serum	ab7475	abcam	Bertha-Benz-Straße 5, 10557 Berlin, Germany
VWF antibody (C-20), Goat-anti-mouse	sc-8068	Santa Cruz Biotechnology, Inc.	10410 Finnell Street Dallas, Texas, 75220 U.S.A.
Cytokeratin 12 antibody (L-15), Goat-anti-mouse	sc-17101	Santa Cruz Biotechnology, Inc.	10410 Finnell Street Dallas, Texas, 75220 U.S.A.
Goat IgG Isotype Control	02-6202	Thermo Fisher Scientific	Neuhofstrasse 11, CH 4153 Reinach, Switzerland
Donkey anti-Goat IgG Secondary Antibody, Alexa Fluor™ 594	A-11058	Invitrogen, Thermo Fisher Scientific	Neuhofstrasse 11, CH 4153 Reinach, Switzerland
ROTI® Mount FluorCare DAPI	HP20.1	Carl Roth GmbH	Schoemperlenstr. 3-5, 76185 Karlsruhe, Germany
Zeiss Axiophot fluorescent microscope		Zeiss	Carl-Zeiss-Strasse 22 73447, Oberkochen Germany
AxioVision		Zeiss	Carl-Zeiss-Strasse 22 73447, Oberkochen Germany

Wild type BALB/c or *Sema4d*$^{-/-}$ mice were inhaled with LPS for 45 minutes and incubated for 4 hours as described in 2.2.14. After the mouse was finally anesthetized with Pentobarbital (240 mg/kg BW), the thorax and abdomen were incised, the abdominal aorta was cut, and the blood in lung circulation was flushed with 10 ml PBS$^{-/-}$ through right ventricle puncture as described in 2.2.16. Then 1 ml formalin was injected into the lung through the tracheal tube, followed by ligature of the trachea to keep the formalin inside the lung. The whole lung was cut out and fixed in a cassette in 4 % formalin for 12 hours. Then the tissue section was dehydrated with graded ethanol with an automatic benchtop tissue processor (Leica, TP1020), embedded in paraffin with Leica modular tissue embedding center (Leica, EG1150) and sectioned with a manual rotary microtome (Leica, RM2235). The tissue sections were put and dried on slides for further processing.

For IF staining, the slides were washed in xylene for 7 minutes 3 times for deparaffinization. Then the slides were rehydrated in graded concentrations of ethanol in water (2 x 100 %, 1 x 96 %, 1 x 70 %, 5 minutes each time), ending in a final rinse in pure deionized water

for 5 minutes twice and once in PBS for 5 minutes. The antigen of sections was then retrieved with Antigen unmasking solution (Vector, H-3300) 1.4 ml in 150 ml dH_2O in a microwave oven 750 w for 7 minutes, followed by cooling for 20 minutes at RT. The slides were then washed once with dH_2O and once with PBS for 5 minutes. The sections were then circled with PAP-Pen. For Sema4d staining, the sections were incubated with 1 % normal goat serum in 5 % BSA + 0.1 % Tween in PBS at RT for an hour to block unspecific staining. Then Sema4d antibody (rabbit anti-mouse, Bioss, Thermo Fisher Scientific, bs-6965R, 1:100 diluted) or normal rabbit IgG (Thermo Fisher Scientific, 31235) as control, or blank for second antibody control, was diluted with 1 % normal goat serum + 1 % BSA + 0.1 % Tween in PBS and incubated with sections at 4 °C in humid chamber overnight. On the second day, the sections were washed with 0.1 % Tween in PBS for 5 minutes 4 times first, followed by incubation with secondary antibody (goat anti-rabbit Alexa Fluor™ 488, Invitrogen, Thermo Fisher Scientific, A-11008) which was diluted 1:500 with 1 % normal goat serum + 1 % BSA + 0.1 % Tween in PBS for 60 minutes at RT in a dark humid chamber. For staining vWF or cytokeratin, the sections were washed with 0.1 % Tween in PBS for 5 minutes 4 times and then incubated with 1 % normal donkey serum in 5 % BSA + 0.1 % Tween in PBS at RT for an hour to block unspecific staining. In the next step, von Willebrand factor antibody (vWF antibody (C-20), goat anti-mouse, Santa Cruz Biotechnology, sc-8068, 1:100 diluted) or Cytokeratin antibody (Cytokeratin antibody (L-15), goat anti-mouse, Santa Cruz Biotechnology, sc-17101, 1:100 diluted) or the normal goat IgG (02-6202, Thermo Fisher Scientific) as control or blank for second antibody control, was diluted with 1 % normal donkey serum + 1% BSA + 0.1 % Tween in PBS and added to sections for incubation at RT for an hour in a dark humid chamber. After washing with 0.1 % Tween in PBS for 5 minutes 4 times, secondary antibody (donkey anti-goat Alexa Fluor™ 594, Invitrogen, Thermo Fisher Scientific, A-11058) was diluted at 1:500 with 1 % normal serum donkey + 1 % BSA + 0.1 % Tween in PBS and incubated on the sections for 60 minutes at RT in a dark humid chamber. Next, the sections were washed with 0.1 % Tween in PBS for 5 minutes 4 times and ROTI Mount FluorCare DAPI was dropped to the sections to mount them on coverslips. The slides were then dried in dark at RT for 2 hours and stored at 4 °C in the dark. The micrographs were acquired on a Zeiss Axiophot fluorescent microscope and analyzed with AxioVision software.

2.2.19 Protein analysis - Bicinchoninic acid assay (BCA)

Product name	Product No.	Company	Headquarter
Pierce™ BCA Protein Assay Kit	23225	Thermo Fisher Scientific	3747 N. Meridian Road. Rockford, Illinois 61101 U.S.A.
96 well microplate	655101	Greiner bio-one, Thermo Fisher Scientific	3747 N. Meridian Road. Rockford, Illinois 61101 U.S.A.
Tecan microplate plate reader	Infinite 200 PRO	Tecan Group Ltd.	Seestrasse 103, 8708 Männedorf Switzerland

Wild type BALB/c or *Sema4d*$^{-/-}$ mice were inhaled with LPS for 45 minutes and incubated for 24 hours in residential cages to induce lung injury. After the mouse was finally anesthetized with Pentobarbital (240 mg/kg BW), the blood in lung circulation was flushed with 10 ml PBS$^{-/-}$ through right ventricle puncture as described in 2.2.16. Following the lung was lavaged 3 times with 0.6 ml PBS. Then the BAL was centrifuged with 500 g for 10 minutes at 4 ^{o}C. Part of the supernatant (1.5ml) was frozen in liquid nitrogen for enzyme-linked immunosorbent assay (ELISA). The pellet and another part of supernatant (250µl) was frozen in liquid nitrogen for BCA Protein Assay and MPO assay. The quantitation of total protein in BAL was acquired with Pierce™ BCA Protein Assay Kit (Thermo Fisher, 23225) in 96 well plates. 25 µl albumin standards, BAL samples and distilled water (blank) were added to wells in duplicates, then freshly prepared 200 µl BCA working reagent (50:1 mixed by Reagent A and Reagent B) were added to the wells and mixed. The plate was then incubated at 37 °C for 25 minutes in the dark. After incubation, the plate was measured for 562 nm absorbance with a Tecan plate reader (Tecan, Infinite M200 PRO) with Magellan 7.1 software.

2.2.20 MPO assay

Product name	Product No.	Company	Headquarter
96 well microplate	655101	Greiner bio-one, Thermo Fisher Scientific	3747 N. Meridian Road. Rockford, Illinois 61101 U.S.A.
Tecan microplate plate reader	Infinite 200 PRO	Tecan Group Ltd.	Seestrasse 103, 8708 Männedorf Switzerland
Citric acid, CAS 77-92-9	818707	Merck, Sigma-Aldrich Chemie GmbH	Eschenstr. 5, 82024, Taufkirchen, Germany
Trisodium citrate dihydrate	S1804	Sigma Aldrich	3050 Spruce Street, Saint Louis, MO 63103, U.S.A.
ABTS	A1888	Sigma Aldrich	3050 Spruce Street, Saint Louis, MO 63103, U.S.A.

Wild type BALB/c or *Sema4d*$^{-/-}$ mice were inhaled with LPS for 45 minutes followed by 24 hours incubation and BAL was harvest as described in 2.2.19. The Myeloperoxidase (MPO) relative concentration in BAL was measured in 96 well microplates. 50 µl BAL samples and distilled water (blank) were added to the wells in duplicates, followed by 50 µl citrate buffer (home-made, 1 mol citric acid (26.3g) + 1 mol trisodium citrate dihydrate (36.8 g) + 250 ml distilled water and adjusted to pH 4.2). Then freshly prepared 100 µl ABTS buffer (5 ml citrate buffer + 45 ml distilled water + 28 mg ABTS (SIGMA, 1888) + 50 µl H_2O_2) were added and mixed well. The plate was then incubated at 37 °C for 30 minutes in the dark. After incubation, the plate was measured with 405 nm absorbance in a Tecan plate reader (Tecan, infinite M200 PRO) with Magellan 7.1 software.

2.2.21 Enzyme-linked immunosorbent assay (ELISA)

Product name	Product No.	Company	Headquarter
ABTS	A1888	Sigma Aldrich	3050 Spruce Street, Saint Louis, MO 63103, U.S.A.
DuoSet ELISA kit TNFα	DY410-05	R&D Systems, Inc.	614 McKinley Place NE Minneapolis, MN 55413, U.S.A.
DuoSet ELISA kit IL6	DY406-05	R&D Systems, Inc.	614 McKinley Place NE Minneapolis, MN 55413, U.S.A.
DuoSet ELISA kit IL1β	DY401-05	R&D Systems, Inc.	614 McKinley Place NE Minneapolis, MN 55413, U.S.A.
DuoSet ELISA kit KC (CXCL1)	DY453-05	R&D Systems, Inc.	614 McKinley Place NE Minneapolis, MN 55413, U.S.A.
DuoSet ELISA kit MIP2 (CXCL2)	DY452-05	R&D Systems, Inc.	614 McKinley Place NE Minneapolis, MN 55413, U.S.A.
96 well microplate	DY990	R&D Systems, Inc.	614 McKinley Place NE Minneapolis, MN 55413, U.S.A.
Tween® 20 for molecular biology	A4974	AppliChem GmbH	Ottoweg 4, D-64291, Darmstadt, Germany
Reagent Diluent	DY995	R&D Systems, Inc.	614 McKinley Place NE Minneapolis, MN 55413, U.S.A.
Plate Sealers	DY992	R&D Systems, Inc.	614 McKinley Place NE Minneapolis, MN 55413, U.S.A.
Substrate Solution	DY999	R&D Systems, Inc.	614 McKinley Place NE Minneapolis, MN 55413, U.S.A.
Stop Solution	DY994	R&D Systems, Inc.	614 McKinley Place NE Minneapolis, MN 55413, U.S.A.
Tecan microplate plate reader	Infinite 200 PRO	Tecan Group Ltd.	Seestrasse 103, 8708 Männedorf, Switzerland

Wild type BALB/c or *Sema4d*$^{-/-}$ mice were inhaled with LPS for 45 minutes followed by 24 hours incubation and BAL was harvest as described in 2.2.19. The concentration of TNFα, IL6, IL1β, KC (CXCL1) and MIP2 (CXCL2) in BAL were measured with the DuoSet ELISA KITs (R&D Systems, DY410-05, DY406-05, DY401-05, DY453-05, DY452-05) following manufactures protocol. In summary, the 96-well microplates were coated with 100 µl pre-diluted capture antibody at RT overnight with adhesive plate sealers (R&D Systems, DY,0992). The next day, the coating buffer was aspirated and the plates were washed twice with 400 µl wash buffer (0.05 % Tween® 20 in PBS, pH 7.2-7.4). Then 300 µl Reagent Diluent (1 % BSA in PBS, pH 7.2-7.4, 0.2 µm filtered; R&D Systems, DY995) were added to the wells for blocking and incubated for an hour at RT, followed by aspiration and washing twice. 100 µl of BAL or standards were diluted with Reagent Diluent and placed to the wells. The plates were incubated for 2 hours at RT with adhesive plate sealers, followed by another aspiration and washing step twice. Then 100 µl detection antibody was placed to wells and incubated at RT for 2 hours with plate sealers, followed by aspiration and washing step twice. 100 µl Streptavidin-HRP in Reagent Diluent was placed and incubated in the dark for 20 minutes at RT. 100 µl substrate solution (1:1 mixed with color reagent A (H_2O_2) and color reagent B (Tetramethylbenzidine), R&D Systems, DY999) were then seeded and incubated for 20 minutes at RT in the dark. After adding 50 µl stop solution (2 N H_2SO_4, R&D Systems, DY994) and mixing, plates were immediately measured for 450 nm absorbance with a Tecan plate reader (Tecan, infinite M200 PRO) with Magellan 7.1 software.

3. Results

3.1 Sema4D inhibits neutrophil rolling and adhesion in inflammation

As described above, leukocyte recruitment is essential for the pathogenesis and progression of ARDS and this pathologic process starts with leukocyte rolling and adhesion on the blood vessel endothelium in an inflammatory venue. Therefore, we investigated whether Sema4D influences neutrophil rolling and adhesion in an in vitro experiment, the flow chamber assay. Glass capillaries were coated with E-selectin to imitate inflammation-activated endothelial cells. Since fibrinogen deposit is a common characteristic of inflammatory or noninflammatory induced tissue injury, we also coated capillaries together with human fibrinogen for a conditional group. Consistent with the literature review, additional human fibrinogen coating significantly increased the amounts of adhered leukocytes and reduced the rolling velocity compared with E-selectin coating alone (Figure 6 A-C). However, on top of E-selectin and fibrinogen, recombinant human Sema4D (rhSema4D) coating decreased the numbers of adhered leukocytes, and coordinately, speeded up the leukocyte rolling, in other words, it inhibited leukocyte adhesion on the surface of E-selectin and fibrinogen (Figure 6 A-C).

Flow cytometry further verified that rhSema4D suppressed the binding capacity of isolated human neutrophils to fibrinogen (Figure 6D), which could partly explain the mechanism of inhibitory function towards leukocyte adhesion in the flow chamber.

Previous literature[60] suggested that fibrinogen prompts neutrophil adhesion through binding to its receptor integrin αMβ2 (Mac-1, CD11b/CD18) and acts as a bridging molecule between endothelial cells and leukocytes. We assessed whether Sema4D influences the expression of integrin αMβ2 and other integrins by flow cytometry in human blood. Contrary to our expectations, Sema4D did not significantly alter the average expression of CD11b, LFA-1, or CD49d (Figure 6E-G), although the expression of LFA-1 and CD11b was apparently increased by fMLP, which has been demonstrated previously.

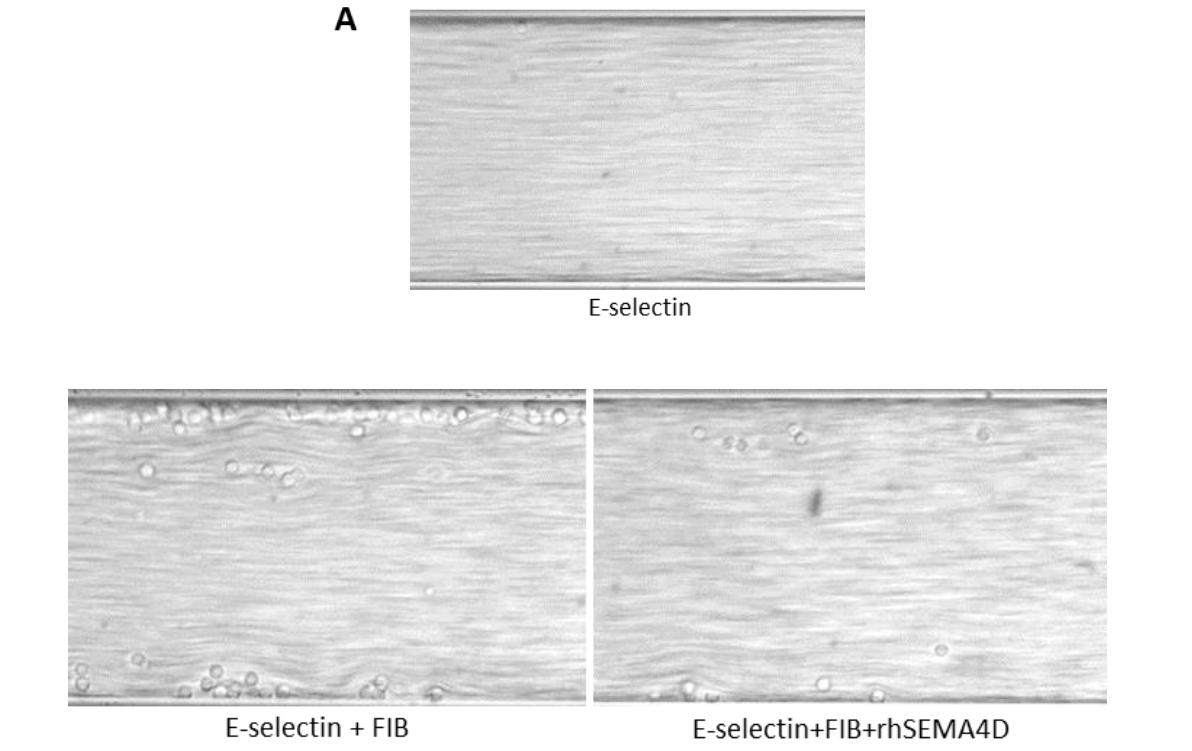
A
E-selectin
E-selectin + FIB
E-selectin+FIB+rhSEMA4D
B
Adhesion Numbers (cells/video)
80
60
40
20
0
***
***
***
C
Rolling Speeds (µm/sec)
50
40
30
20
10
0
**
***
**
Coating conditions
E-selectin
E-selectin+FIB
E-selectin+FIB+rhSEME4D
D
Fibrinogen binding (norm. MFI APC)
1250
1200
1150
1100
1050
1000
*
*
NaCl
fMLP
PBS
rhSEMA4D

E

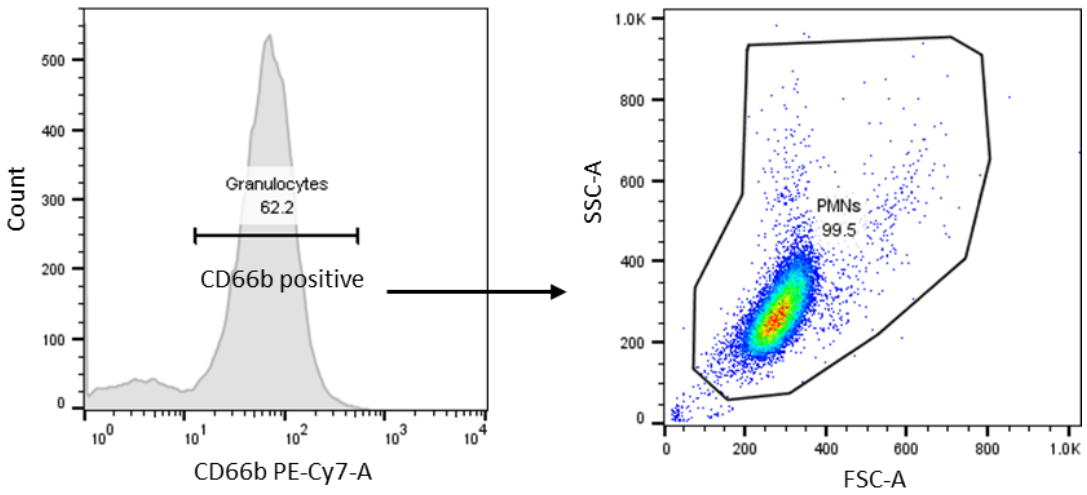
Count
Granulocytes
62.2
CD66b positive
CD66b PE-Cy7-A
SSC-A
PMNs
99.5
FSC-A

F

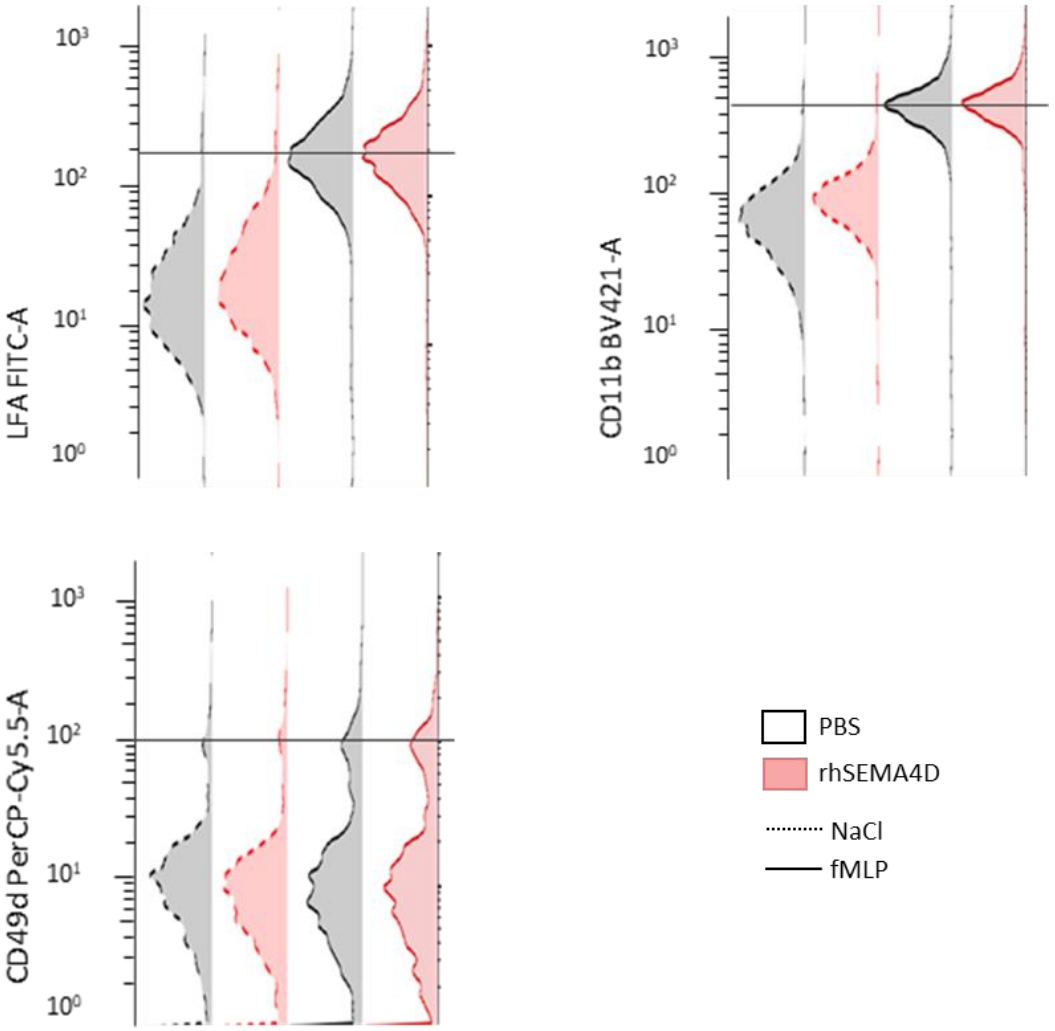
LFA FITC-A
CD11b BV421-A
CD49d PerCP-Cy5.5-A
PBS
rhSEMA4D
NaCl
fMLP

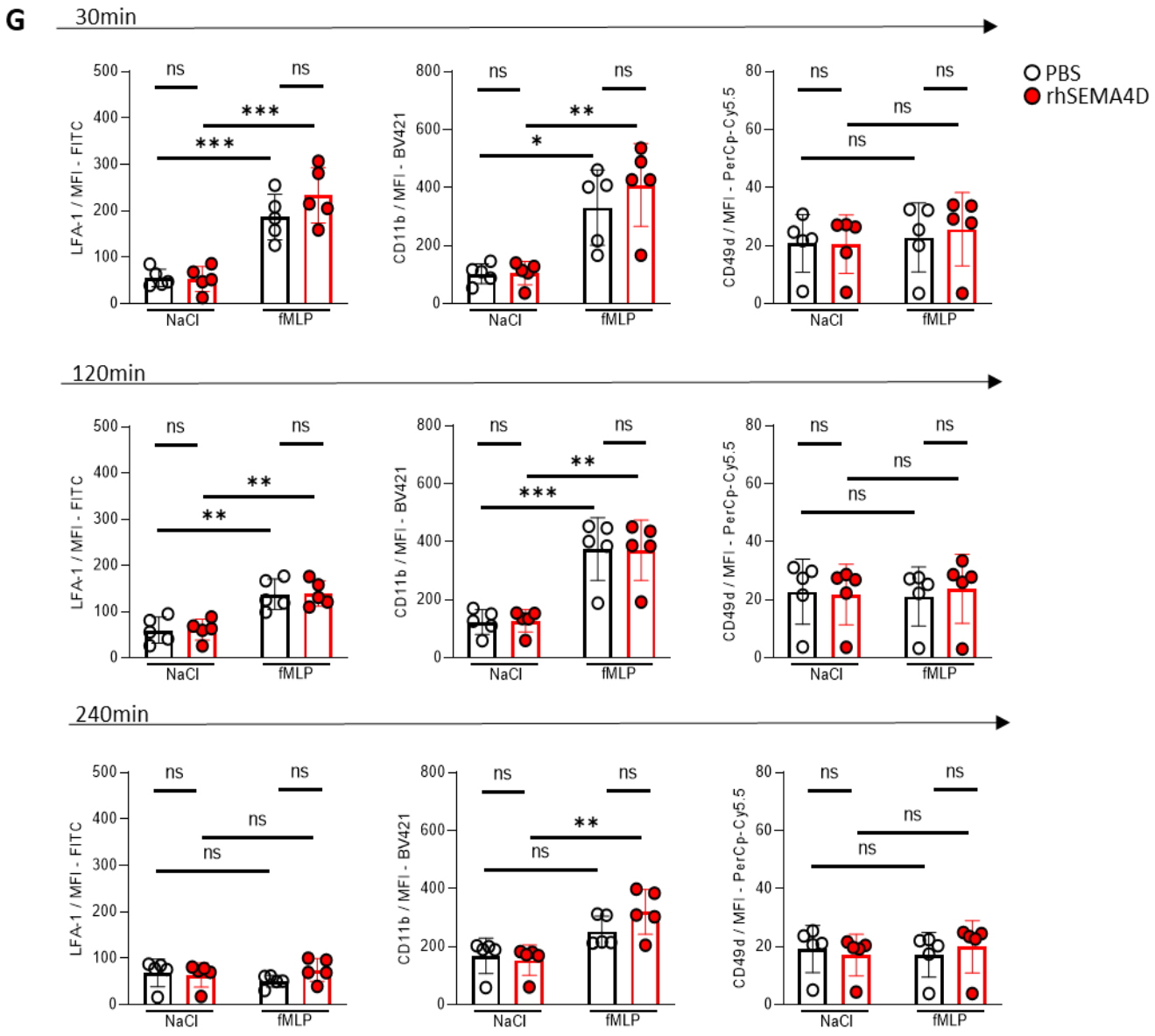

Figure 6. Sema4D inhibits neutrophil adhesion in inflammation.

(A) Representative images from videos of rolling and adhered human leukocytes from flow chamber experiments which were performed in E-selectin (3.0 µg/ml), fibrinogen (100 µg/ml), and rhSEMA4D (2 µg/ml) pre-coated rectangular glass capillaries. Videos were recorded for 10 seconds on a Leitz microscope with a 20× lens equipped with a black-and-white digital camera (Hamamatsu, Herrsching-Germany). Software Nikon 'NIS-Element AR420: 02' and 'NIS-Elements AR Analysis 4.20.00' were employed for recording and analysis. n=3 donors; 9-11 videos per group. **(B)** Quantification of adhered leukocyte number in videos from flow chamber experiments. n = 52-57 videos from 3 independent

experiments from 3 donors. **(C)** Quantification of leukocytes rolling velocity in videos from flow chamber experiments. n = 22-37 cells from 3 independent experiments from 3 healthy donors. **(D)** Fibrinogen binding assay with flow cytometry. Human neutrophils (2 $\times 10^5$ /group) were isolated from healthy donors with MACS system with magnetic beads and CD15 antibody, and stimulated with or without rhSema4D (2.5 µg/ml), fMLP (10 ng/ml) or PBS, together with AlexaFluor 647 conjugated human fibrinogen for 5 minutes at 37 ^{o}C. **(E)** Flow cytometry gating strategy. Human whole blood was incubated with or without rhSEMA4D, and / or fMLP for 30, 120, and 240 minutes. Neutrophils were determined by CD66b positive events and FSA - SSC gating. **(F)** Representative histograms for LFA, CD11b, and CD49d on human neutrophils (30 minutes). **(G)** Mean fluorescence intensity (MFI) of LFA, CD11b, and CD49d on human neutrophils at the indicated time points (30 minutes, 120 minutes, and 240 minutes). For E-G, n = 3 donors with duplicate, in 3 independent experiments. * $P < 0.05$; ** $P < 0.01$; *** $P < 0.001$, as determined by ordinary one-way analysis of variance (ANOVA), followed by multiple comparisons with Tukey's test or Šídák's test. Values are means ± SD.

3.2 Sema4D inhibits neutrophil polarization and PSGL-1 redistribution in inflammation

Polarization is one of the characteristics of neutrophil activation in inflammation, and it enables efficient migration. Therefore, we performed a chemotaxis assay to explore the function of Sema4D in the neutrophil polarization process. Human neutrophils were isolated from peripheral whole blood of healthy donors using a Percoll-based density gradient (isolation quality control is shown on Figure 7A). Next, we stimulated neutrophil polarization by a fMLP concentration gradient in a chemotaxis chamber (Figure 7B). From the analysis of the length-width ratio of neutrophils in the micrographs, we demonstrated again that fMLP concentration gradients effectively stimulated neutrophils to polarize from stationary round shape to irregular long oval shape. However, pre-incubation with rhSema4D significantly suppressed neutrophil polarization in a stimulus concentration gradient, which is shown in the representative micrographs and the quantification of the length-width ratio of neutrophils (Figure 7C-E).

Neutrophil polarization does not only mean transformation but also redistribution of the membranal proteins, which promotes better cooperation of neutrophils with

other types of cells in the circumstance, for example, endothelial cells and platelets. In our chemotaxis experiments, we found that when neutrophils get activated and polarized, PSGL-1 was redistributed from all over the plasma membrane evenly concentrated to the backside of the neutrophils, while CD11b was not concentrated at a specific location. Preincubation with rhSema4D inhibited this conversion obviously (Figure 7E). The polarization of PSGL-1 and CD11b could be quantified by their immunofluorescence density ratio of the uropod-located half-part to the other half-part. In accordance with the representative pictures, the immunofluorescence density of PSGL-1 got polarized with fMLP stimulation, and this did not happen to CD11b and rhSema4d restrained the asymmetrical redistribution (Figure 7F).

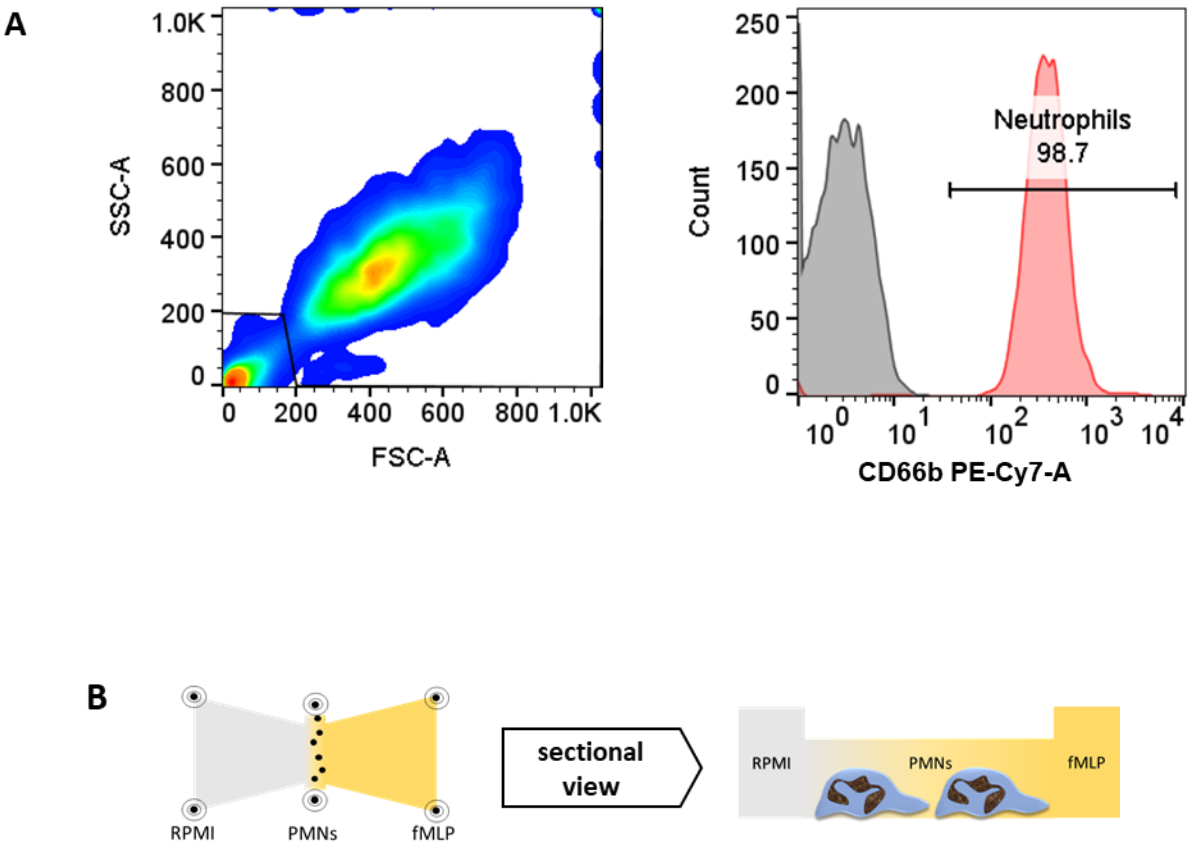

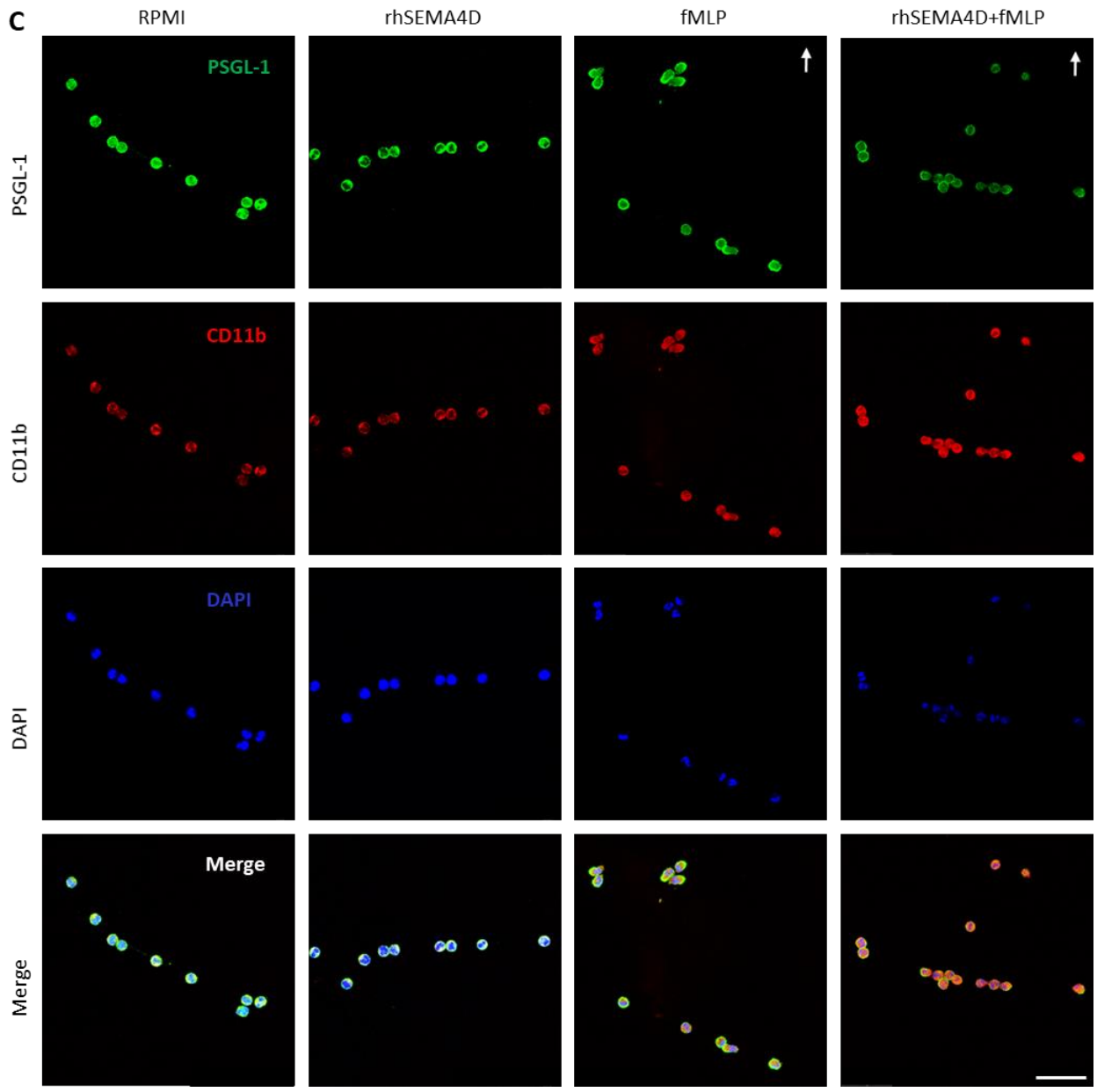
C
RPMI
rhSEMA4D
fMLP
rhSEMA4D+fMLP
PSGL-1
CD11b
DAPI
Merge
D
ns
***
***
PBS
rhSEMA4D
length width ratio-hPMNs
4
2
2
1
NaCl
fMLP

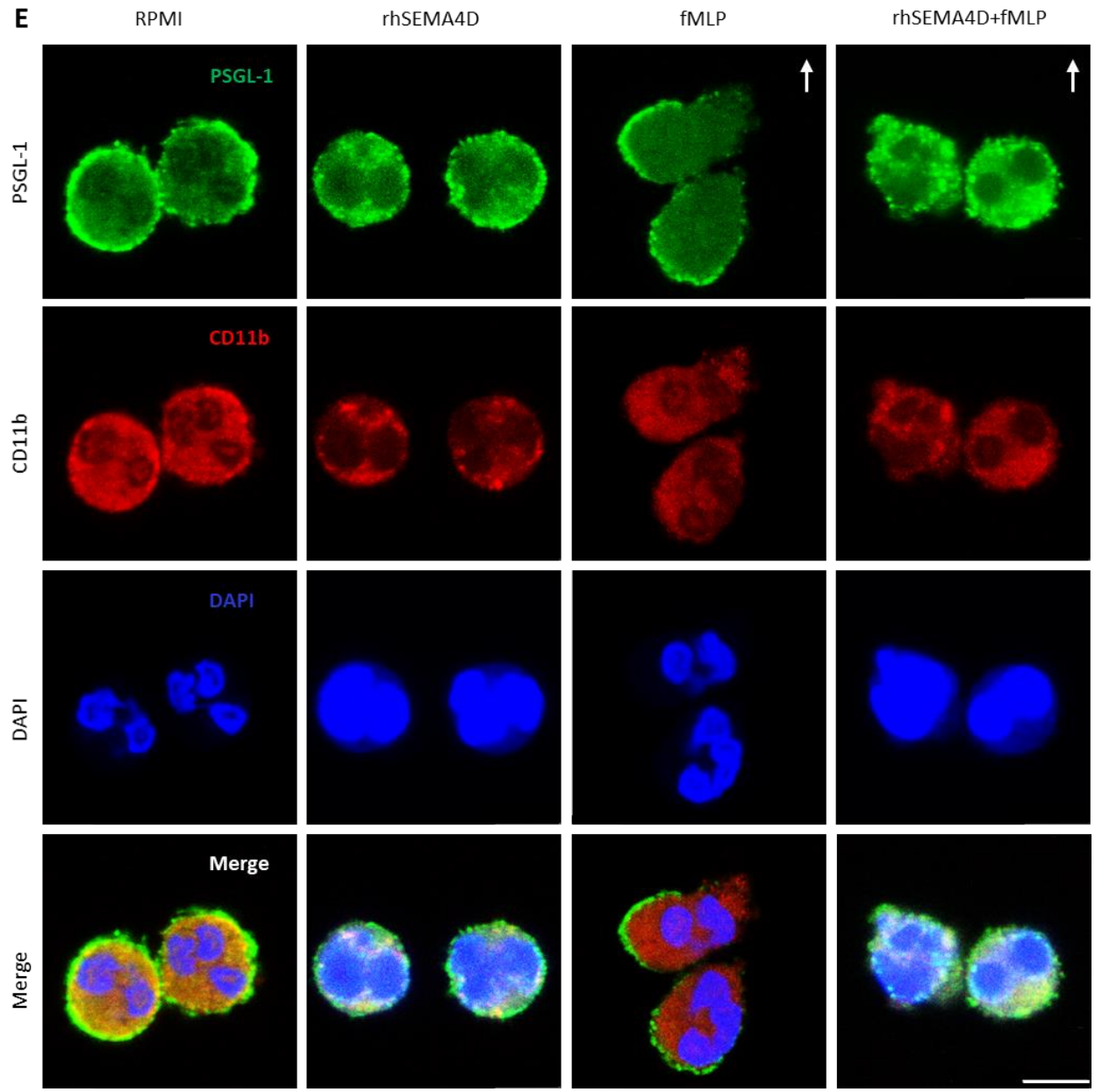
E
RPMI
rhSEMA4D
fMLP
rhSEMA4D+fMLP
PSGL-1
CD11b
DAPI
Merge
F
PSGL-1 polarization ratio
CD11b polarization ratio
NaCl
fMLP
ns
***
PBS
rhSEMA4D

Figure 7. Sema4D inhibits neutrophil polarization and PSGL-1 redistribution in inflammation.

(A) Flow cytometry for quality control of neutrophil isolation with percoll-based density gradient. Cells were gated to exclude debris with FSC-SSC. Neutrophils were determined as CD66b / PE-Cy7 positive population. **(B)** Schematic diagram of fMLP based concentration gradient in the chemotaxis chamber. **(C)** Representative micrographs of human neutrophils pre-incubated with or without rhSEMA4D (1 µg/ml) followed by exposure to fMLP concentration gradient (arrows point to the direction of higher concentrations) for 15 minutes. **(D)** Quantification of neutrophil polarization by analyzing micrographs of these experiments to determine length-width ratios; n = 150 - 235 cells from 3 independent experiments with 3 healthy donors. **(E)** Detail micrographs of human neutrophils of these experiments. **(F)** Quantification of PSGL-1 and CD11b polarization ratio in micrographs from the same experiments; n = 81 - 109 cells from 3 independent experiments with 3 healthy donors. * $P < 0.05$; ** $P < 0.01$; *** $P < 0.001$, ns $P > 0.05$; as determined by ordinary one-way ANOVA, followed by multiple comparisons with Tukey's test or Šídák's test. Scale bar = 35 µm (B), 5 µm(D).

3.3 Sema4D inhibits neutrophil uropod formation and firm adhesion in inflammation

The process of neutrophil polarization leads to uropod formation at the cell backside. Literature[46,47] has proven that uropod formation is critical for neutrophils firm adhesion and transmigration process, but the mechanism is still unspecified. Our chemotaxis experiment clearly showed that the isolated neutrophils could form a uropod in the backside after exposure to the fMLP concentration gradient (Figure 6A-B): If neutrophils were pre-incubated with rhSema4D, less neutrophils formed a uropod (Figure 8A-C). Simultaneously with the formation of uropods, the concentration of PSGL-1 but not CD11b changed on the plasma membrane of these uropods and rhSema4D suppressed the PSGL-1 concentration on the activated neutrophils significantly. (Figure 8A-C).

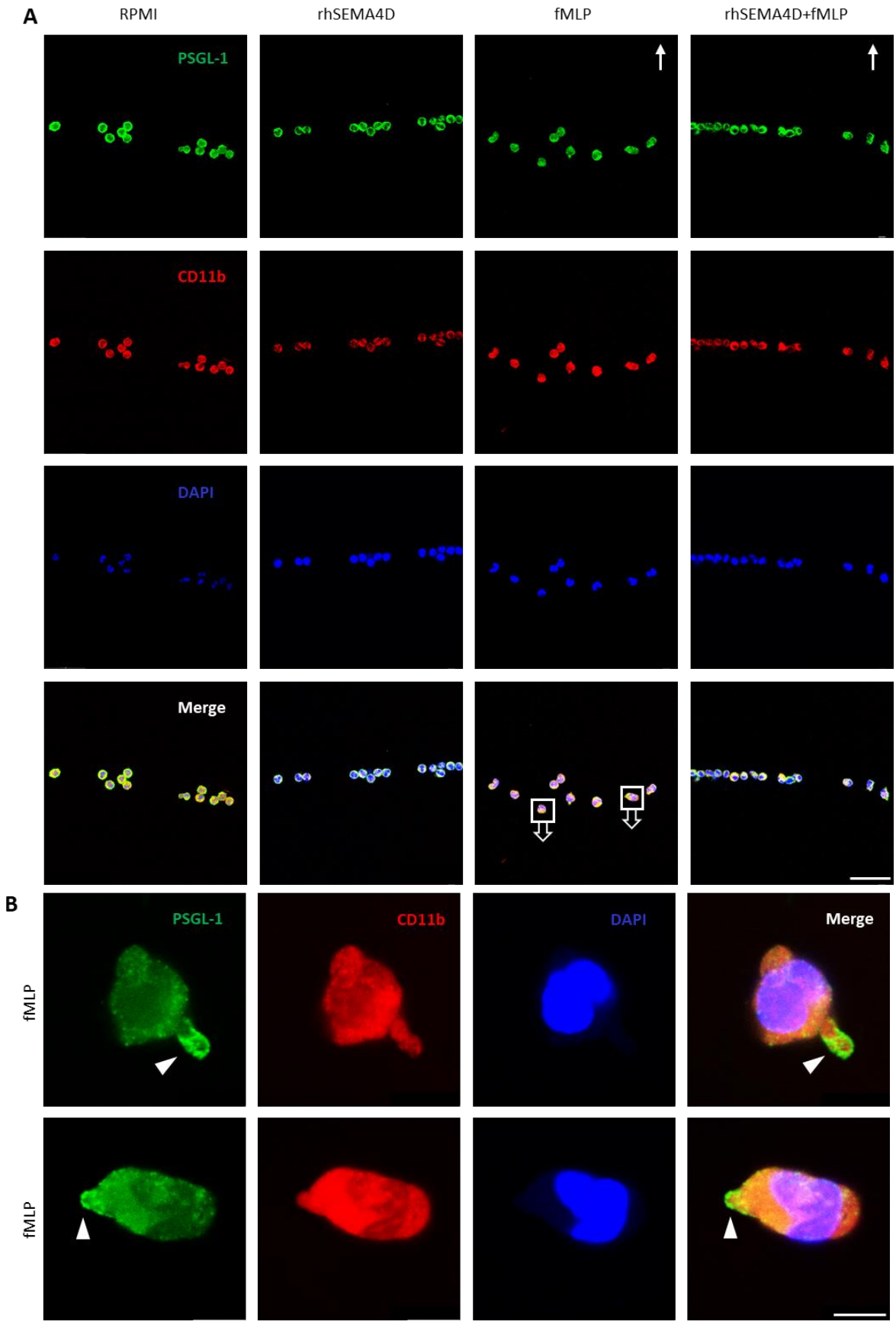
A
RPMI
rhSEMA4D
fMLP
rhSEMA4D+fMLP
PSGL-1
CD11b
DAPI
Merge
B
fMLP
fMLP
PSGL-1
CD11b
DAPI
Merge

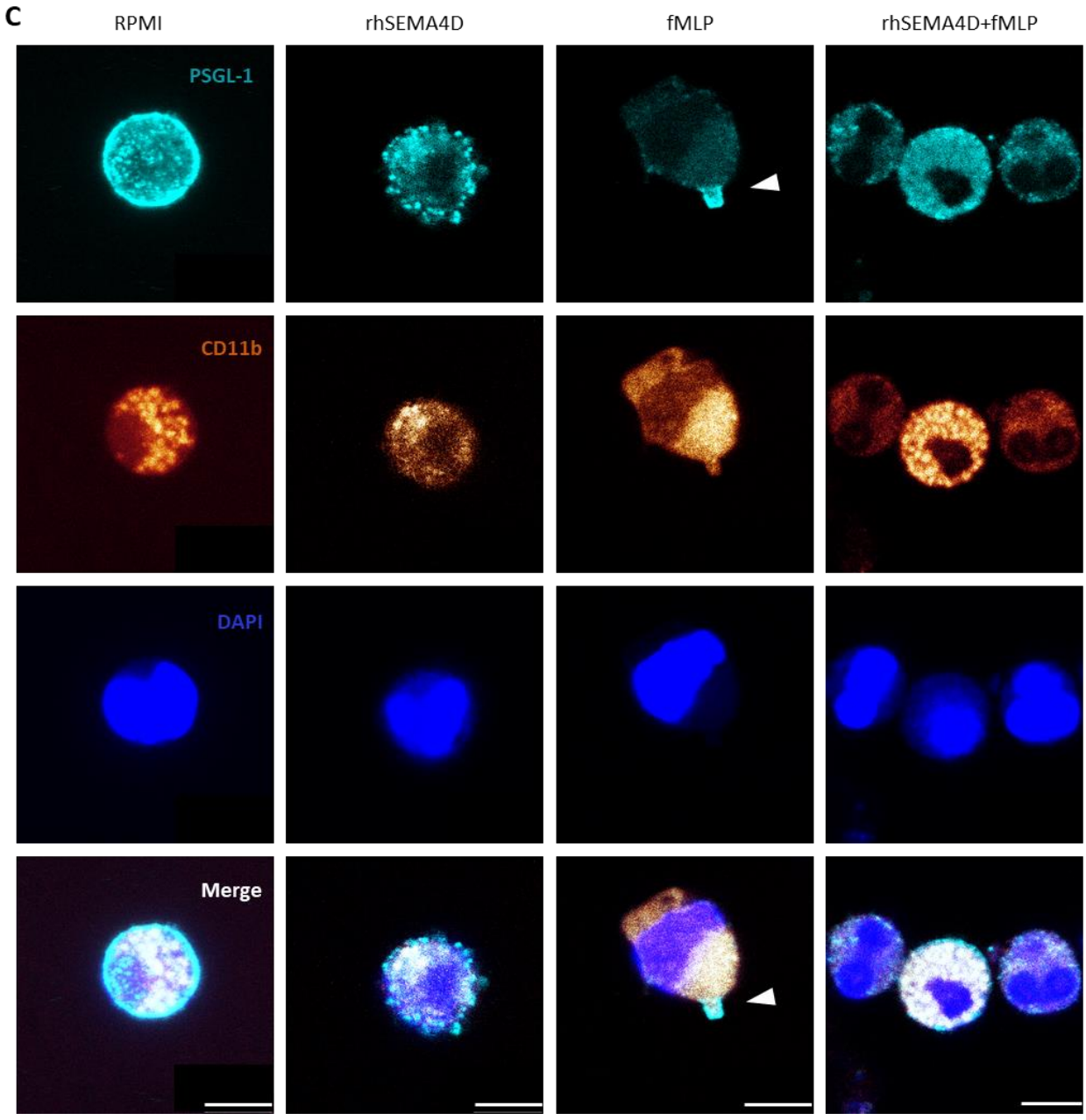
C
RPMI
rhSEMA4D
fMLP
rhSEMA4D+fMLP
PSGL-1
CD11b
DAPI
Merge

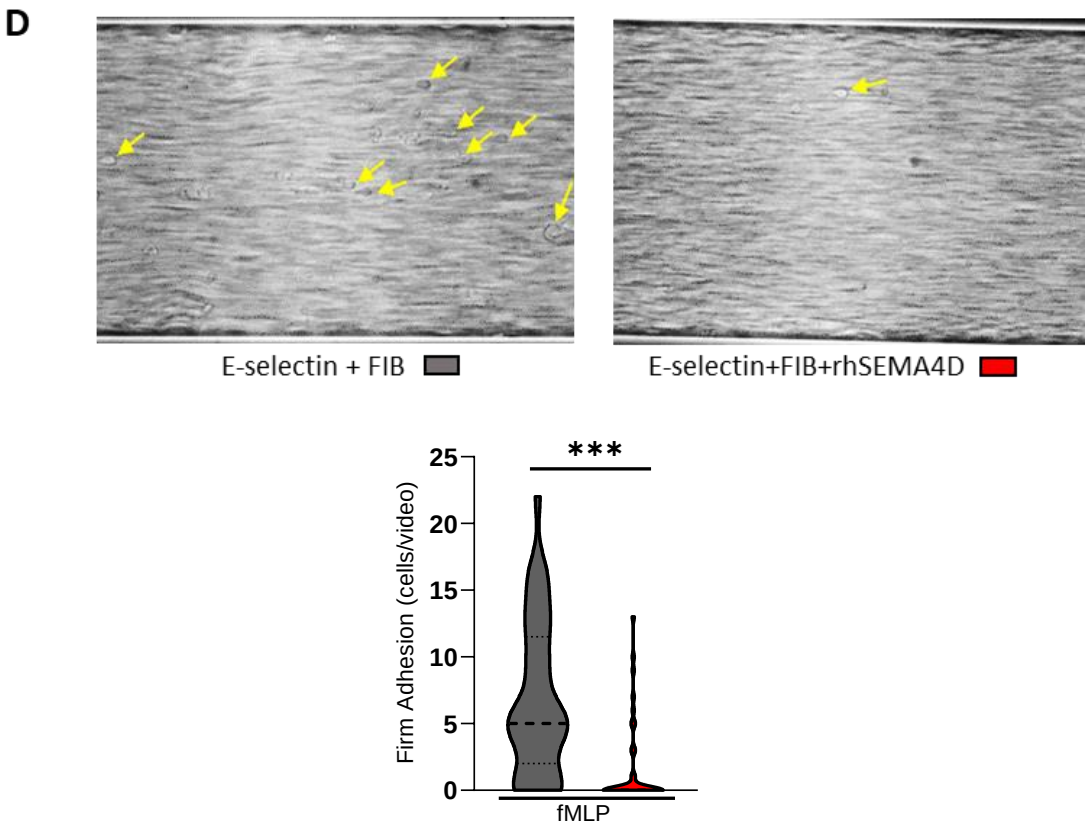

Figure 8. Sema4D inhibits neutrophil uropod formation and firm adhesion in inflammation.

(A) Representative micrographs of human neutrophils incubated with or without rhSEMA4D (1 µg/ml) followed by exposure to fMLP concentration gradient (arrows point to the direction of higher concentration) for 15 minutes. Two neutrophils marked with squares were zoomed-in to show the detailed cell shape and distribution of proteins. Arrowheads point to the uropod **(B). (C)** Representative zoom-in micrographs of human neutrophils for all the groups from the same experiments show the detailed cell shape and uropod of neutrophils (arrowheads). **(D)** Representative pictures from videos of firmly adhered human leukocytes in flow chamber experiments which were performed in E-selectin (3.0 µg/ml), fibrinogen (100 µg/ml), and/or rhSEMA4D (2 µg/ml) pre-coated capillaries. Human whole blood was initially stimulated with fMLP (10 ng/ml) for 210 minutes. Blood was taken from 3 independent donors, n=3; *** $P < 0.001$, as determined by a two-tailed unpaired t-test. Scale bar, (A) 35µm, (B) & (C) 5µm.

As uropod formation is critical for firm adhesion of neutrophils, we performed flow chamber experiments to explore whether Sema4D influences leukocyte firm

adhesion. Human whole blood was pre-incubated with fMLP for 3.5 hours and then examined in capillaries pre-coated with E-selectin and fibrinogen. Under these conditions some of the leukocytes got firmly adhered to the capillary surface and could not be flushed away by strong shear stress induced by the high-speed blood flow. Without fMLP stimulation or exclusively with an E-selectin coating, there is no firm adhesion of leukocytes to the surface. Interestingly the firmly adhered leukocytes were fixed locally only by a small area at the backward of the cells (similar to the uropod), while the main body of the cells was floating and were stretched into the shape of a droplet (Figure 8D). Supporting our previous observations in rhSema4D coated capillaries, much fewer fMLP-stimulated leukocytes got firmly adhered to the pre-coated E-Selectin and fibrinogen capillary-surface (Figure 8D).

3.4 Sema4D regulates the Rho GTPase family proteins and consequently influences the intracellular cytoskeleton in neutrophils

After the chemoattractant binds to GPCR on neutrophils, the small Rho GTPase activates and re-arranges the intracellular cytoskeleton system, which provides mechanical force for polarization. In general, Rac1 or Cdc42 are activated in the leading edge to promote F-actin polymerization which pushes the cell membrane to protrude forward. Simultaneously RhoA is activated in the cell rear and stimulates the myosin contraction to form the uropod. After we found that Sema4D inhibits the neutrophil polarization in a chemoattractant concentration gradient, we hypothesized that Sema4D performs this function by influencing the Rho GTPase family and the intracellular cytoskeleton. To verify this, isolated neutrophils were exposed to fMLP with or without rhSema4D pre-incubation. Then IF analysis was performed to observe changes in RhoA and F-actin expression levels. Consistently with previous literature, the expression of RhoA and F-actin was not polarized in stationary neutrophils, while after exposure to the fMLP concentration gradient, F-actin polymerization led to protrusion of neutrophils in the leading edge, whereas at the same time, RhoA was intensively localized in the rear where the F-actin polymerization was significantly inhibited (arrow in Figure 9A). Following this, we investigated the influence of Sema4D on the cytoskeleton. F-actin polymerization

was significantly increased after fMLP stimulation and rhSema4D inhibited F-actin polymerization in activated neutrophils (Figure 9B-C).

To further understand the function of Sema4D comprehensively and quantitatively, we performed proteomics analysis with isolated human neutrophils which were incubated with or without rhSema4D for 15 minutes. In the heatmap obtained from proteomics analysis (Figure 9D), we could see that protein members of the Rho GTPase family, including RhoA (RHOA) and Rac2 (RAC2), were regulated after rhSema4D treatment. Subsequently the intracellular cytoskeleton system, for example, actin (ACTB) and myosin units (MYH10, MYH1) were influenced. At the same time, Sema4D also significantly regulated radixin (RDX) and alpha-actinin-1 (ACTN1) in neutrophils, which are critical for anchoring actin to the plasma membrane, or for linking the actin to intracellular structures, respectively. From the enrichment ratio analysis (Figure 9E), we verified again that the MAPK signaling pathway, the Rho GTPase pathway, and the actin cytoskeleton pathway in the neutrophils were regulated by Sema4D. These fundamental changes could subsequently influence the pathways of leukocyte chemotaxis function, leukocyte migration function, negative regulation of leukocyte cell-cell adhesion and adherens junction interactions.

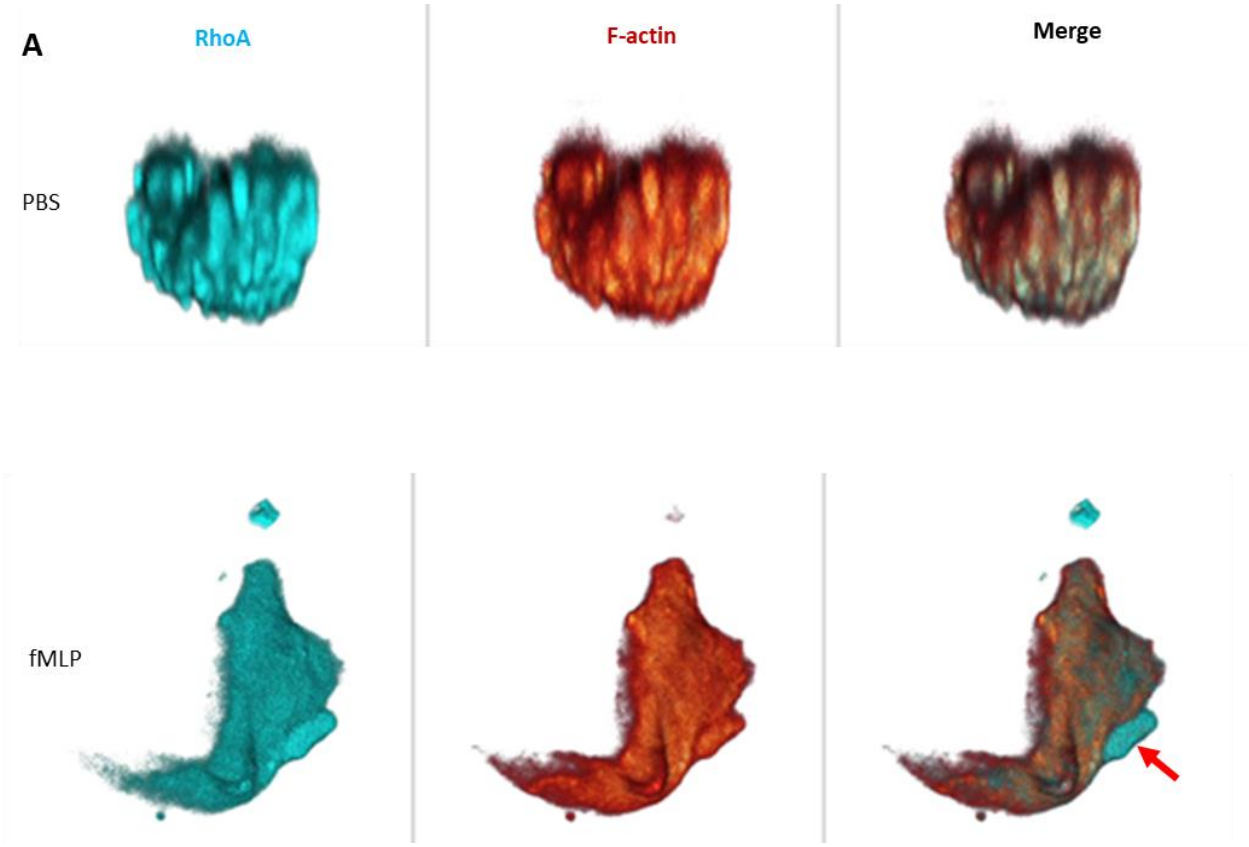
A
RhoA
F-actin
Merge
PBS
fMLP

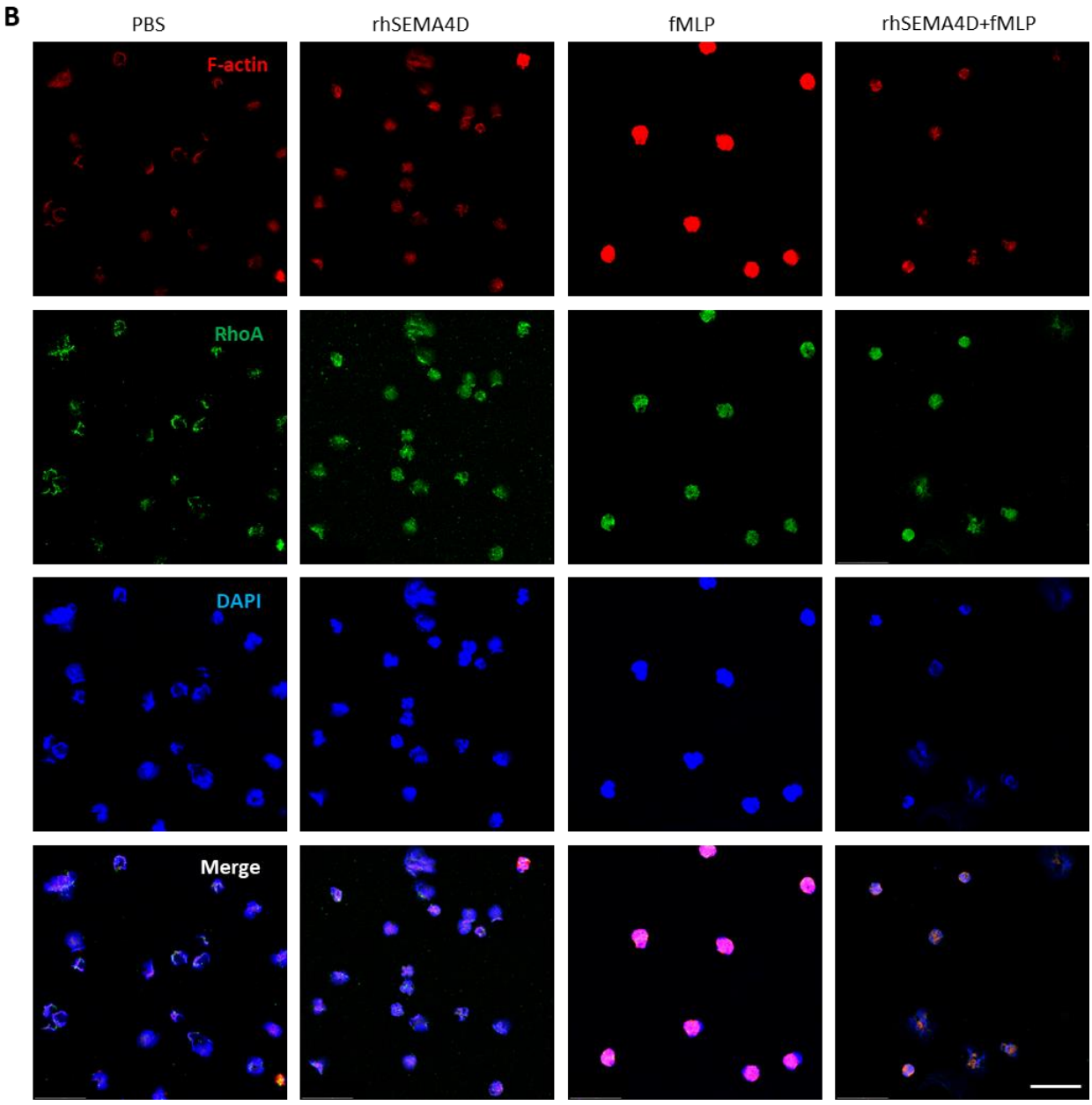
B
PBS
rhSEMA4D
fMLP
rhSEMA4D+fMLP
F-actin
RhoA
DAPI
Merge
C
***
***
***
100
50
0
F-actin / norm. IF intensity
NaCl
fMLP
PBS
rhSEMA4D

D

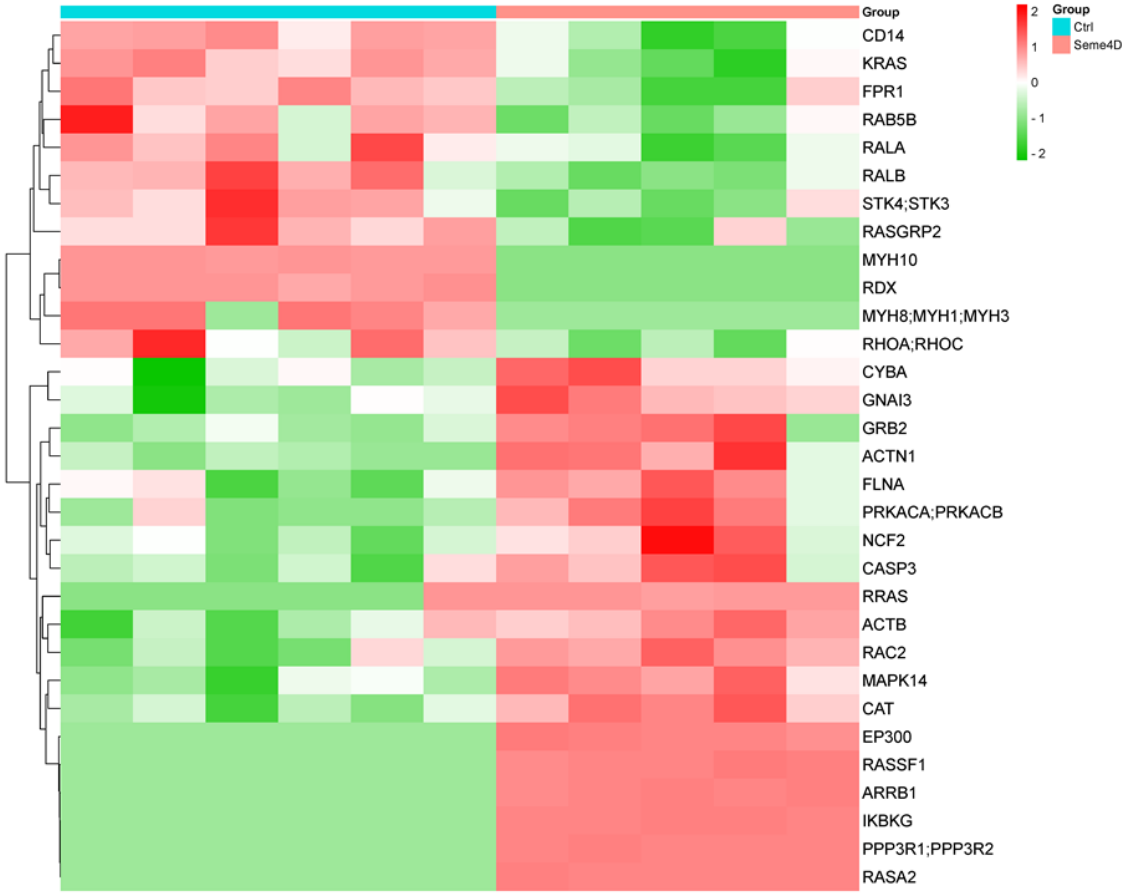
Group
CD14
KRAS
FPR1
RAB5B
RALA
RALB
STK4;STK3
RASGRP2
MYH10
RDX
MYH8;MYH1;MYH3
RHOA;RHOC
CYBA
GNAI3
GRB2
ACTN1
FLNA
PRKACA;PRKACB
NCF2
CASP3
RRAS
ACTB
RAC2
MAPK14
CAT
EP300
RASSF1
ARRB1
IKBKG
PPP3R1;PPP3R2
RASA2
Group
Ctrl
Seme4D
2
1
0
- 1
- 2

E

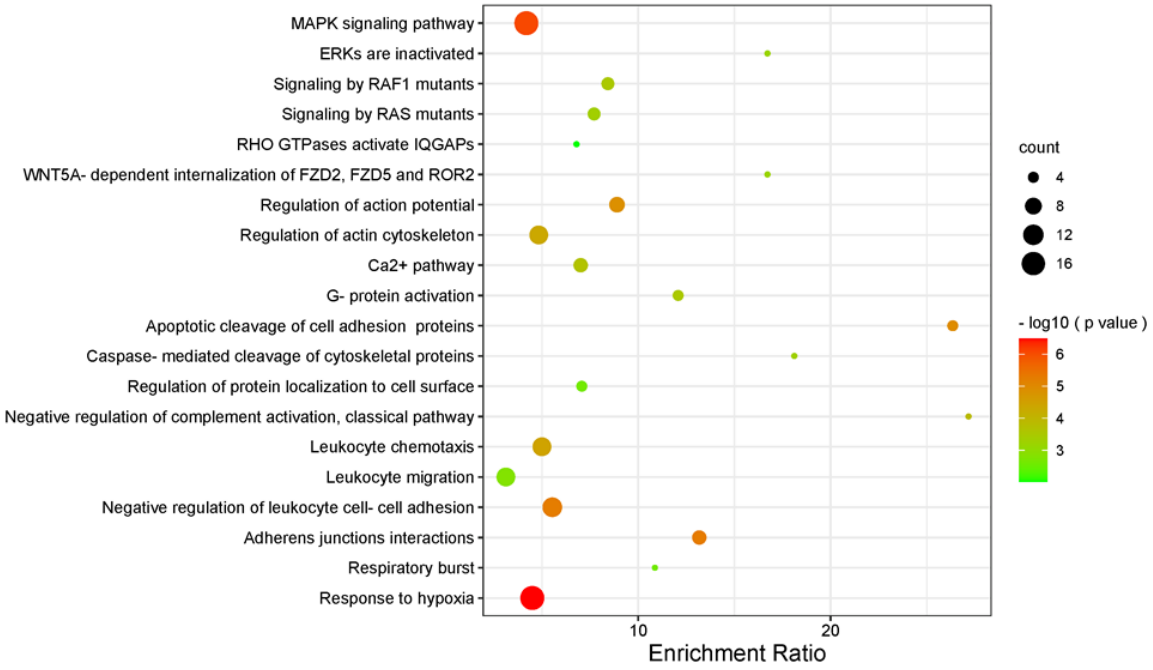
MAPK signaling pathway
ERKs are inactivated
Signaling by RAF1 mutants
Signaling by RAS mutants
RHO GTPases activate IQGAPs
WNT5A- dependent internalization of FZD2, FZD5 and ROR2
Regulation of action potential
Regulation of actin cytoskeleton
Ca2+ pathway
G- protein activation
Apoptotic cleavage of cell adhesion proteins
Caspase- mediated cleavage of cytoskeletal proteins
Regulation of protein localization to cell surface
Negative regulation of complement activation, classical pathway
Leukocyte chemotaxis
Leukocyte migration
Negative regulation of leukocyte cell- cell adhesion
Adherens junctions interactions
Respiratory burst
Response to hypoxia
10
20
Enrichment Ratio
count
4
8
12
16
- log10 (p value)
6
5
4
3

Figure 9. Sema4D regulates Rho GTPase family proteins and consequently influences the intracellular cytoskeleton in neutrophils.

(A) Expression of RhoA and F-actin on human neutrophils in chemotaxis. Percoll density gradient - isolated human neutrophils were exposed to fMLP concentration gradient or PBS in chemotaxis chambers for 15 minutes. Immunofluorescence was performed with anti-RhoA antibody and rhodamine Phalloidin for F-actin staining. **(B)** Representative micrographs of RhoA and F-actin expression on human neutrophils which were pre-incubated with or without rhSEMA4D (1 µg/ml) followed by exposure to fMLP (10 ng/ml) or NaCl for 15 minutes. **(C)** Quantification of immunofluorescence intensity of F-actin on neutrophils of these experiments. **(D, E)** Proteomics analysis of human neutrophils isolated with percoll density gradient method and incubated with or without rhSEMA4D (1 µg/ml). The enrichment ratio **(E)** was calculated with https://metascape.org. Enrichment plot **(E)** and heatmap **(D)** were plotted by http://www.bioinformatics.com.cn. For A and B, n = 171 - 233 cells from 3 independent experiments with 3 healthy donors. * $P < 0.05$; ** $P < 0.01$; *** $P < 0.001$, as determined by an ordinary one-way ANOVA, followed by multiple comparisons with Šídák's test. Scale bar, 35 µm.

3.5 Sema4D inhibits neutrophil polarization through binding to its receptors PlxnB1 and PlxnB2.

After we confirmed that Sema4D inhibits neutrophil polarization by regulating the intracellular cytoskeleton, we investigated how Sema4D executes its influence through its receptors. There are three main receptors for Sema4D from previous literature: PlxnB1, PlxnB2, and CD72. BioGPS cDNA database and previous literature show that PlxnB1 and PlxnB2 are highly expressed on myeloid lineage cells, including neutrophils. CD72 is only highly expressed on $CD19^+$ B cells but not myeloid lineage cells and therefore we focused on the role of PlxnB1 and PlxnB2 in our project. We again performed chemotaxis experiments using the human neutrophils isolated with percoll density gradient method. Neutrophils were pre-incubated with anti-PlxnB1 or anti-PlxnB2 antibody, with or without rhSema4D, followed by exposure to fMLP concentration gradient for 15 minutes. Analysis of the length-width ratio revealed that when PlxnB1 or PlxnB2 receptors are blocked, the variation between neutrophils with and without Sema4D incubation was not significant anymore (Figure 10A, B). Both blocking the PlxnB1 receptor and the

PlxnB2 receptor eliminated the inhibitive function of Sema4D. Interestingly, without giving Sema4D, only blocking PlxnB1 or PlxnB2 on stimulated neutrophils leads to a contrary change in neutrophils polarization: blocking PlxnB1 reduced the polarization of neutrophils, while blocking PlxnB2 leads to an increased transformation of neutrophils, what shows in the length-width ratio in the micrographs (Figure 10A, B).

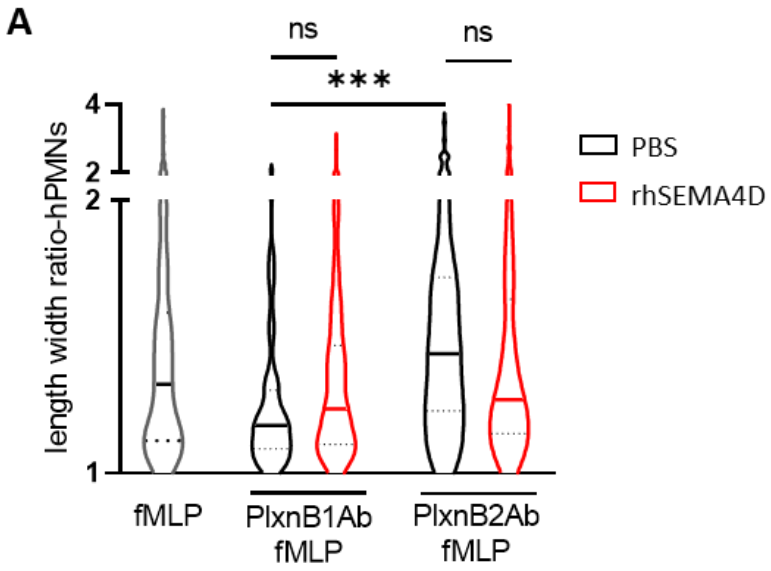

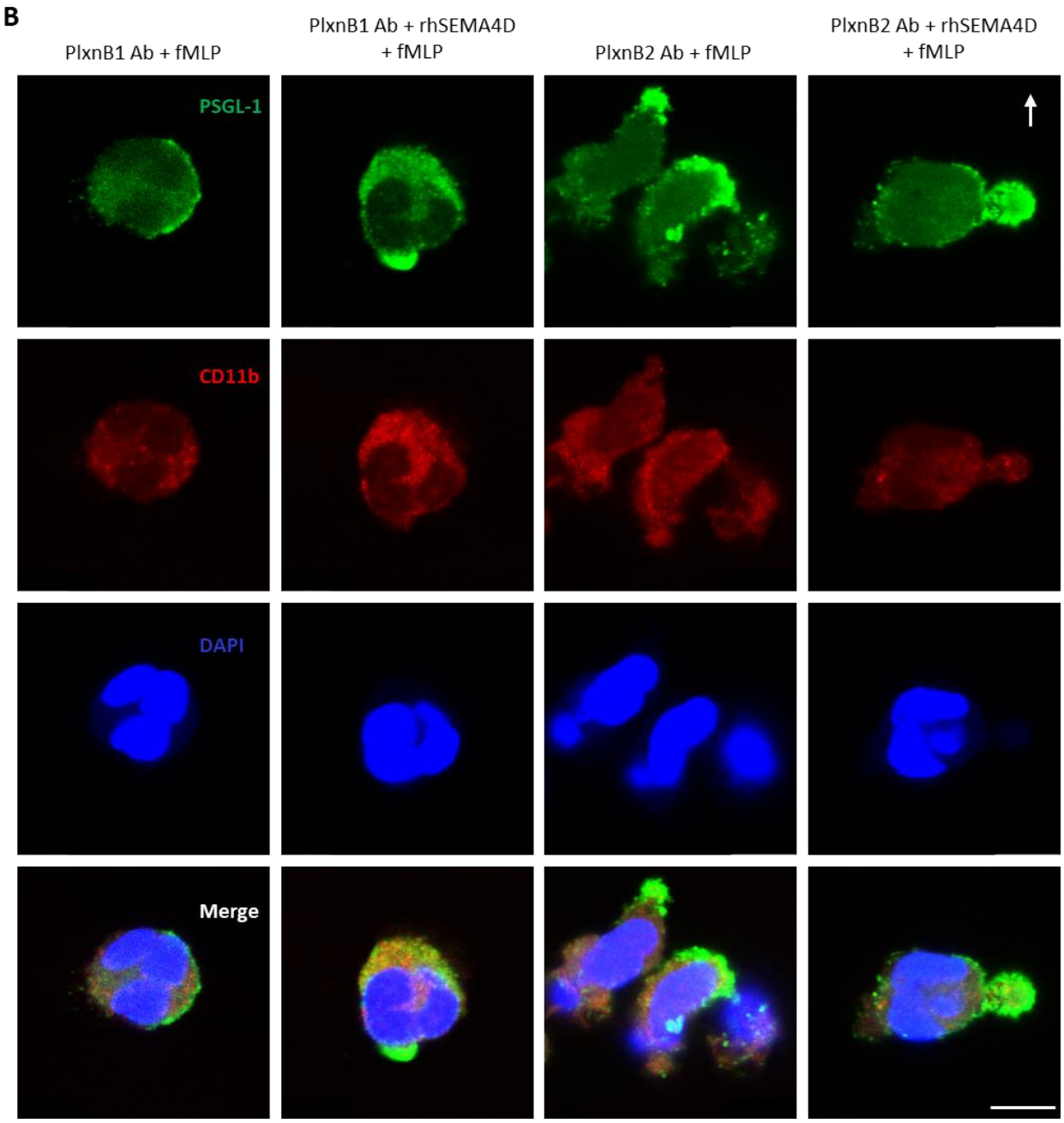

Figure 10. Sema4D inhibits neutrophil polarization through binding to its receptors PlxnB1 and PlxnB2.

(A) Representative micrographs of human neutrophils which were isolated with percoll density gradient and pre-incubated with PlxnB1 antibody (PlxnB1Ab; 10 µg/ml) or PlxnB2 antibody (PlxnB2Ab; 10 µg/ml), subsequently with or without rhSEMA4D (1 µg/ml) treatment, followed by exposure to fMLP concentration gradient for 15 minutes. **(B)** Quantification of neutrophil polarization in micrographs from these experiments by length-width ratio; n = 86 - 208 cells from 3 independent experiments with 3 healthy donors. *** P

< 0.001, ns = not significant, P > 0.05, as determined by an ordinary one-way ANOVA, followed by multiple comparisons with Šídák's test. Scale bar, 5μm.

3.6 The expression of Sema4D and its receptors on neutrophils declines in inflammation

Neutrophils are the first recruited defensive immune cells in inflammation and their activation is critical for inflammatory actions. We proved that Sema4D inhibits neutrophils adhesion and polarization through its receptors PlxnB1 and PlxnB2. Subsequently, we wondered whether this inhibitive function controls all neutrophils in the peripheral blood continuously, even when it is necessary for neutrophils to be activated in inflammation. Therefore, we evaluated the expression of Sema4D and its receptors on neutrophils under primary and inflammatory conditions. We performed IF staining to investigate their expression levels in isolated human neutrophils which were stimulated with fMLP or NaCl as control. Micrographs illustrated strong expression of Sema4D and PlxnB2 on stationary neutrophils, while after fMLP stimulation neutrophil Sema4D and PlxnB2 expression declined (Figure 11A-C). Subsequently, we verified this expression reduction in vivo in LPS induced lung injury model. WT BALB/c mice were inhaled with LPS for 45 minutes and incubated for 4 hours to induce acute lung injury. Neutrophils in blood and BAL were then examined with flow cytometry as the Ly6G positive population in samples. The expression of Sema4D on neutrophils in whole peripheral blood was not changed significantly. On the contrary, the transmigrated neutrophils (in BAL) expressed significantly less Sema4D in acute lung injury (Figure 11D).

We also performed flow cytometry to assess the expression of PlxnB1 and PlxnB2 on neutrophils in blood, BAL, or resected and digested left lungs in murine LPS induced acute lung injury model. In lung injury mice, the number of neutrophils that have transmigrated into BAL, or adhered in the lung significantly increased compared to control mice (Figure 11E), which is consistent with the expectation. The expression of PlxnB1 and PlxnB2 on neutrophils reduced dramatically, especially on the adherent and transmigrated neutrophils, but not on the circulating neutrophils in peripheral blood (Figure 11F, G).

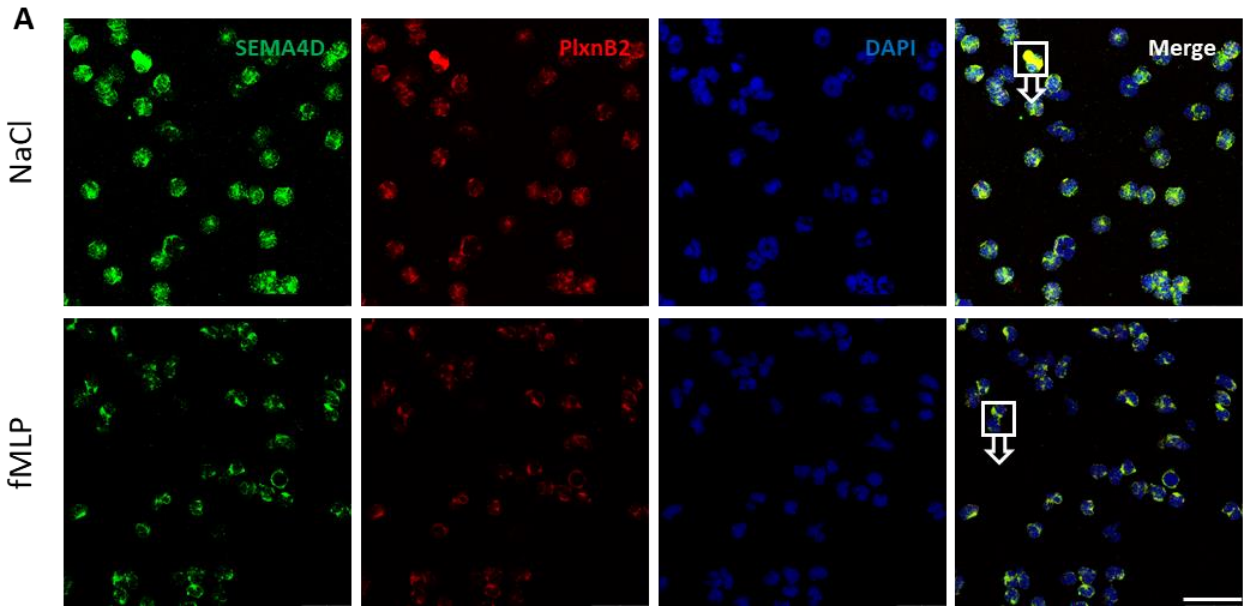
A
NaCl
fMLP
SEMA4D
PlxnB2
DAPI
Merge

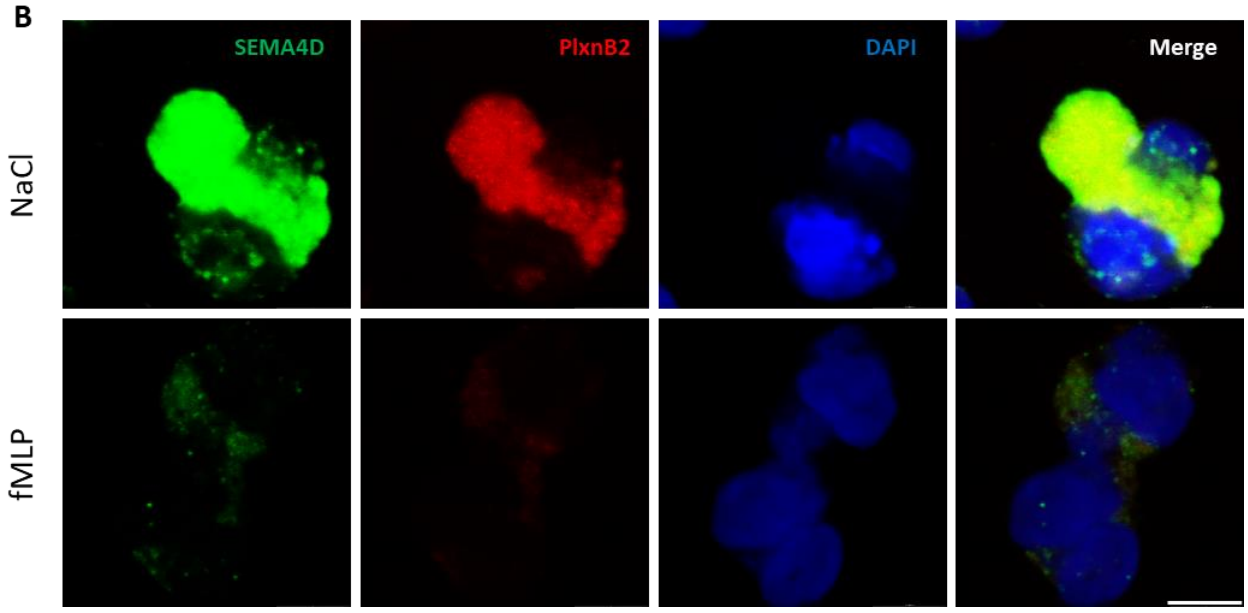
B
NaCl
fMLP
SEMA4D
PlxnB2
DAPI
Merge

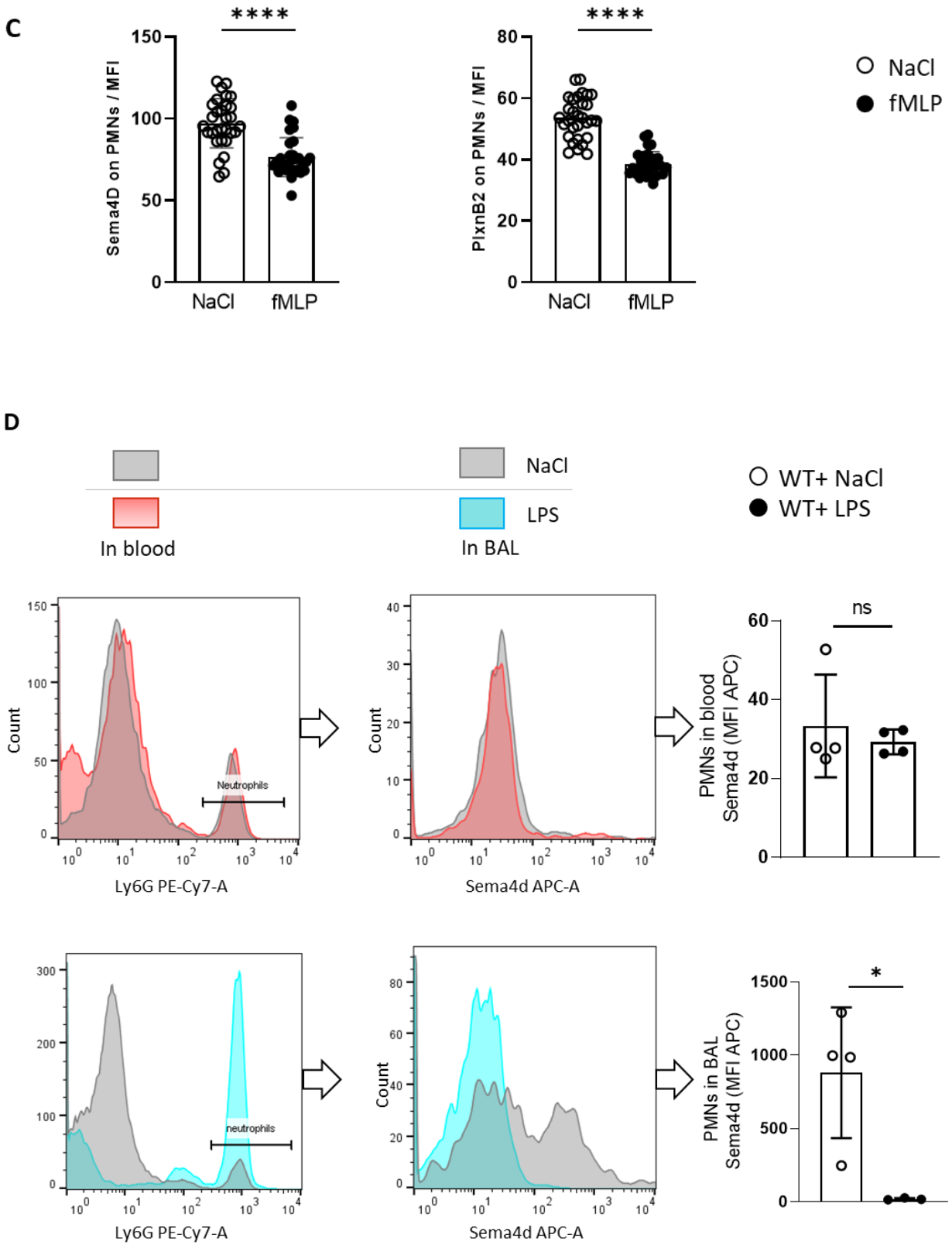
C
****
Sema4D on PMNs / MFI
150
100
50
0
NaCl
fMLP
****
PlxnB2 on PMNs / MFI
80
60
40
20
0
NaCl
fMLP
NaCl
fMLP
D
NaCl
LPS
In blood
In BAL
WT+ NaCl
WT+ LPS
Count
Neutrophils
Ly6G PE-Cy7-A
Sema4d APC-A
PMNs in blood
Sema4d (MFI APC)
ns
neutrophils
PMNs in BAL
*

E

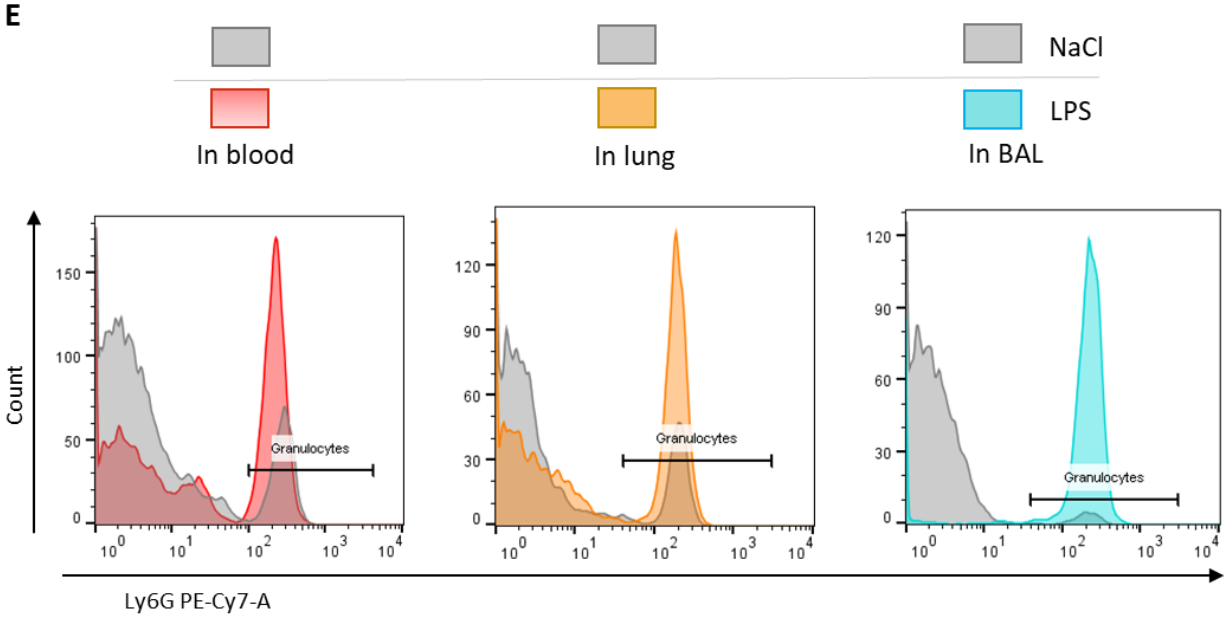
NaCl
LPS
In blood
In lung
In BAL
Count
Granulocytes
Granulocytes
Granulocytes
Ly6G PE-Cy7-A

F

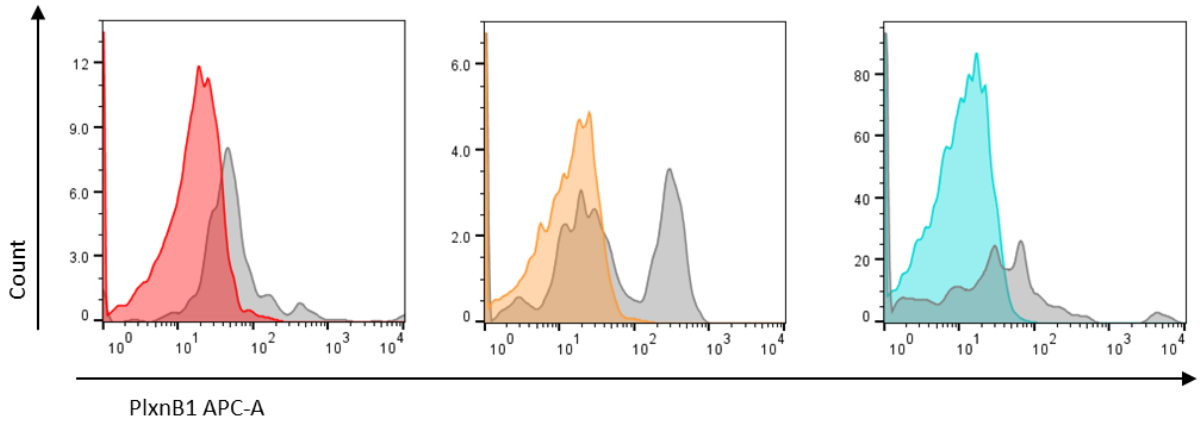
Count
PlxnB1 APC-A

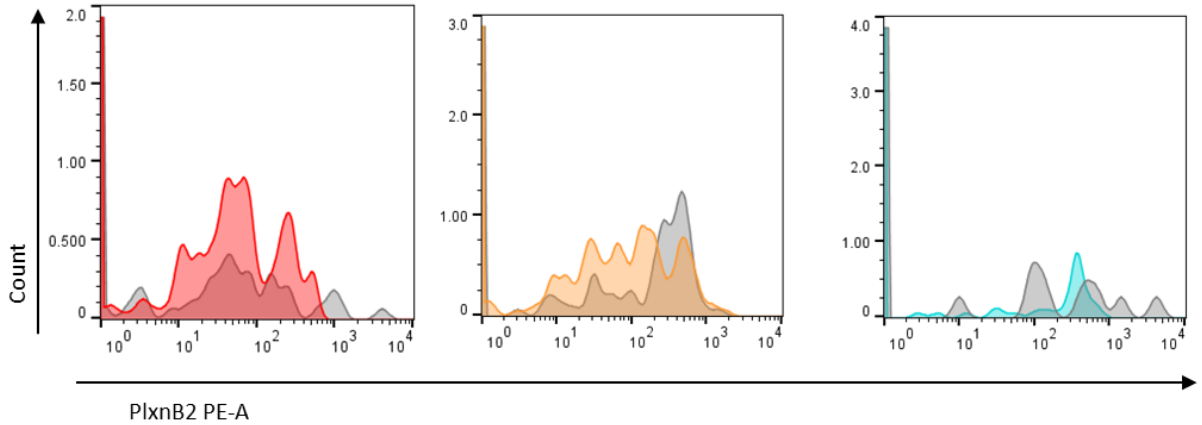
Count
PlxnB2 PE-A

G

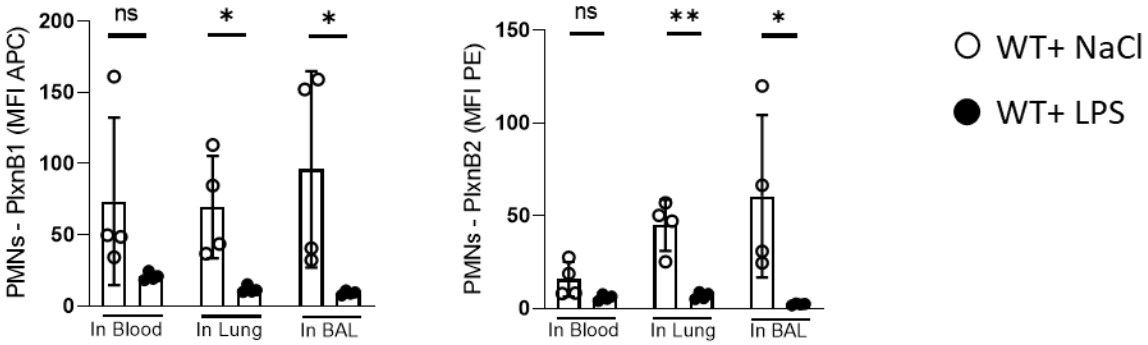

Figure 11. Expression of Sema4D and its receptors on neutrophils declines in inflammation.

(A) & **(B)** Representative micrographs of IF for Sema4D and PlxnB2 expression on human neutrophils exposed to NaCl or fMLP (10 ng/ml) for 15 minutes. **(C)** Quantification of MFI for Sema4D and PlexinB2 on PMNs in the micrographs in the same experiment. **(D)** Flow cytometry for Sema4d expression on neutrophils in blood and BAL from mice. NaCl or LPS inhalation was performed in WT BALB/c mice for 45 minutes followed by 4 hours incubation. Neutrophils were determined as Ly6G positive population. **(E)** Representative histogram and gating strategy for neutrophils by flow cytometry for PlxnB1 and PlxnB2 expression. NaCl or LPS inhalation was performed in WT BAL/c mice for 45 minutes and incubated for 4 hours. Neutrophils in blood and BAL were harvested directly after lysis the erythrocytes in samples. Neutrophils in the lungs were isolated from resected and digested left lungs. In analysis, neutrophils were determined as Ly6G positive population. **(F)** Representative histogram graphs for PlxnB1 and PlxnB2 expression on neutrophils in blood, lung, and BAL from NaCl or LPS inhaled mice. **(G)** MFI of PlxnB1 and PlxnB2 on neutrophils in blood, lung, and BAL from NaCl or LPS inhaled mice. For A, n=3 independent experiments from 3 donors. For B-E, n=4 mice. * $P < 0.05$; ** $P < 0.01$; *** $P < 0.001$, ns = not significant, $P > 0.05$, as determined by a two-tailed unpaired t-test. Values are presented as means ± SD. Scale bar 35 µm (A), 5 µm (B).

3.7 Inflammation induces increase in Sema4D expression on pulmonary endothelial and epithelial cells

Pulmonary endothelial and epithelial cells play an important role in ARDS, as they regulate the tissue liquid homeostasis and inflammatory cell accumulation in the lung interstitium and alveolar space during inflammation. Therefore, we explored

the expression of Sema4D on pulmonary endothelial and epithelial cells and its change in inflammation. We performed flow cytometry with pulmonary cells which were isolated from flushed, resected, and digested left lungs in murine LPS induced acute lung injury model. The endothelial cells were gated as CD144 (vascular endothelial cadherin, VE-cadherin) positive population and epithelial cells as CD326 (Epithelial cell adhesion molecule, EpCAM) positive population (Figure 10 A). In acute injury lung, both epithelial and endothelial cells expressed more Sema4d than under noninflammatory conditions (Figure 12A). The IF micrographs of lung tissue illustrated the same tendency, that on vWF marked endothelium (Figure 12B) and cytokeratin marked epithelium (Figure 12C), the expression of Sema4d increased significantly after LPS inhalation.

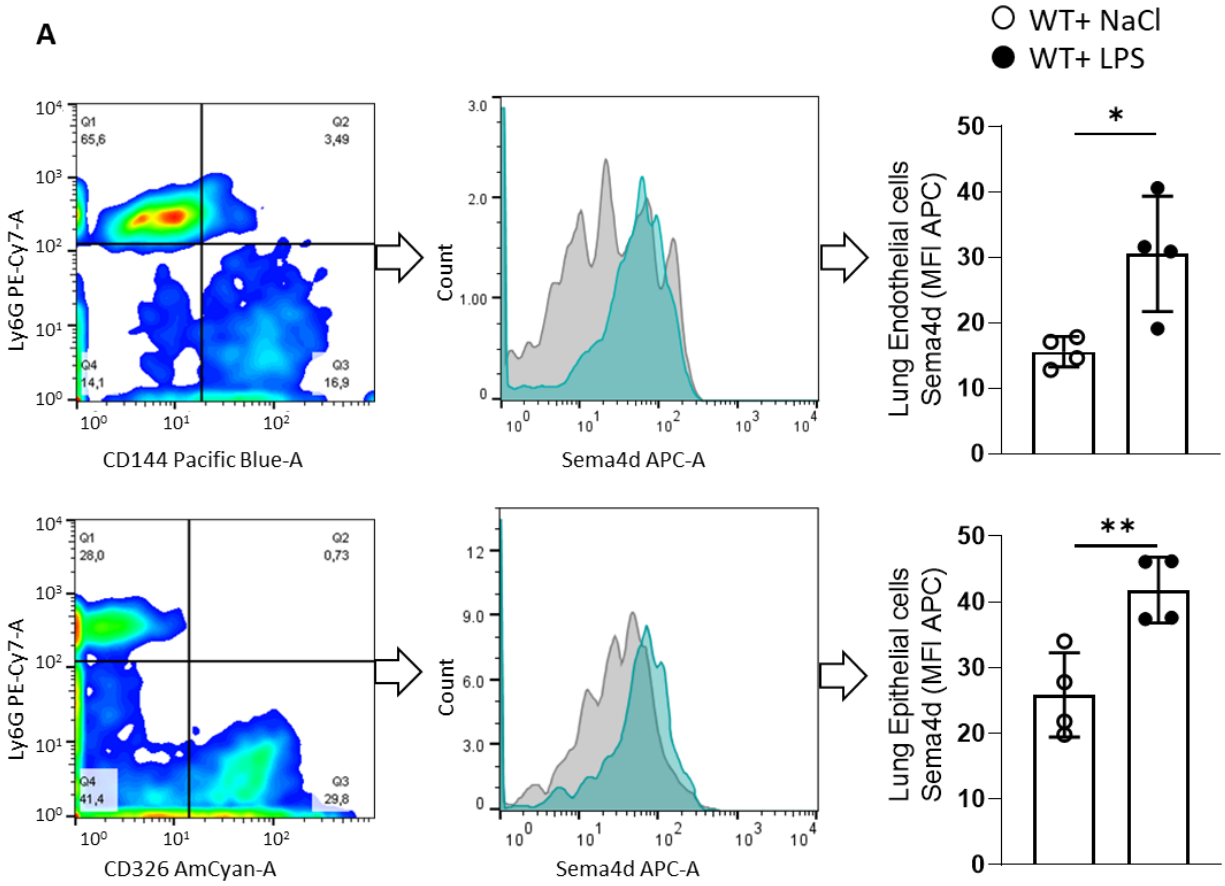

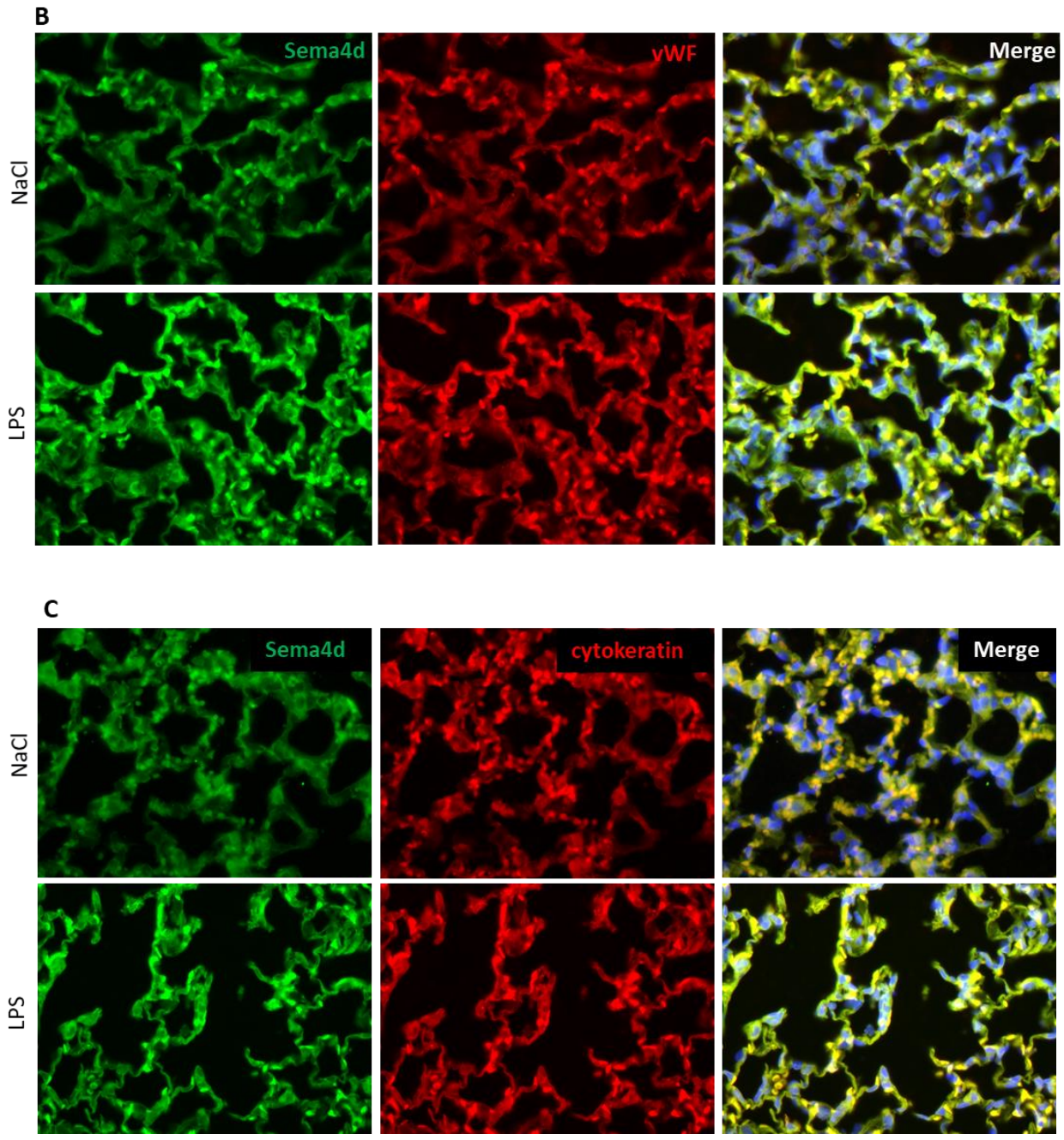

Figure 12. The expression of Sema4D on pulmonary epithelial and endothelial cells increases in inflammation.

(A) Flow cytometry for Sema4d expression on murine pulmonary epithelial and endothelial cells. NaCl or LPS inhalation was performed in WT BALB/c mice for 45 minutes followed by 4 hours incubation time. Pulmonary cells were isolated from flushed, resected, and digested left lungs. Endothelial cells were determined as $CD144^{+}$ $Ly6G^{-}$ population, and epithelial cells were determined as $CD326^{+}$ $Ly6G^{-}$ population. **(B-C)** Representative

micrographs of Sema4d expression on pulmonary endothelial cells (marked with vWF) **(B)** and epithelial cells (marked with cytokeratin) **(C)** in mice after NaCl or LPS inhalation. Micrographs were taken with the magnification x400. For A, n=4. For B, n=3. * $P < 0.05$; ** $P < 0.01$; *** $P < 0.001$, as determined by a two-tailed unpaired t-test. Values are shown as means ± SD.

3.8 Sema4D deficiency leads to a more aggressive inflammatory reaction in acute lung injury

To verify the significance of Sema4D in acute lung injury, we employed Sema4d-deficient (*Sema4d*$^{-/-}$) and WT BALB/c mice in the LPS inhalation model. Bronchoalveolar lavage (BAL) was harvested and investigated after 45 minutes of LPS inhalation and 24 hours of incubation. Under non-inflammatory conditions, both WT and *Sema4d*$^{-/-}$ mice recruited only a few cells in BAL. While in the acute lung injury the number of accumulated cells in BAL increased in both groups as expected, while *Sema4d*$^{-/-}$ mice recruited significantly more cells than the WT mice (Figure 13A). For the concentration of protein and inflammatory cytokines (TNFα, IL6, and MIP2) in BAL, even in the NaCl inhalation group *Sema4d*$^{-/-}$ mice are significantly higher than in WT mice (Figure 13B, D). After LPS induced acute lung injury, *Sema4d*$^{-/-}$ mice showed significantly higher concentration of protein, TNFα, IL6, and MIP2 than the WT mice (Figure 13B, D). Of note, Sema4d deficiency did not significantly influence MPO or KC in BAL in LPS induced lung injury, despite pulmonary inflammation led to a dramatic increase (Figure 13C, D).

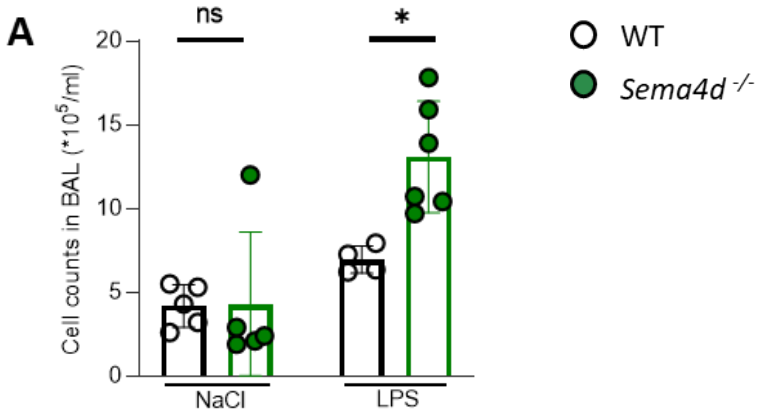

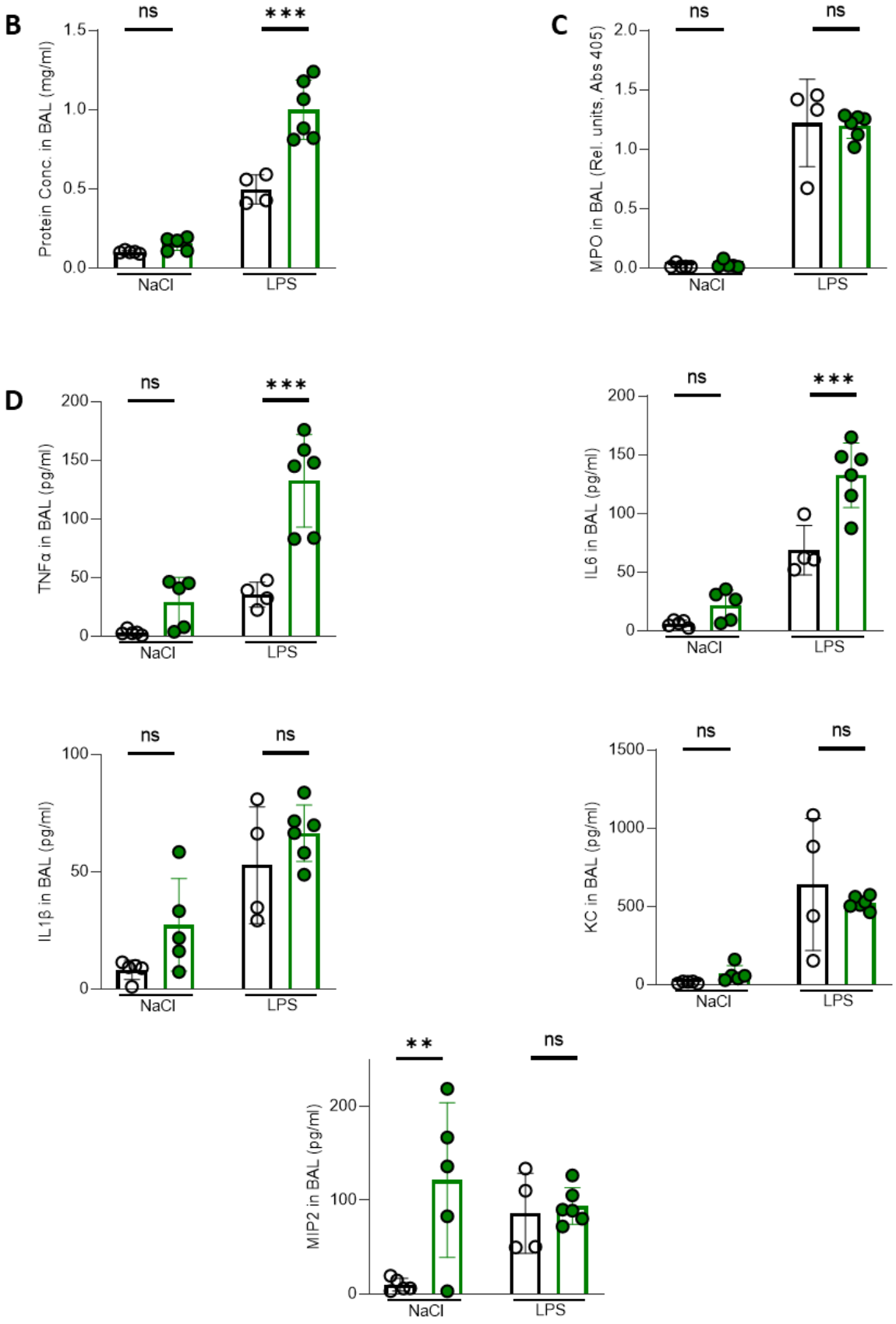
B
Protein Conc. in BAL (mg/ml)
1.5
1.0
0.5
0.0
ns
***
NaCl
LPS
C
MPO in BAL (Rel. units, Abs 405)
2.0
1.5
1.0
0.5
0.0
ns
ns
NaCl
LPS
D
TNFα in BAL (pg/ml)
200
150
100
50
0
ns
***
NaCl
LPS
IL6 in BAL (pg/ml)
200
150
100
50
0
ns
***
NaCl
LPS
IL1β in BAL (pg/ml)
100
50
0
ns
ns
NaCl
LPS
KC in BAL (pg/ml)
1500
1000
500
0
ns
ns
NaCl
LPS
MIP2 in BAL (pg/ml)
200
100
0
**
ns
NaCl
LPS

Figure 13. Sema4D deficiency leads to a more aggressive inflammatory reaction in acute lung injury.

NaCl or LPS inhalation was administered in *Sema4d*$^{-/-}$ and WT BALB/c mice for 45 minutes followed by 24 hours incubation time to induce lung injury. Bronchoalveolar lavage (BAL) was harvested and investigated for **(A)** cell counts, **(B)** protein concentration, **(C)** MPO assay, and **(D)** inflammatory cytokines TNFα, IL6, IL1β, KC and MIP2 (ELISAs). n = 4 - 6 mice per group. * $P < 0.05$; ** $P < 0.01$; *** $P < 0.001$, ns = not significant $P > 0.05$; as determined by an ordinary one-way ANOVA, followed by multiple comparisons with Šídák's test. Values are displayed as means ± SD.

4. Discussion

ARDS is a high mortality syndrome with excessive public health impact[4-6]. It is the common reason for acute respiratory failure and mechanical ventilation in ICUs all over the world[5,6] and the pandemic of COVID-19 undoubtedly increases the incidence of ARDS fiercely. It is of great significance to search for interventions that can prevent or treat ARDS.

In pathophysiology, ARDS is characterized by aggressive inflammation which consequently induces, or synchronously companies with epithelial and endothelial barrier function injury[23-27]. In the process of inflammation, leukocytes, especially neutrophils recruitment into the lung interstitial or alveolar space plays fundamental roles[34-36]. In this research project, we illustrate for the first time that Sema4D and its receptors PlxnB1 and PlxnB2 inhibit neutrophil polarization and adhesion, and subsequently influence the recruitment of neutrophils into lung interstitial and alveolar space. For these reasons, they control the extent and severity of the inflammation in the lungs.

The neutrophil extravasation cascade is initiated by the process of neutrophil adhesion, which is mainly dependent on the interactions of selectins with PSGL-1 and integrins with adhesion molecules and fibrinogen[43,53,54,60-62,66-70]. Our study showed that Sema4D significantly inhibits leukocytes adhesion to inflammatory endothelium which is characterized by expression of E-selectin and fibrinogen. Although we did not find a significant influence of Sema4D on the cell surface expression of integrins, including LFA-1 (CD11a/CD18), MAC-1 (CD11b/CD18), and VLA4 (CD49d/CD29). The fibrinogen binding assay reveal the obvious inhibitive function of Sema4D, which could explain the mechanism for Sema4D inhibitive function towards leukocyte adhesion on fibrinogen coating surface. As we know from the literature[60] that neutrophils bind to fibrinogen through Mac-1, but the expression level of Mac-1 on neutrophils were not significantly influenced by Sema4d in our experiments, so we hypothesize that Sema4D reduces the affinity of neutrophils MAC-1 to its ligand fibrinogen. In accordance with a previous study, E-selectin expressed on the inflammatory endothelial cells is critical in inducing neutrophil adhesion and its binding to PSGL-1 on neutrophils triggers an affinity

modification of MAC-1 but without changing the expression level[63].This may account why in our flow chamber studies, in the absence of E-selectin coating, leukocytes did not adhere to the capillary surface. Comprehensive analysis of the above results suggests that Sema4D inhibits E-selectin – PSGL-1 interaction induced affinity upregulation of MAC-1 to its ligand fibrinogen, and this inhibition reduces neutrophil adhesion onto the inflammatory endothelial cells.

Neutrophil polarization provides the primary force for cell motility and subsequently is critical for effective neutrophil recruitment to the site of inflammation. When neutrophils polarize, they form a leading edge towards the chemoattractant gradient and a uropod on the averted side, which transforms neutrophils from round to irregular shape. Synchronously the membranal proteins are trafficked and redistributed to cooperate with other components in the surrounding environment. For the first time our experiments show that Sema4D suppresses the polarization of neutrophils in a chemoattractant concentration gradient. In addition to inhibition of neutrophil morphological change which is evaluated with length-width ratio, Sema4D also restrains the concentrated redistribution of PSGL-1 from the overall membrane to the uropod which plays critical roles to influence neutrophils adhesion and transmigration[46,53,54]. Redistribution and accumulation of PSGL-1 at the uropod enhances firm adhesion of the uropod while releasing the leading edge of neutrophils to facilitate subsequent crawling and searching for proper transmigration sites. Just as we have seen in our flow chamber experiments, the firm adhered neutrophils were fixed on the capillary surface by a small ‘contact point’ at the backsides, while the main cell bodies were floating freely in the blood flow in droplet shape, and Sema4D reduced the amount of firmly adhered neutrophils onto the E-selectin and fibrinogen coated capillaries significantly.

Both neutrophil morphological change and redistribution of membranal proteins are dependent on the rearrangement of the cytoskeleton, including actin polymerization and myosin activation, which is regulated by the small Rho GTPases[39-41]. In great concordance with literature[39-41], we proved in our study again that, exposure of neutrophils to chemoattract gradient induced F-actin to polymerization at the leading edge and produced protrusions, meanwhile on the

backside RhoA aggregated to activate myosin contraction. Sema4D inhibits F-actin polymerization significantly in inflammation-activated neutrophils, which explains the mechanism of its inhibitive function in neutrophil polarization.

Proteomics analysis revealed that Sema4D regulates the small Rho GTPases RhoA and Rac, subsequently influence myosin and actin. In detail, Sema4D inhibits the activation of myosin heavy chain 10 (MYH10, also named non-muscle myosin IIB) significantly, which is critical for cell polarization, adhesion, and migration[140]. MYH10 regulates cell protrusion through cooperation with actin filaments[141], controls the maturation of cell adhesion through influencing integrins clustering and affinity[142], and promotes cell polarization by contracting to form the rear of the cells to break cell symmetry[143]. Additionally, Sema4D probably also regulates neutrophil myosin I activation which is critical for nucleus dynamic deformation during transmigration through 3D enviroments[144].

The proteomics analysis proved that actin is also regulated by Sema4D, together with filamin A (FLNA) which links the cytoskeleton to membranal receptors including integrins and therefore influences neutrophils adhesion[145]. Different from the inhibitory function of Sema4D towards RhoA and myosin, our proteomics analysis showed that Sema4D upregulates the expression of Rac and actin polymerization. One possible reason is that our proteomics analysis was performed under non-inflammatory conditions. In immunofluorescence experiments Sema4D also seems to promote actin polymerization in noninflammatory condition. However, in inflammatory condition Sema4D restrains the polymerization of actin.

Our proteomics analysis suggested that Rac2, but not Rac1, is significantly regulated by Sema4D in neutrophils, this result is slightly inconsistent from previous study which shows that Sema4D inhibits activation of Rac1 significantly by $PlxnB_2$[130]. Rac subfamily includes Rac1, Rac2, Rac3 and RhoG. The expression and distribution of Rac1-3 is different, Rac1 is expressed in various tissues, Rac3 expression is restricted to central nervous system (CNS), while Rac2 is mainly expressed by hematopoietic cell lineages[146]. Rac2 is critical for the recruitment of neutrophils and macrophages to the inflammatory sites, but exogenous expression of Rac1 could comparatively restore neutrophils motility in $Rac2^{-/-}$ zebrafish[146],

indicating that the functions of Rac1 and Rac2 are to some extent overlapping. This subject can be further clarified in the upcoming research.

Nevertheless, we should keep in mind that all small GTPases employ GTP/GDP binding switch to fulfil their dynamic responsibility towards cytoskeletons. Guanine nucleotide exchange factors (GEFs) induce the GDP releasing and GTP binding to activate them, and GTPase activating proteins (GAPs) promote GTP hydrolysis to inactivate the small GTPases[147]. The regulation of Sema4D towards Rac and Cdc42 mainly depends on this mechanism[42-44]. The guanine dissociation inhibitors (GDIs) inhibit the dissociation of GDP from RhoA to keep it inactive, and Sema4D blocks Rho GDI to activate RhoA[43,45]. The alternation of GTP/GDP binding could not be investigated by proteomics analysis but by other specialized experiments which will be conducted hereafter.

The inhibitory function of Sema4D in neutrophil polarization depends on both receptors PlxnB1 and PlxnB2. In our research we demonstrated that blocking of both receptors abolished the suppressing effect of Sema4D towards neutrophils polarization. Previous study suggested that Sema4D activates PlxnB1 by phosphorylating its intracellular tyrosine residues and subsequently mediates RhoA activation[148,149], while PlxnB2 interacts with Rac and Cdc42 and downregulates activation and subsequently inhibits cell motility[150]. Inside the neutrophils the intensive cooperation and interaction of RhoA, Rac and Cdc42 for cell motility have been well revealed[151,152]. In general, Rho is activated at the posterior part of cells to trigger the actin-myosin-based contractile stress fibers formation, while Rac and Cdc42 are activated in the leading edge of cells to promote actin polymerization and the formation of lamellipodia and filopodia, respectively[151,152]. Cdc42 increase could subsequently induces Rac and RhoA activation[153]. Combining all the information and the proteomics analysis we assume that Sema4D binds to PlxnB1 to inhibit the activation of RhoA and to suppress the actin-myosin-based contractile stress fibers formation. But in our proteomics analysis the Rac2 and actin were upregulated by Sema4D in non-inflammatory condition, which was also proven by IF for F-actin. This confliction of results probably is induced by different neutrophils condition, since the fMLP-stimulated

neutrophils showed significantly inhibited F-actin polymerization by Sema4D, which is perhaps due to PlxnB2 activation by Sema4D.

Interestingly we found in our study that only blocking PlxnB1 in inflammatory condition led to relative round and less polarized neutrophils, while blocking PlxnB2 induced neutrophil aggressive polarization and lamellipodia and filopodia formation at the leading edge. This phenotype is consistent with studies that have proven that PlxnB2 knockout macrophages show higher motility [150]. We assume that probably blocking PlxnB1 activates RhoA through loss of the inhibitory effect, and subsequently myosin is activated to contract and restrict the protrusion of cell. While blocking PlxnB2 leads to Rac and Cdc42 activation to promote the formation of lamellipodia and filopodia. Further detailed studies are needed to finally confirm these conclusions.

From above, we can conclude that Sema4D inhibits the polarization and activation of neutrophils by binding to its receptors PlxnB1 and PlxnB2. Is this inhibitory function of Sema4D permanently active? What if neutrophils need to polarize and transmigrate effectively, for instance, in inflammatory conditions? Our study revealed that the expression of PlxnB1 and PlxnB2 on activated neutrophils declines significantly, especially on the neutrophils which have adhered to the pulmonary vessel or transmigrated into the lung alveolar space, while their expression on neutrophils in the peripheral blood still keeps in the high level. This significant decrease of PlxnB1 and PlxnB2 expression will diminish the inhibitory function of Sema4D towards neutrophils and theoretically produce the same phenotype as blocking these receptors, which is activation of the small GTPase and subsequently reorganizes the intercellular cytoskeleton. The mechanism of downregulated expression of PlxnB1 and PlxnB2 is still not totally clarified by now.

Consistent with previous reports in the literature[129,130], our study also demonstrated that Sema4D is cleaved off from neutrophils membrane under inflammatory conditions. The cleavage of Sema4D is mainly performed by a disintegrin and metalloprotease 17 (ADAM17), and releases a soluble fragment of Sema4D (sSema4D)[130,154]. In concordance with this, the concentration of sSema4D in human serum or plasma has been shown to be increased in various

inflammatory diseases, including different types of autoimmune disease such as multiple sclerosis (MS)[155], rheumatoid arthritis (RA)[156] and infections[124]. The level of sSema4D correlates with severity of inflammatory disease[129]. The evidence to date on the immunological function of sSEMA4D is contradictory. Some researchers demonstrated sSema4D as a proinflammatory stimulator which could prompts inflammatory cytokines IL-12[157], TNFα, and IL-6[156] release. However, it has also been proven to inhibit monocytes and DCs migration[158].

On the contrary with declined expression of Sema4D on neutrophils, its expression on pulmonary endothelial cells and epithelial cells are increased in inflammation. Sema4D has been proven to trigger invasive growth of epithelial cells by binding to PlxnB1, in which Sema4D promotes cell dissociation, unanchored growth, and the occurrence of branching morphology[159]. It has also been confirmed to facilitate angiogenesis by inducing endothelial cells chemotaxis and tube formation through PlxnB1 on endothelial cells[148]. Sema4D is significantly induced in head and neck squamous cell carcinoma (HNSCC) cells in hypoxia and contributes to the adaptive responses to lower oxygen concentration[160]. But the function of Sema4D expressed on endothelial cells or epithelial cells has not been well established by now. In our research we demonstrate the inhibitory function of Sema4D towards neutrophils activation, polarization and transmigration, and in this circumstance, the increased expression of Sema4D on pulmonary endothelial and epithelial cells in inflammation is not surprisingly unexpected. We hypothesize that the increased expression of Sema4D is probably a negative feedback mechanism, which inhibits excessive neutrophils migration into the lung interstitial and alveolar spaces in inflammation, and therefore controls the severity of pulmonary inflammation. Concurrent with the decreased expression of PlxnB1 and PlxnB2 on activated neutrophils, these sophisticated changes orchestrate a perfect working mechanism that on one hand ensures efficient migration of activated neutrophils, while on the other hand restraining the activation and transmigration of neutrophils in the peripheral circulation.

This hypothesis was also to some extent demonstrated in our in vivo experiments which showed that *Sema4D*$^{-/-}$ mice experienced more severe inflammatory reaction

than WT mice under equivalent exogenous injury stimuli. *Sema4D*$^{-/-}$ mice recruited more leukocytes into the alveolar space, and consonant with higher concentration of pro-inflammatory cytokines, including TNFα and IL6. Knocking-out Sema4D leads to an aggressive inflammatory reaction in acute lung injury. This again demonstrates the importance of the inhibitory function of Sema4D for neutrophil activation and recruitment in inflammation, but the concentration of myeloperoxidase (MPO) in BAL was not significantly increased in *Sema4D*$^{-/-}$. We could not find direct scientific knowledge to explain these seemingly contradictory results. We assume that this is because Sema4D also plays important roles in the intracellular oxygen metabolism, which has been proven by numerous researches in various cell lines[160,161].

In summary, our research initially demonstrates that Sema4D regulates the activation of small GTPase RhoA and Rac in neutrophils, which subsequently regulates the activation of intracellular cytoskeleton, including F-actin and myosin, and ultimately inhibits neutrophils polarization, adhesion and activation. This function depends on binding to its receptors PlxnB1 and PlxnB2. In inflammatory condition, activated neutrophils decrease the expression of PlxnB1 and PlxnB2 on the cell surface, which abolishes the inhibitory function of Sema4D and ensures the necessary adhesion, polarization and transmigration of neutrophils. In inflammatory lung, epithelial and endothelial cells express more Sema4D on their surface and probably this is an important negative feedback mechanism to restrain the severity of pulmonary inflammation.

5. Summary

Objectives Acute respiratory distress syndrome (ARDS) is a high mortality syndrome with excessive public health impact. It is of great significance to search for interventions that can prevent or treat ARDS effectively. In pathophysiology, ARDS is characterized by aggressive inflammation in which neutrophils recruitment into the lung interstitial or alveolar space plays a fundamental role. This research aimed to investigate the function of semaphorin4D (Sema4D) in regulating neutrophils adhesion, polarization, and transmigration, consequently illustrate its involvement in the pathogenesis of ARDS.

Methods Leukocyte adhesion was evaluated in flow chamber experiments. The fibrinogen binding assay and the expression of integrins on neutrophils were performed by flow cytometry (FACS). The neutrophil polarization was induced by fMLP concentration gradient in chemotaxis chambers and investigated by immunofluorescence (IF). Proteomics assay and IF was employed for the pathway molecular mechanism investigation. The expression of Sema4D and its receptors PlxnB1 and PlxnB2 was evaluated with IF and flow cytometry in vitro and in vivo model. Sema4D knock-out mice were used to determine the severity of inflammation in the lung with BCA assay for protein concentration, ELISA for inflammatory cytokines, and MPO assay.

Results Sema4D inhibited leukocytes adhesion at the inflammatory site by influencing their affinity for binding fibrinogen. Sema4D suppressed neutrophils polarization, the redistribution of PSGL-1 to the uropod, and subsequently neutrophil firm adhesion in inflammation. These processes are depending on Sema4D binding to its receptors PlxnB1 and PlxnB2. The proteomics analysis showed that Sema4D regulated the activation of RhoA and Rac, and subsequently influenced the F-actin and myosin activation. In inflammation, the expression of Sema4D and its receptors declined on neutrophils, but the expression of Sema4D on pulmonary endothelial and epithelial cells increased significantly. Sema4D deficiency led to increased inflammatory action in the lung.

Conclusions Sema4D inhibits neutrophils polarization and adhesion, subsequently influence the recruitment of neutrophils into lung interstitial and alveolar space, and control the severity of inflammatory action in the lung. This function depends on its binding to PlxnB1 and PlxnB2 through which Sema4D regulates the activation of RhoA and Rac,

subsequently influences the intracellular cytoskeleton activation. This enables Sema4D to become a promising therapeutic target for ARDS.

6. German summary

Objectives Das akute Atemnotsyndrom (ARDS) ist ein Syndrom mit hoher Sterblichkeit und erheblichen Auswirkungen auf die öffentliche Gesundheit. Es ist von großer Bedeutung Maßnahmen zu finden, die eine ARDS wirksam verhindern oder behandeln und heilen können. In der Pathophysiologie ist das ARDS durch eine aggressive Entzündung gekennzeichnet, bei der die Rekrutierung von Neutrophilen Granulozyten in den interstitiellen oder alveolären Raum der Lunge eine wesentliche Rolle spielt. Ziel dieser Forschung war es, die Funktion von Semaphorin4D (Sema4D) bei der Regulierung der Adhäsion, Polarisierung und Transmigration von Neutrophilen Granulozyten zu untersuchen und seine Beteiligung an der Pathogenese des ARDS zu verdeutlichen.

Methoden Die Adhäsionsfunktion von Leukozyten wurde in Flusskammerexperimenten untersucht. Der Fibrinogenbindungsassay und die Expression von Integrinen auf Neutrophilen Granulozyten wurden mittels Durchflusszytometrie durchgeführt. Die Polarisierung der Neutrophilen Granulozyten wurde in einer Chemotaxiskammer über einen fMLP-Konzentrationsgradienten induziert und über Immunfluoreszenz (IF) dargestellt und analysiert. Für die Untersuchung des molekularen Mechanismus wurden Proteomics-Untersuchungen und IF eingesetzt. Die Expression von Sema4D und seinen Rezeptoren wurde mit IF dargestellt und mittels Durchflusszytometrie in vitro und in vivo gemessen. Mit Sema4D-Knock-out-Mäusen wurde der Schweregrad der Entzündung in der Lunge mittels Proteinkonzentration (BAC-Assay), ELISAs für ausgewählte entzündliche Zytokine und MPO-Assay untersucht.

Ergebnisse Indem Sema4D die Affinität der Bindung von Fibrinogen beeinflusste, hemmte es die die Adhäsion von Leukozyten am Entzündungsherd. Sema4D unterdrückte die Polarisierung der Neutrophilen, in dem es die Umverteilung und Konzentration von PSGL-1 am Uropod unterdrückte und folglich die feste Adhäsion der Neutrophilen verhinderte. Die Wirkung von Sema4D war abhängig von seinen Rezeptoren PlxnB1 und PlxnB2. Die Analyse des molekularen Mechanismus zeigte, dass Sema4D die Aktivierung von RhoA und Rac reguliert und somit die Aktivierung von F-Actin und Myosin beeinflusst. In Entzündung verringerte sich die Expression von Sema4D und seinen Rezeptoren auf den neutrophilen Granulozyten, aber die Expression von Sema4D

auf Lungenendothel- und -epithelzellen nahm deutlich zu. Ein Mangel an Sema4D führte in der Lunge zu einer aggressiveren Entzündungsreaktion.

Schlussfolgerungen Sema4D hemmt die Polarisierung und Adhäsion von Neutrophilen, beeinflusst die Rekrutierung von neutrophilen Granulozyten im interstitiellen und alveolären Lungenraum und kontrolliert den Schweregrad der Entzündungsreaktion in der Lunge. Die durch Sema4D ausgelösten Entzündungsreaktionen sind abhängig von der Bindung an die Rezeptoren PlxnB1 und PlxnB2. Über diese Bindungen wird die Aktivierung von RhoA und Rac reguliert, wodurch die Aktivierung des intrazellulären Zytoskelett und somit die Zellmotilität beeinflusst wird. Dies macht Sema4D zu einem vielversprechenden therapeutischen Ziel im ARDS.

7. References

1. Matthay, M.A*., et al.* Acute respiratory distress syndrome. *Nat Rev Dis Primers* **5**, 18 (2019).
2. Ashbaugh, D.G., Bigelow, D.B., Petty, T.L. & Levine, B.E. Acute respiratory distress in adults. *Lancet* **2**, 319-323 (1967).
3. Bernard, G.R*., et al.* The American-European Consensus Conference on ARDS. Definitions, mechanisms, relevant outcomes, and clinical trial coordination. *Am J Respir Crit Care Med* **149**, 818-824 (1994).
4. Force, A.D.T*., et al.* Acute respiratory distress syndrome: the Berlin Definition. *JAMA : the journal of the American Medical Association* **307**, 2526-2533 (2012).
5. Rubenfeld, G.D*., et al.* Incidence and outcomes of acute lung injury. *N Engl J Med* **353**, 1685-1693 (2005).
6. Bellani, G*., et al.* Epidemiology, Patterns of Care, and Mortality for Patients With Acute Respiratory Distress Syndrome in Intensive Care Units in 50 Countries. *JAMA : the journal of the American Medical Association* **315**, 788-800 (2016).
7. Thille, A.W*., et al.* Comparison of the Berlin definition for acute respiratory distress syndrome with autopsy. *Am J Respir Crit Care Med* **187**, 761-767 (2013).
8. Ley, K., Laudanna, C., Cybulsky, M.I. & Nourshargh, S. Getting to the site of inflammation: the leukocyte adhesion cascade updated. *Nat Rev Immunol* **7**, 678-689 (2007).
9. Aghapour, M., Raee, P., Moghaddam, S.J., Hiemstra, P.S. & Heijink, I.H. Airway Epithelial Barrier Dysfunction in Chronic Obstructive Pulmonary Disease: Role of Cigarette Smoke Exposure. *Am J Respir Cell Mol Biol* **58**, 157-169 (2018).
10. Tilley, A.E., Walters, M.S., Shaykhiev, R. & Crystal, R.G. Cilia dysfunction in lung disease. *Annu Rev Physiol* **77**, 379-406 (2015).
11. Guillot, L*., et al.* Alveolar epithelial cells: master regulators of lung homeostasis. *Int J Biochem Cell Biol* **45**, 2568-2573 (2013).
12. Noreng, S., Bharadwaj, A., Posert, R., Yoshioka, C. & Baconguis, I. Structure of the human epithelial sodium channel by cryo-electron microscopy. *Elife* **7**(2018).
13. Enuka, Y., Hanukoglu, I., Edelheit, O., Vaknine, H. & Hanukoglu, A. Epithelial sodium channels (ENaC) are uniformly distributed on motile cilia in the oviduct and the respiratory airways. *Histochem Cell Biol* **137**, 339-353 (2012).
14. Sun, Y., Minshall, R.D. & Hu, G. Role of claudins in oxidant-induced alveolar epithelial barrier dysfunction. *Methods Mol Biol* **762**, 291-301 (2011).
15. Wittekindt, O.H. Tight junctions in pulmonary epithelia during lung inflammation. *Pflugers Arch* **469**, 135-147 (2017).
16. Dagenais, A*., et al.* Downregulation of ENaC activity and expression by TNF-alpha in alveolar epithelial cells. *Am J Physiol Lung Cell Mol Physiol* **286**, L301-311 (2004).
17. Komarova, Y.A., Kruse, K., Mehta, D. & Malik, A.B. Protein Interactions at Endothelial Junctions and Signaling Mechanisms Regulating Endothelial Permeability. *Circ Res* **120**, 179-206 (2017).
18. Del Vecchio, P.J*., et al.* Endothelial monolayer permeability to macromolecules. *Fed Proc* **46**, 2511-2515 (1987).
19. Corada, M*., et al.* Monoclonal antibodies directed to different regions of vascular endothelial cadherin extracellular domain affect adhesion and clustering of the protein and modulate endothelial permeability. *Blood* **97**, 1679-1684 (2001).
20. Carmeliet, P*., et al.* Targeted deficiency or cytosolic truncation of the VE-cadherin gene in mice impairs VEGF-mediated endothelial survival and angiogenesis. *Cell* **98**, 147-157 (1999).
21. Bach, T.L*., et al.* VE-Cadherin mediates endothelial cell capillary tube formation in fibrin and collagen gels. *Exp Cell Res* **238**, 324-334 (1998).

22. Potter, M.D., Barbero, S. & Cheresh, D.A. Tyrosine phosphorylation of VE-cadherin prevents binding of p120- and beta-catenin and maintains the cellular mesenchymal state. *J Biol Chem* **280**, 31906-31912 (2005).
23. Xiong, S.*, et al.* IL-1beta suppression of VE-cadherin transcription underlies sepsis-induced inflammatory lung injury. *J Clin Invest* **130**, 3684-3698 (2020).
24. Broermann, A.*, et al.* Dissociation of VE-PTP from VE-cadherin is required for leukocyte extravasation and for VEGF-induced vascular permeability in vivo. *J Exp Med* **208**, 2393-2401 (2011).
25. Ozaki, H.*, et al.* Cutting edge: combined treatment of TNF-alpha and IFN-gamma causes redistribution of junctional adhesion molecule in human endothelial cells. *J Immunol* **163**, 553-557 (1999).
26. Ostermann, G., Weber, K.S., Zernecke, A., Schroder, A. & Weber, C. JAM-1 is a ligand of the beta(2) integrin LFA-1 involved in transendothelial migration of leukocytes. *Nat Immunol* **3**, 151-158 (2002).
27. Ludwig, R.J.*, et al.* Junctional adhesion molecule (JAM)-B supports lymphocyte rolling and adhesion through interaction with alpha4beta1 integrin. *Immunology* **128**, 196-205 (2009).
28. Woodfin, A.*, et al.* The junctional adhesion molecule JAM-C regulates polarized transendothelial migration of neutrophils in vivo. *Nat Immunol* **12**, 761-769 (2011).
29. Bradfield, P.F.*, et al.* JAM-C regulates unidirectional monocyte transendothelial migration in inflammation. *Blood* **110**, 2545-2555 (2007).
30. Goodenough, D.A. & Paul, D.L. Gap junctions. *Cold Spring Harb Perspect Biol* **1**, a002576 (2009).
31. Liao, Y., Day, K.H., Damon, D.N. & Duling, B.R. Endothelial cell-specific knockout of connexin 43 causes hypotension and bradycardia in mice. *Proc Natl Acad Sci U S A* **98**, 9989-9994 (2001).
32. Krattinger, N.*, et al.* Connexin40 regulates renin production and blood pressure. *Kidney Int* **72**, 814-822 (2007).
33. Parthasarathi, K.*, et al.* Connexin 43 mediates spread of Ca2+-dependent proinflammatory responses in lung capillaries. *J Clin Invest* **116**, 2193-2200 (2006).
34. Steinberg, K.P.*, et al.* Evolution of bronchoalveolar cell populations in the adult respiratory distress syndrome. *Am J Respir Crit Care Med* **150**, 113-122 (1994).
35. Parsons, P.E., Fowler, A.A., Hyers, T.M. & Henson, P.M. Chemotactic activity in bronchoalveolar lavage fluid from patients with adult respiratory distress syndrome. *Am Rev Respir Dis* **132**, 490-493 (1985).
36. Weiland, J.E.*, et al.* Lung neutrophils in the adult respiratory distress syndrome. Clinical and pathophysiologic significance. *Am Rev Respir Dis* **133**, 218-225 (1986).
37. Mantripragada, K.C. & Quesenberry, P.J. Polarization of neutrophil granules - A characteristic of inflammatory states. *Blood Cells Mol Dis* **69**, 74 (2018).
38. Fais, S. & Malorni, W. Leukocyte uropod formation and membrane/cytoskeleton linkage in immune interactions. *J Leukoc Biol* **73**, 556-563 (2003).
39. Luo, H.R. & Mondal, S. Molecular control of PtdIns(3,4,5)P3 signaling in neutrophils. *EMBO reports* **16**, 149-163 (2015).
40. Suire, S.*, et al.* GPCR activation of Ras and PI3Kc in neutrophils depends on PLCb2/b3 and the RasGEF RasGRP4. *EMBO J* **31**, 3118-3129 (2012).
41. Welch, H.C., Coadwell, W.J., Stephens, L.R. & Hawkins, P.T. Phosphoinositide 3-kinase-dependent activation of Rac. *FEBS Lett* **546**, 93-97 (2003).
42. Welch, H.C.*, et al.* P-Rex1, a PtdIns(3,4,5)P3- and Gbetagamma-regulated guanine-nucleotide exchange factor for Rac. *Cell* **108**, 809-821 (2002).
43. Tsai, T.Y.*, et al.* Efficient Front-Rear Coupling in Neutrophil Chemotaxis by Dynamic Myosin II Localization. *Dev Cell* **49**, 189-205 e186 (2019).

44. Sanchez-Madrid, F. & del Pozo, M.A. Leukocyte polarization in cell migration and immune interactions. *EMBO J* **18**, 501-511 (1999).
45. Wong, K., Pertz, O., Hahn, K. & Bourne, H. Neutrophil polarization: spatiotemporal dynamics of RhoA activity support a self-organizing mechanism. *Proc Natl Acad Sci U S A* **103**, 3639-3644 (2006).
46. Hind, L.E., Vincent, W.J. & Huttenlocher, A. Leading from the Back: The Role of the Uropod in Neutrophil Polarization and Migration. *Dev Cell* **38**, 161-169 (2016).
47. Smith, L.A., Aranda-Espinoza, H., Haun, J.B., Dembo, M. & Hammer, D.A. Neutrophil traction stresses are concentrated in the uropod during migration. *Biophys J* **92**, L58-60 (2007).
48. Vadillo, E.*, et al.* Intermittent rolling is a defect of the extravasation cascade caused by Myosin1e-deficiency in neutrophils. *Proc Natl Acad Sci U S A* (2019).
49. Saez de Guinoa, J., Barrio, L. & Carrasco, Y.R. Vinculin arrests motile B cells by stabilizing integrin clustering at the immune synapse. *J Immunol* **191**, 2742-2751 (2013).
50. Hyun, Y.M.*, et al.* Uropod elongation is a common final step in leukocyte extravasation through inflamed vessels. *J Exp Med* **209**, 1349-1362 (2012).
51. Bruehl, R.E.*, et al.* Leukocyte activation induces surface redistribution of P-selectin glycoprotein ligand-1. *J Leukoc Biol* **61**, 489-499 (1997).
52. Nagata, K., Tsuji, T., Matsushima, K., Hanai, N. & Irimura, T. Redistribution of selectin counter-ligands induced by cytokines. *Int Immunol* **12**, 487-492 (2000).
53. Sreeramkumar, V.*, et al.* Neutrophils scan for activated platelets to initiate inflammation. *Science* **346**, 1234-1238 (2014).
54. Itoh, S., Susuki, C., Takeshita, K., Nagata, K. & Tsuji, T. Redistribution of P-selectin glycoprotein ligand-1 (PSGL-1) in chemokine-treated neutrophils: a role of lipid microdomains. *J Leukoc Biol* **81**, 1414-1421 (2007).
55. McEver, R.P., Beckstead, J.H., Moore, K.L., Marshall-Carlson, L. & Bainton, D.F. GMP-140, a platelet alpha-granule membrane protein, is also synthesized by vascular endothelial cells and is localized in Weibel-Palade bodies. *J Clin Invest* **84**, 92-99 (1989).
56. Berman, C.L.*, et al.* A platelet alpha granule membrane protein that is associated with the plasma membrane after activation. Characterization and subcellular localization of platelet activation-dependent granule-external membrane protein. *J Clin Invest* **78**, 130-137 (1986).
57. Purdy, M., Obi, A., Myers, D. & Wakefield, T. P- and E- selectin in venous thrombosis and non-venous pathologies. *J Thromb Haemost* **20**, 1056-1066 (2022).
58. Timmerman, I., Daniel, A.E., Kroon, J. & van Buul, J.D. Leukocytes Crossing the Endothelium: A Matter of Communication. *Int Rev Cell Mol Biol* **322**, 281-329 (2016).
59. Leeuwenberg, J.F.*, et al.* E-selectin and intercellular adhesion molecule-1 are released by activated human endothelial cells in vitro. *Immunology* **77**, 543-549 (1992).
60. Abbassi, O., Kishimoto, T.K., McIntire, L.V. & Smith, C.W. Neutrophil adhesion to endothelial cells. *Blood Cells* **19**, 245-259; discussion 259-260 (1993).
61. Shyjan, A.M., Bertagnolli, M., Kenney, C.J. & Briskin, M.J. Human mucosal addressin cell adhesion molecule-1 (MAdCAM-1) demonstrates structural and functional similarities to the alpha 4 beta 7-integrin binding domains of murine MAdCAM-1, but extreme divergence of mucin-like sequences. *J Immunol* **156**, 2851-2857 (1996).
62. Ivetic, A., Hoskins Green, H.L. & Hart, S.J. L-selectin: A Major Regulator of Leukocyte Adhesion, Migration and Signaling. *Front Immunol* **10**, 1068 (2019).
63. Wang, H.B.*, et al.* P-selectin primes leukocyte integrin activation during inflammation. *Nat Immunol* **8**, 882-892 (2007).
64. Miner, J.J.*, et al.* Separable requirements for cytoplasmic domain of PSGL-1 in leukocyte rolling and signaling under flow. *Blood* **112**, 2035-2045 (2008).

65. Vestweber, D. How leukocytes cross the vascular endothelium. *Nat Rev Immunol* **15**, 692-704 (2015).
66. Campbell, I.D. & Humphries, M.J. Integrin structure, activation, and interactions. *Cold Spring Harb Perspect Biol* **3**(2011).
67. Barczyk, M., Carracedo, S. & Gullberg, D. Integrins. *Cell Tissue Res* **339**, 269-280 (2010).
68. Heit, B., Colarusso, P. & Kubes, P. Fundamentally different roles for LFA-1, Mac-1 and alpha4-integrin in neutrophil chemotaxis. *J Cell Sci* **118**, 5205-5220 (2005).
69. Berton, G. & Lowell, C.A. Integrin signalling in neutrophils and macrophages. *Cell Signal* **11**, 621-635 (1999).
70. Li, N.*, et al.* Ligand-specific binding forces of LFA-1 and Mac-1 in neutrophil adhesion and crawling. *Mol Biol Cell* **29**, 408-418 (2018).
71. Smith, C.W. Leukocyte-endothelial cell interactions. *Semin Hematol* **30**, 45-53; discussion 54-45 (1993).
72. Luscinskas, F.W.*, et al.* Cytokine-activated human endothelial monolayers support enhanced neutrophil transmigration via a mechanism involving both endothelial-leukocyte adhesion molecule-1 and intercellular adhesion molecule-1. *J Immunol* **146**, 1617-1625 (1991).
73. Wang, Y.*, et al.* Leukocyte engagement of platelet glycoprotein Ibalpha via the integrin Mac-1 is critical for the biological response to vascular injury. *Circulation* **112**, 2993-3000 (2005).
74. Luyendyk, J.P., Schoenecker, J.G. & Flick, M.J. The multifaceted role of fibrinogen in tissue injury and inflammation. *Blood* **133**, 511-520 (2019).
75. Caswell, P.T., Vadrevu, S. & Norman, J.C. Integrins: masters and slaves of endocytic transport. *Nat Rev Mol Cell Biol* **10**, 843-853 (2009).
76. Pflugfelder, S.C., Stern, M., Zhang, S. & Shojaei, A. LFA-1/ICAM-1 Interaction as a Therapeutic Target in Dry Eye Disease. *J Ocul Pharmacol Ther* **33**, 5-12 (2017).
77. Senetar, M.A., Moncman, C.L. & McCann, R.O. Talin2 is induced during striated muscle differentiation and is targeted to stable adhesion complexes in mature muscle. *Cell Motil Cytoskeleton* **64**, 157-173 (2007).
78. Larjava, H., Plow, E.F. & Wu, C. Kindlins: essential regulators of integrin signalling and cell-matrix adhesion. *EMBO Rep* **9**, 1203-1208 (2008).
79. Kiema, T.*, et al.* The molecular basis of filamin binding to integrins and competition with talin. *Mol Cell* **21**, 337-347 (2006).
80. McGilvray, I.D.*, et al.* VLA-4 integrin cross-linking on human monocytic THP-1 cells induces tissue factor expression by a mechanism involving mitogen-activated protein kinase. *J Biol Chem* **272**, 10287-10294 (1997).
81. Zheng, L., Sjolander, A., Eckerdal, J. & Andersson, T. Antibody-induced engagement of beta 2 integrins on adherent human neutrophils triggers activation of p21ras through tyrosine phosphorylation of the protooncogene product Vav. *Proc Natl Acad Sci U S A* **93**, 8431-8436 (1996).
82. Miyamoto, S.*, et al.* Integrin function: molecular hierarchies of cytoskeletal and signaling molecules. *J Cell Biol* **131**, 791-805 (1995).
83. Lowell, C.A., Fumagalli, L. & Berton, G. Deficiency of Src family kinases p59/61hck and p58c-fgr results in defective adhesion-dependent neutrophil functions. *J Cell Biol* **133**, 895-910 (1996).
84. Berton, G., Laudanna, C., Sorio, C. & Rossi, F. Generation of signals activating neutrophil functions by leukocyte integrins: LFA-1 and gp150/95, but not CR3, are able to stimulate the respiratory burst of human neutrophils. *J Cell Biol* **116**, 1007-1017 (1992).
85. Suchard, S.J. & Boxer, L.A. Exocytosis of a subpopulation of specific granules coincides with H2O2 production in adherent human neutrophils. *J Immunol* **152**, 290-300 (1994).
86. Savill, J. Apoptosis in resolution of inflammation. *J Leukoc Biol* **61**, 375-380 (1997).

87. Sumagin, R. & Sarelius, I.H. Intercellular adhesion molecule-1 enrichment near tricellular endothelial junctions is preferentially associated with leukocyte transmigration and signals for reorganization of these junctions to accommodate leukocyte passage. *J Immunol* **184**, 5242-5252 (2010).
88. Wojciechowski, J.C. & Sarelius, I.H. Preferential binding of leukocytes to the endothelial junction region in venules in situ. *Microcirculation* **12**, 349-359 (2005).
89. Luu, N.T., Rainger, G.E. & Nash, G.B. Kinetics of the different steps during neutrophil migration through cultured endothelial monolayers treated with tumour necrosis factor-alpha. *J Vasc Res* **36**, 477-485 (1999).
90. Ohashi, K.L., Tung, D.K., Wilson, J., Zweifach, B.W. & Schmid-Schonbein, G.W. Transvascular and interstitial migration of neutrophils in rat mesentery. *Microcirculation* **3**, 199-210 (1996).
91. Sumagin, R., Prizant, H., Lomakina, E., Waugh, R.E. & Sarelius, I.H. LFA-1 and Mac-1 define characteristically different intralumenal crawling and emigration patterns for monocytes and neutrophils in situ. *J Immunol* **185**, 7057-7066 (2010).
92. Phillipson, M*., et al.* Intraluminal crawling of neutrophils to emigration sites: a molecularly distinct process from adhesion in the recruitment cascade. *J Exp Med* **203**, 2569-2575 (2006).
93. Zhelev, D.V. & Alteraifi, A. Signaling in the motility responses of the human neutrophil. *Ann Biomed Eng* **30**, 356-370 (2002).
94. Halai, K., Whiteford, J., Ma, B., Nourshargh, S. & Woodfin, A. ICAM-2 facilitates luminal interactions between neutrophils and endothelial cells in vivo. *J Cell Sci* **127**, 620-629 (2014).
95. Barreiro, O*., et al.* Dynamic interaction of VCAM-1 and ICAM-1 with moesin and ezrin in a novel endothelial docking structure for adherent leukocytes. *J Cell Biol* **157**, 1233-1245 (2002).
96. Carman, C.V., Jun, C.D., Salas, A. & Springer, T.A. Endothelial cells proactively form microvilli-like membrane projections upon intercellular adhesion molecule 1 engagement of leukocyte LFA-1. *J Immunol* **171**, 6135-6144 (2003).
97. Woodfin, A*., et al.* Endothelial cell activation leads to neutrophil transmigration as supported by the sequential roles of ICAM-2, JAM-A, and PECAM-1. *Blood* **113**, 6246-6257 (2009).
98. Woodfin, A*., et al.* JAM-A mediates neutrophil transmigration in a stimulus-specific manner in vivo: evidence for sequential roles for JAM-A and PECAM-1 in neutrophil transmigration. *Blood* **110**, 1848-1856 (2007).
99. Schenkel, A.R., Mamdouh, Z., Chen, X., Liebman, R.M. & Muller, W.A. CD99 plays a major role in the migration of monocytes through endothelial junctions. *Nat Immunol* **3**, 143-150 (2002).
100. Bixel, M.G*., et al.* CD99 and CD99L2 act at the same site as, but independently of, PECAM-1 during leukocyte diapedesis. *Blood* **116**, 1172-1184 (2010).
101. Bixel, M.G*., et al.* A CD99-related antigen on endothelial cells mediates neutrophil but not lymphocyte extravasation in vivo. *Blood* **109**, 5327-5336 (2007).
102. Mamdouh, Z., Kreitzer, G.E. & Muller, W.A. Leukocyte transmigration requires kinesin-mediated microtubule-dependent membrane trafficking from the lateral border recycling compartment. *J Exp Med* **205**, 951-966 (2008).
103. Muller, W.A. Transendothelial migration: unifying principles from the endothelial perspective. *Immunol Rev* **273**, 61-75 (2016).
104. Burn, G.L., Foti, A., Marsman, G., Patel, D.F. & Zychlinsky, A. The Neutrophil. *Immunity* **54**, 1377-1391 (2021).
105. Cowland, J.B. & Borregaard, N. Granulopoiesis and granules of human neutrophils. *Immunol Rev* **273**, 11-28 (2016).
106. Mollinedo, F. Neutrophil Degranulation, Plasticity, and Cancer Metastasis. *Trends Immunol* **40**, 228-242 (2019).
107. Borregaard, N., Sorensen, O.E. & Theilgaard-Monch, K. Neutrophil granules: a library of innate immunity proteins. *Trends Immunol* **28**, 340-345 (2007).

108. Brumell, J.H.*, et al.* Subcellular distribution of docking/fusion proteins in neutrophils, secretory cells with multiple exocytic compartments. *J Immunol* **155**, 5750-5759 (1995).
109. Mylvaganam, S., Freeman, S.A. & Grinstein, S. The cytoskeleton in phagocytosis and macropinocytosis. *Curr Biol* **31**, R619-R632 (2021).
110. Ravindran, M., Khan, M.A. & Palaniyar, N. Neutrophil Extracellular Trap Formation: Physiology, Pathology, and Pharmacology. *Biomolecules* **9**(2019).
111. Yipp, B.G. & Kubes, P. NETosis: how vital is it? *Blood* **122**, 2784-2794 (2013).
112. Yipp, B.G*., et al.* Infection-induced NETosis is a dynamic process involving neutrophil multitasking in vivo. *Nat Med* **18**, 1386-1393 (2012).
113. Mirakaj, V. & Rosenberger, P. Immunomodulatory Functions of Neuronal Guidance Proteins. *Trends Immunol* **38**, 444-456 (2017).
114. Kolodkin, A.L., Matthes, D.J. & Goodman, C.S. The semaphorin genes encode a family of transmembrane and secreted growth cone guidance molecules. *Cell* **75**, 1389-1399 (1993).
115. Limoni, G. Modelling and Refining Neuronal Circuits with Guidance Cues: Involvement of Semaphorins. *Int J Mol Sci* **22**(2021).
116. Xie, Z., Huganir, R.L. & Penzes, P. Activity-dependent dendritic spine structural plasticity is regulated by small GTPase Rap1 and its target AF-6. *Neuron* **48**, 605-618 (2005).
117. Vanderhaeghen, P. & Cheng, H.J. Guidance molecules in axon pruning and cell death. *Cold Spring Harb Perspect Biol* **2**, a001859 (2010).
118. Antipenko, A*., et al.* Structure of the semaphorin-3A receptor binding module. *Neuron* **39**, 589-598 (2003).
119. Rozbesky, D*., et al.* Diversity of oligomerization in Drosophila semaphorins suggests a mechanism of functional fine-tuning. *Nat Commun* **10**, 3691 (2019).
120. Moretti, S., Procopio, A., Boemi, M. & Catalano, A. Neuronal semaphorins regulate a primary immune response. *Curr Neurovasc Res* **3**, 295-305 (2006).
121. Nakayama, H., Kusumoto, C., Nakahara, M., Fujiwara, A. & Higashiyama, S. Semaphorin 3F and Netrin-1: The Novel Function as a Regulator of Tumor Microenvironment. *Front Physiol* **9**, 1662 (2018).
122. Treps, L., Le Guelte, A. & Gavard, J. Emerging roles of Semaphorins in the regulation of epithelial and endothelial junctions. *Tissue Barriers* **1**, e23272 (2013).
123. Svitkina, T. The Actin Cytoskeleton and Actin-Based Motility. *Cold Spring Harb Perspect Biol* **10**(2018).
124. Catalano, A*., et al.* Semaphorin-3A is expressed by tumor cells and alters T-cell signal transduction and function. *Blood* **107**, 3321-3329 (2006).
125. Kumanogoh, A*., et al.* Nonredundant roles of Sema4A in the immune system: defective T cell priming and Th1/Th2 regulation in Sema4A-deficient mice. *Immunity* **22**, 305-316 (2005).
126. Roth, J.M., Kohler, D., Schneider, M., Granja, T.F. & Rosenberger, P. Semaphorin 7A Aggravates Pulmonary Inflammation during Lung Injury. *PLoS One* **11**, e0146930 (2016).
127. Kohler, D*., et al.* Red blood cell-derived semaphorin 7A promotes thrombo-inflammation in myocardial ischemia-reperfusion injury through platelet GPIb. *Nat Commun* **11**, 1315 (2020).
128. Suzuki, K., Kumanogoh, A. & Kikutani, H. CD100/Sema4D, a lymphocyte semaphorin involved in the regulation of humoral and cellular immune responses. *Cytokine Growth Factor Rev* **14**, 17-24 (2003).
129. Maleki, K.T., Cornillet, M. & Bjorkstrom, N.K. Soluble SEMA4D/CD100: A novel immunoregulator in infectious and inflammatory diseases. *Clin Immunol* **163**, 52-59 (2016).
130. Nishide, M*., et al.* Semaphorin 4D inhibits neutrophil activation and is involved in the pathogenesis of neutrophil-mediated autoimmune vasculitis. *Ann Rheum Dis* **76**, 1440-1448 (2017).

131. Bougeret, C*., et al.* Increased surface expression of a newly identified 150-kDa dimer early after human T lymphocyte activation. *J Immunol* **148**, 318-323 (1992).
132. Hall, K.T*., et al.* Human CD100, a novel leukocyte semaphorin that promotes B-cell aggregation and differentiation. *Proc Natl Acad Sci U S A* **93**, 11780-11785 (1996).
133. Love, C.A*., et al.* The ligand-binding face of the semaphorins revealed by the high-resolution crystal structure of SEMA4D. *Nat Struct Biol* **10**, 843-848 (2003).
134. Wang, X*., et al.* Functional soluble CD100/Sema4D released from activated lymphocytes: possible role in normal and pathologic immune responses. *Blood* **97**, 3498-3504 (2001).
135. Mou, P*., et al.* Identification of a calmodulin-binding domain in Sema4D that regulates its exodomain shedding in platelets. *Blood* **121**, 4221-4230 (2013).
136. Kumanogoh, A. & Kikutani, H. Immunological functions of the neuropilins and plexins as receptors for semaphorins. *Nat Rev Immunol* **13**, 802-814 (2013).
137. Kumanogoh, A*., et al.* Identification of CD72 as a lymphocyte receptor for the class IV semaphorin CD100: a novel mechanism for regulating B cell signaling. *Immunity* **13**, 621-631 (2000).
138. Chabbert-de Ponnat, I*., et al.* Soluble CD100 functions on human monocytes and immature dendritic cells require plexin C1 and plexin B1, respectively. *Int Immunol* **17**, 439-447 (2005).
139. Li, M*., et al.* Endogenous CD100 promotes glomerular injury and macrophage recruitment in experimental crescentic glomerulonephritis. *Immunology* **128**, 114-122 (2009).
140. Vicente-Manzanares, M., Ma, X., Adelstein, R.S. & Horwitz, A.R. Non-muscle myosin II takes centre stage in cell adhesion and migration. *Nat Rev Mol Cell Biol* **10**, 778-790 (2009).
141. Ponti, A., Machacek, M., Gupton, S.L., Waterman-Storer, C.M. & Danuser, G. Two distinct actin networks drive the protrusion of migrating cells. *Science* **305**, 1782-1786 (2004).
142. Friedland, J.C., Lee, M.H. & Boettiger, D. Mechanically activated integrin switch controls alpha5beta1 function. *Science* **323**, 642-644 (2009).
143. Verkhovsky, A.B., Svitkina, T.M. & Borisy, G.G. Self-polarization and directional motility of cytoplasm. *Curr Biol* **9**, 11-20 (1999).
144. Salvermoser, M*., et al.* Myosin 1f is specifically required for neutrophil migration in 3D environments during acute inflammation. *Blood* **131**, 1887-1898 (2018).
145. Uotila, L.M., Guenther, C., Savinko, T., Lehti, T.A. & Fagerholm, S.C. Filamin A Regulates Neutrophil Adhesion, Production of Reactive Oxygen Species, and Neutrophil Extracellular Trap Release. *J Immunol* **199**, 3644-3653 (2017).
146. Rosowski, E.E., Deng, Q., Keller, N.P. & Huttenlocher, A. Rac2 Functions in Both Neutrophils and Macrophages To Mediate Motility and Host Defense in Larval Zebrafish. *J Immunol* **197**, 4780-4790 (2016).
147. Cherfils, J. & Zeghouf, M. Regulation of small GTPases by GEFs, GAPs, and GDIs. *Physiol Rev* **93**, 269-309 (2013).
148. Basile, J.R., Barac, A., Zhu, T., Guan, K.L. & Gutkind, J.S. Class IV semaphorins promote angiogenesis by stimulating Rho-initiated pathways through plexin-B. *Cancer Res* **64**, 5212-5224 (2004).
149. Driessens, M.H., Olivo, C., Nagata, K., Inagaki, M. & Collard, J.G. B plexins activate Rho through PDZ-RhoGEF. *FEBS Lett* **529**, 168-172 (2002).
150. Roney, K.E*., et al.* Plexin-B2 negatively regulates macrophage motility, Rac, and Cdc42 activation. *PLoS One* **6**, e24795 (2011).
151. Machesky, L.M. & Hall, A. Role of actin polymerization and adhesion to extracellular matrix in Rac- and Rho-induced cytoskeletal reorganization. *J Cell Biol* **138**, 913-926 (1997).
152. Olson, M.F., Ashworth, A. & Hall, A. An essential role for Rho, Rac, and Cdc42 GTPases in cell cycle progression through G1. *Science* **269**, 1270-1272 (1995).

153. Nobes, C.D. & Hall, A. Rho, rac, and cdc42 GTPases regulate the assembly of multimolecular focal complexes associated with actin stress fibers, lamellipodia, and filopodia. *Cell* **81**, 53-62 (1995).
154. Motani, K. & Kosako, H. Activation of stimulator of interferon genes (STING) induces ADAM17-mediated shedding of the immune semaphorin SEMA4D. *J Biol Chem* **293**, 7717-7726 (2018).
155. Smith, E.S.*, et al.* SEMA4D compromises blood-brain barrier, activates microglia, and inhibits remyelination in neurodegenerative disease. *Neurobiol Dis* **73**, 254-268 (2015).
156. Yoshida, Y.*, et al.* Semaphorin 4D Contributes to Rheumatoid Arthritis by Inducing Inflammatory Cytokine Production: Pathogenic and Therapeutic Implications. *Arthritis Rheumatol* **67**, 1481-1490 (2015).
157. Ishida, I.*, et al.* Involvement of CD100, a lymphocyte semaphorin, in the activation of the human immune system via CD72: implications for the regulation of immune and inflammatory responses. *Int Immunol* **15**, 1027-1034 (2003).
158. Delaire, S.*, et al.* Biological activity of soluble CD100. II. Soluble CD100, similarly to H-SemaIII, inhibits immune cell migration. *J Immunol* **166**, 4348-4354 (2001).
159. Giordano, S.*, et al.* The semaphorin 4D receptor controls invasive growth by coupling with Met. *Nat Cell Biol* **4**, 720-724 (2002).
160. Sun, Q., Zhou, H., Binmadi, N.O. & Basile, J.R. Hypoxia-inducible factor-1-mediated regulation of semaphorin 4D affects tumor growth and vascularity. *J Biol Chem* **284**, 32066-32074 (2009).
161. Qiu, L.*, et al.* Regulatory sequence analysis of semaphorin 4D 5' non-coding region. *J Cancer* **10**, 903-910 (2019).

8. Declaration of Contributions to the Dissertation

The dissertation work was carried out at the Department of Anaesthesiology and Intensive Medicine in University Hospital Tübingen under the supervision of Prof. Dr. med. Peter Rosenberger.

The study was designed by Prof. Dr. med. Peter Rosenberger, Linyan Tang and Dr. Tiago Folgosa Granja.

After training by Dr. Tiago Granja and Michaela Hoch-Gutbrod, I carried out all experiments independently except the staining for Sema4D on pulmonary epithelial and endothelial cells in Figure 12 which was performed together with Dr. rer. nat. Claudia Eggstein.

Statistical analysis was carried out independently by myself.

I confirm that I wrote the manuscript myself under the supervision of Prof. Dr. med. Peter Rosenberger and that any additional sources of information have been duly cited. Dr. rer. nat. David Köhler and Dr. Kalin Heck-Swain have reviewed the dissertation.

Signed_____

on 08.02.2023 in Tübingen

9. Awards

2022 Best Poster Award at the Ph.D. Retreat of the Medicine Faculty - University Tübingen in Bad Urach 2022

10. Acknowledgments

I would like to express my deepest appreciation to my supervisor Prof. Dr. Peter Rosenberger. This endeavor would not have been possible without his professional guidance, suggestions and invaluable encouragement. I am also deeply grateful to Prof. Dr. Robert Lukowski and Prof. Dr. Tamam Bakchoul on my doctoral committee, who have generously provided helpful suggestions with their wide knowledge and expertise.

I would like to extend my sincere thanks to Dr. Tiago Folgosa Granja for his patient supervision, generous teaching, and warm help. I am also sincerely thankful for Dr. rer. nat. David Köhler and Dr. rer. nat. Claudia Eggstein who have given me professional suggestions and expert support and revising my thesis. I would also like to thank Dr. Kalin Heck-Swain for reviewing my thesis.

Special thanks to Michaela Hoch-Gutbrod for her assistance and help with experiments and techniques. I would like to acknowledge Irene Vollmer, Alice Mager and Tatjana Schreiber for their support in the lab.

I would like to thank Dr. Inka Montero and Dr. Lina Maria Bandholz-Cajamarca for their warm and considerate help and instructions in so many situations during this Ph. D. program.

Last but not least I am extremely grateful to my beloved family for their sacrifice and support in these years. And I would also like to thank my closest friends, especially Claudia Holt for her warm accompaniment and emotional support.